

**FORAMINIFERAL AND CORALLINE BARIUM
AS PALEOCEANOGRAPHIC TRACERS**

by

David Wallace Lea

B.S., Haverford College

(1984)

SUBMITTED IN PARTIAL FULFILLMENT
OF THE REQUIREMENTS FOR THE DEGREE OF
DOCTOR OF PHILOSOPHY

at the

MASSACHUSETTS INSTITUTE OF TECHNOLOGY
and the
WOODS HOLE OCEANOGRAPHIC INSTITUTION

September, 1989

©Massachusetts Institute of Technology 1989

Signature of Author _____

Department of Earth, Atmospheric, and Planetary Sciences,
Massachusetts Institute of Technology, and the Joint Program in
Oceanography, Massachusetts Institute of Technology/Woods Hole
Oceanographic Institution, September 1989

Certified by _____

Edward A. Boyle, Thesis Supervisor

Accepted by _____

Philip M. Gschwend, Chairman, Joint Committee for Chemical
Oceanography, Massachusetts Institute of Technology/Woods Hole
Oceanographic Institution

Lindgren

WITHDRAWN
MASSACHUSETTS INSTITUTE
OF TECHNOLOGY
FROM
NOV 06 1989
MIT LIBRARIES
LIBRARIES

FORAMINIFERAL AND CORALLINE BARIUM AS PALEOCEANOGRAPHIC TRACERS

by

David W. Lea

Submitted to the Department of Earth, Atmospheric, and Planetary Sciences on October 6, 1989 in partial fulfillment of the requirements for the Degree of Doctor of Philosophy in Oceanography

Abstract

The distribution of Ba in the ocean is similar to the refractory components, silica and alkalinity. Therefore reconstructions of Ba in ancient water masses can be used to probe the circulation and chemistry of past oceans. Paleo-Ba distributions are recovered from the aragonite skeletons of corals and the calcite shells of planktonic and benthic foraminifera, since Ba substitutes for Ca in the lattice of these biogenic phases. The shell or coral material is treated with a rigorous cleaning procedure to remove spurious Ba associated with residual sedimentary phases. The Ba/Ca ratio of the purified foraminiferal calcite or coralline aragonite is quantified by a combination of isotope dilution flow injection on an ICP-MS for Ba and flame atomic absorption for Ca.

A quarter-annual record of coralline Ba recovered from a cored sample of *Pavona clavus* from the Galapagos Islands demonstrates that variability in Ba can be related to temporal variability in upwelling of source waters to the surface ocean. Ba/Ca ratios vary between about 4 and 5 $\mu\text{mol/mol}$, with the highest values associated with bands formed during periods of cold sea surface temperatures. Upwelling in the equatorial Pacific transports cold, Ba-rich upper thermocline waters to the surface ocean, causing the coincidence between Ba and sea surface temperature. Depression of the thermocline during El Niño/Southern Oscillation (ENSO) events results in the coincidence of negative Ba anomalies with the positive temperature anomalies characteristic of ENSO events. Sr/Ca ratios in the same coral record vary between about 9.2 and 9.8 mmol/mol, presumably in response to a temperature effect on Sr incorporation. Similarities between Ba and Sr records in the coral suggest that the Ba/Ca ratio of corals may be partially controlled by a temperature effect.

Planktonic foraminifera *Globigerinoides sacculifera*, *ruber*, *conglobatus*, *Orbulina spp.* and *Neogloboquadrina dutertrei* from the Panama Basin, North Atlantic, and Mediterranean have Ba/Ca ratios between 0.6 and 1.0 $\mu\text{mol/mol}$. Variation in foraminiferal Ba contents between the three basins is consistent with the trend in surface seawater Ba. The distribution coefficient for Ba incorporation in these 5 species is 0.19 ± 0.05 . Records of planktonic-Ba reaching back to the end of the last glacial period do not reveal any large change in the Ba concentration of North-West Atlantic and Eastern Equatorial Pacific surface waters. *Globorotalia* have Ba/Ca ratios as high as 10 $\mu\text{mol/mol}$; these anomalously high Ba contents are inconsistent with coprecipitation of Ba

in the shell. High Ba contents of *Globorotalia* could result from diatom-rich food sources, since precipitation of barite in marine biogenic particulate matter is apparently associated with diatom frustules.

The Ba/Ca ratios of the benthic foraminifera *Cibicidoides* and *Uvigerina* recovered from sedimentary core-tops range from 2 to 5 $\mu\text{mol/mol}$; ratios can be directly related to local bottom water Ba. The calculated benthic distribution coefficient is 0.37 ± 0.06 . Ba/Ca of benthic foraminifera recovered from glacial sections (15-25 kyr) of cores from the Atlantic indicates that waters deeper than 2900 m had ~30-60% higher Ba. These changes are consistent with previously observed nutrient shifts based on foraminiferal Cd and $\delta^{13}\text{C}$. Increases in Atlantic deep water nutrient contents can be explained by reduction in NADW formation during the last glacial maximum (LGM). Ba/Ca of benthic foraminifera from the glacial sections of intermediate depth Atlantic cores are equal or lower to Holocene values. This Ba evidence argues against the Mediterranean as a greatly increased source to Atlantic intermediate waters during the LGM, since the Mediterranean is enriched in Ba today and apparently remained enriched during the LGM. Deep waters of the Glacial Pacific were about 25% lower in Ba (~3000 m). The Ba content of waters of the deep Atlantic, Antarctic and Pacific were similar at the last glacial maximum.

The main difference between LGM foraminiferal Ba and Cd distributions is that Cd remains significantly lower in the deep Atlantic relative to the Pacific. A simple seven-box ocean model is used to explore several scenarios for reconciling LGM Ba and Cd distributions. While the changed distribution of both tracers suggests diminishment in the flux of nutrient depleted waters to the deep Atlantic during the LGM, increased Atlantic upwelling rates and consequently enhanced Ba-particle fluxes can account for the the lack of Ba fractionation between the deep Atlantic and Pacific. The model suggests that Ba can be transferred efficiently to the deep Atlantic by enhanced upwelling because the vast majority of the Ba is regenerated in the deep Atlantic box.

A 212 kyr record of benthic foraminiferal Ba has been recovered from CHN82 Sta24 Core4PC at 3427m water depth in the North-West Atlantic. Ba/Ca ranges from a low of about 2 $\mu\text{mol/mol}$ during interglacial periods to a high of 4 $\mu\text{mol/mol}$ during glacial periods. These variations are consistent with reduced NADW formation during glacial periods. Variability in benthic Ba is not strictly linked to a glacial-interglacial pattern. Spectral analysis of the Ba time series indicates dominance of the 23 kyr period of precession of the earth's axis. Since power at the precessional frequencies is far greater in the Ba time series than in the time series of Cd and carbon isotopes from the same core, Ba variations apparently record a second process distinct from variations in the flux of nutrient depleted water to the site of the core. One possible explanation for this second mechanism might be the increase in Atlantic upwelling and the consequently enhanced particulate Ba fluxes suggested to explain the observed differences in Ba and Cd at the LGM.

Thesis Supervisor: Dr. Edward A. Boyle, Associate Professor of Oceanography, MIT

Dedicated to Patti and my parents

Acknowledgements

Perhaps every Ph.D. candidate feels this way, but I can't imagine anyone ever having had as much valuable help as I have had! First and foremost I would like to thank my advisor Ed Boyle; Ed taught me how to do science, involved me in a very exciting endeavor, and always found time (and had the patience) to answer the plethora of questions and queries with which I presented him.

I want to thank the members of my thesis committee, Wallace Broecker, Lloyd Keigwin and Mike Bacon for their insights and help as my work progressed. Many other scientists have been generous with their time and expertise; among them I would like to especially thank John Edmond, Ellen Druffel, Bill Curry, Phil Gschwend, Harry Elderfield, Nick Shackleton, Chris Measures, Mark Kurz, Jim Bishop, John Trefry, Peggy Delaney and Werner Deuser.

Many samples were generously provided for my work. Werner Deuser, Ellen Druffel and Sus Honjo provided sediment trap samples, Lloyd Keigwin, Glen Jones, Wallace Broecker and Ed Sholkovitz provided sediment samples, Lex van Geen provided seawater samples, Ted McConnaughey, Glen Shen and Ellen Druffel provided coral samples and at the last minute on short notice Delia Oppo provided some critical Mediterranean foraminifera samples. Samples were provided by core repositories at WHOI, LDGO (via Ed Boyle's companion study), URI and OSU. Jim Broda and Eben Franks were always willing to lend their help in the WHOI core lab.

The acquisition of an ICP-MS at MIT was a key to the success of my thesis work. I want to thank John Edmond and Kelly Kenison Falkner for making that possible, and I especially want to acknowledge Kelly and Andy Campbell for sharing their insights about the plasmaquad. I could not have completed all the Ba measurements without their generous help.

Both Glen Shen and Art Spivack were important influences when I first arrived in the lab, and I am especially grateful to Glen for his instruction in trace metal analysis as well as introduction to the acquisition of historical coral records. Glen also generously provided all the samples I used for coral studies in my thesis.

Susan Chapnick, Paula Rosener and Irene Ellis kept our lab running smoothly as well as sharing their expertise in analytical chemistry.

I have had the pleasure of two great office mates, Michael Baker and Debra Colodner; both offered the ideal combination of humor and scientific debate! Lab mates Lex van Geen, Rob Sherrell and Yair Rosenthal were fun to work with and a great help numerous times, and fellow students Eric Brown, Ed Brook, Neil Slowey and many others provided additional diversion and/or stimulating discussion.

Any foraminiferal thesis must acknowledge the true heroes: the foram pickers! I could not have done it all without the unfailing work of Najla Azadzi, Pei Ling Du, Lorraine Cirillo, An-Na Liu and Bijal Trivedi.

Patti Murakami was my companion and Henry Richardson and Sheba Akhtar my friends through thick and thin. Without all of Patti's help and encouragement these last 5 years would have been far more difficult.

My parents have given me tremendous support over all these years. They never questioned my switching from Bach to Barium, even if Milankovitch harmonics might seem a bit less melodious than those from the oboe. I thank them for their trust in me.

This research was supported by NSF grant OCE8710168 (to Edward A Boyle) and a Joint Oceanographic Institutions/Ocean Drilling Program Fellowship for 1987-1988.

Table of Contents

	<u>Page</u>
Abstract	iii
Dedication	v
Acknowledgements	vi
Table of Contents	viii
List of Figures	x
List of Tables	xii
Chapter 1. INTRODUCTION	
1.1 General Introduction	1
1.2 Barium in the ocean	2
1.3 Records of Ba in ancient oceans	5
1.4 Content of the thesis	6
Chapter 2. METHODS	
2.1 Introduction	9
2.2 Purification of benthic foraminifera shells for Ba/Ca analysis	9
2.3 Analysis of benthic foraminiferal Ba/Ca ratios	15
2.4 Determination of Ba/Ca ratios in coral aragonite	23
Chapter 3. CORALLINE BARIUM RECORDS TEMPORAL VARIABILITY IN EQUATORIAL PACIFIC UPWELLING	28
Chapter 4. BARIUM IN PLANKTONIC FORAMINIFERA	
4.1 Introduction	41
4.2 Analytical Methods	42
4.3 Cleaning Method	43
4.4 Additional notes on cleaning	50
4.5 Ba/Ca in Holocene <i>Globigerinoides</i>	52
4.6 Ba in <i>Globorotalia</i>	59
4.7 Reconstruction of surface Ba in the Atlantic over the last 14 kyr	61
4.8 Conclusions	65
4.9 Appendix to Chapter 4: simple 2-box model for surface Ba	68
Chapter 5. BARIUM CONTENT OF BENTHIC FORAMINIFERA CONTROLLED BY BOTTOM WATER COMPOSITION	74
Chapter 6. BARIUM IN THE GLACIAL OCEANS	
6.1 Introduction	83
6.2 Core Selection	85
6.3 Methods	88
6.4 Core Data	89
6.5 Changes in the inter-basin distribution of Ba in the glacial oceans	108
6.6 Comparison of glacial distributions of Cd and ¹³ C to Ba	110
6.7 Consideration of factors unique to Ba	111
6.8 Reconciling Cd and Ba distributions in the Glacial oceans	114
6.9 Intermediate waters of the Atlantic; was the Mediterranean a more important source during glacial periods?	125
6.10 Conclusions	129
Chapter 7: 210 KYR RECORD OF BARIUM IN THE DEEP NORTH ATLANTIC	
7.1 Introduction	135
7.2 Features of the Ba record	143

7.3 Discussion	146
7.4 Time series analysis	147
7.5 Conclusions and speculation	153
Chapter 8: GENERAL CONCLUSIONS	160
Appendix 1: Analyses of Ba in seawater	165
Appendix 2: Description of model VIV*	168
Biographical Note	173

List of Figures

	<u>Page</u>
Figure 1.1 GEOSECS phosphate, silica and Ba profiles.	4
Figure 2.1 Core TR163-31B <i>Uvigerina</i> cleaning comparison.	11
Figure 2.2 Core TR163-31B <i>Uvigerina</i> cleaning comparison: x-y plot.	12
Figure 2.3 Core-top benthic foraminifera cleaning comparison.	13
Figure 2.4 Partial dissolutions of three species of benthic foraminifera.	16
Figure 2.5 Ba/Ca in semi-annual bands of Punta Pitt coral, 1950-1959.	25
Figure 3.1 Comparison of Ba in the Punta Pitt coral record with local SST.	29
Figure 3.2 Quarterly anomalies of Ba/Ca compared with SST anomalies.	34
Figure 3.3 Comparison of Ba and Cd in the Punta Pitt coral record.	35
Figure 3.4 Comparison of Ba and Sr in the Punta Pitt coral record.	38
Figure 4.1 SEM image of <i>N. dutertrei</i> shell with adhering barite.	45
Figure 4.2 Comparison of cleaned and uncleaned planktonic foraminifera.	47
Figure 4.3 Comparative cleaning of <i>N. dutertrei</i> shells from Panama Basin Sediment Trap.	51
Figure 4.4 Comparison of average Ba in planktonic foraminifera from core-tops and sediment traps/plankton tows.	54
Figure 4.5 Partial dissolution of two planktonic foraminifera.	56
Figure 4.6 Average Ba/Ca of planktonic foraminifera from three basins vs. surface water Ba.	58
Figure 4.7 Effect of alkaline-DTPA treatment on <i>G. truncatulinoides</i> shells.	60
Figure 4.8 Core EN120-GGC1 planktonic Ba/Ca record for last 14 kyr.	63
Figure 4.9 2-box model to describe surface Ba control.	69
Figure 4.10 Model derived relationship of surface Ba to mean P and mean Ba.	72
Figure 5.1 Paired Ba and alkalinity data for 9 GEOSECS stations.	76
Figure 5.2 Core-top calibrations for three benthic foraminifera.	78

Figure 6.1	Locations of cores.	87
Figure 6.2	Benthic Ba/Ca records from three North Atlantic CHN82 records.	90
Figure 6.3	Comparison of benthic $\delta^{18}\text{O}$, Cd and Ba for CHN82 Sta31 Core11PC, 0-140 cm.	94
Figure 6.4	Benthic $\delta^{18}\text{O}$ and Ba from core KNR64 Sta5 Core5PG.	96
Figure 6.5	Planktonic and benthic Ba/Ca from core TR163-31B.	99
Figure 6.6	Map of Holocene and LGM Ba/Ca from the Atlantic Ocean.	105
Figure 6.7	Holocene and LGM Ba hydrography for the North-West Atlantic.	106
Figure 6.8	Glacial Ba/Ca for the Eastern Equatorial Pacific.	107
Figure 6.9	Benthic Ba/Ca for Atlantic and Pacific cores on coincident time scales for the last 30 kyrs.	109
Figure 6.10	Benthic Ba vs. Cd of deep water masses in the Holocene and Glacial oceans.	115
Figure 6.11	7-Box Model with Holocene conditions.	118
Figure 6.12	Model run G3.	121
Figure 6.13	Model run G6.	123
Figure 6.14	Model sensitivity experiment for Ba and P in the deep Atlantic and Pacific.	124
Figure 6.15	Seawater Ba in the Mediterranean.	127
Figure 7.1	Benthic $\delta^{18}\text{O}$, $\delta^{13}\text{C}$, Cd and Ba from core CHN82 Sta24 Core4PC.	138
Figure 7.2	Benthic $\delta^{18}\text{O}$ and Ba vs. age in CHN82 Sta24 Core4PC.	144
Figure 7.3	Periodogram and log power spectrum for the Core4PC Ba record.	149
Figure 7.4	Comparison of log power spectra for $\delta^{18}\text{O}$, $\delta^{13}\text{C}$, Cd and Ba from core CHN82 Sta24 Core4PC and ETP index.	151
Figure 7.5	Comparison of the Core4PC Ba record with precession index.	154

List of Tables

	<u>Page</u>
Table 2.1 Ba isotope ratios of spike and natural sample.	18
Table 2.2 Concentrations of precision of determinations of Ba/Ca in consistency standards.	18
Table 2.3 Ba isotope dilution determinations as a function of 135/138 ratio.	21
Table 2.4 Ba determination in solutions of varying Ca concentration.	21
Table 2.5 Ba/Ca averages for 1950-59 Punta Pitt coral record.	26
Table 3.1 Ba/Ca and Sr/Ca for the 1965-1979 Punta Pitt coral record.	30
Table 4.1 Cleaning steps used to remove specific Ba-bearing phases.	44
Table 4.2 Ba in various species of planktonic foraminifera.	48
Table 4.3 Mean Ba/Ca for certain planktonic foraminifera.	53
Table 4.4 Calculation of planktonic foraminiferal Ba distribution coefficients.	57
Table 4.5 Planktonic Ba from core EN120-GGC1.	64
Table 5.1 Ba/Ca in benthic foraminifera from Recent core tops.	79
Table 6.1 Ba/Ca in benthic foraminifera from LGM core sections.	86
Table 6.2a Ba/Ca in benthic foraminifera from CHN82 Sta31 Core11PC.	91
Table 6.2b Ba/Ca in benthic foraminifera from CHN82 Sta41 Core15PC.	92
Table 6.3 Ba/Ca in benthic foraminifera from KNR64 Sta5 Core5PG.	97
Table 6.4 Ba/Ca in benthic foraminifera from core TR163-31B.	100
Table 7.1 Ba/Ca in benthic foraminifera from CHN82 Sta24 Core4PC.	139
Table 7.2 Spectral coherence of ETP and measured parameters with benthic Ba in CHN82 Sta24 Core4PC.	152

Chapter 1: Introduction

1.1 General Introduction

Determination of the distribution of oceanic nutrients such as P and Si in ancient water masses is a key to characterizing temporal change in the ocean-climate system. Climate, atmospheric composition and biological productivity all can be linked to nutrient distributions. Changes in the patterns of nutrient distributions in the deep ocean can reveal shifts in thermohaline circulation, while variation in surface water nutrients provides clues to changes in shallow wind-driven circulation and the origin of source waters. Precise measurement of nutrients in seawater is a relatively routine procedure, but gathering paleo-nutrient distributions is not simple. Such distributions must be recovered from records preserved in marine sediments. Biogenic components that accumulate in sediments are precipitated in seawater, so they are the most promising phases for this objective; however, as far as is known these components do not directly record the nutrient content of the waters in which they grew.

The distribution of trace metals in sea water reveals that many of these metals imitate the oceanic behavior of nutrients (Bruland, 1983). Characterization of the distribution of such metals in past oceans therefore provides a proxy for nutrients in past oceans. Since many trace metals are known to occur in biogenic phases, an indirect method of nutrient determination is possible. For example, the trace metal Cd imitates the oceanic behavior of the labile nutrient PO_4 in the present oceans (Boyle, 1976). Boyle (1988) has shown that the Cd content of the calcite shells of benthic foraminifera can be used to reconstruct the distribution of PO_4 in the Quaternary oceans; Shen *et al.* (1987) has shown that the Cd content of the aragonitic skeleton of massive corals can be used to reconstruct Cd in surface waters. As a result of their work

it is now possible to characterize the distribution of labile nutrients in past water masses.

No means has existed to reconstruct the distribution of the refractory nutrients, silica and alkalinity, in ancient oceans. These dissolved components are regenerated deep in the water column and/or in the sediments from the slowly dissolving phases opal, aragonite and calcite. Knowledge of the distribution of both labile and refractory nutrients in past water masses would be a significant step towards better understanding of temporal change in oceanic chemistry and circulation. Parameters such as partial pressure of CO_2 in oceanic waters or saturation with respect to CaCO_3 are a direct function of the ratio of alkalinity (refractory) to ΣCO_2 (labile). Thermohaline circulation of the oceans is reflected differently by the labile nutrients (shallow regeneration) and the refractory nutrients (deep regeneration). Since the oceanic behavior of the trace element barium is similar to the refractory nutrients, the distribution of Ba in the paleo-oceans can provide an indirect means of reconstructing the distribution of this nutrient class.

1.2 Barium in the ocean

The marine geochemistry of Ba has been a subject of interest since the early 1960's (Bacon and Edmond, 1972; Bender *et al.*, 1972; Bishop, 1988; Chan *et al.*, 1977; Chan *et al.*, 1976; Chow and Goldberg, 1960; Church and Wolgemuth, 1972; Dehairs *et al.*, 1980; Turekian and Johnson, 1966; Wolgemuth, 1970; Wolgemuth and Broecker, 1970). This interest arose principally out of the notion that Ba would prove to be a useful tracer of both chemical processes in the ocean and of physical circulation (Chan *et al.*, 1977). The distribution of dissolved Ba in the oceans was mapped in detail as part of the GEOSECS program, mainly out of the desire to use Ba as a stable chemical

analogue of ^{226}Ra . Although Ra/Ba proved limited as an oceanic tracer, the high precision Ba measurements from GEOSECS make Ba the most extensively characterized trace element in the oceans (Bruland, 1983).

Ba is removed from surface waters via biological activity, apparently by precipitation of barite (BaSO_4) in decaying marine particulate matter (Bishop, 1988; Chan *et al.*, 1977; Chow and Goldberg, 1960; Dehairs *et al.*, 1980). The barite in the sinking particulates dissolves deep in the water column and/or in the sediments, creating deep water maxima through-out the world's oceans (Chan *et al.*, 1977). The overprint of thermohaline circulation on this cycle of uptake and regeneration results in fractionation of Ba between the major ocean basins, with enriched values in the older deep waters of the Pacific and Indian oceans contrasting with depleted values in more recently ventilated deep Atlantic waters. Figure 1.1 shows GEOSECS profiles from the North Atlantic and North Pacific to illustrate this fractionation and compare Ba profiles to the nutrients P and Si .

Ba has unique properties which make it an appropriate candidate as a new paleo-tracer. Ba is constrained by different boundary conditions than labile nutrients, since it is principally regenerated at the bottom of oceanic basins. Ba is also less bio-active than Cd , as evidenced by its surface water depletion of no more than a factor of 5, compared to Cd depletions of nearly 3 orders of magnitude. This difference is especially important in coral studies, because Cd and Ba have very different depth gradients in the upper thermocline. Finally, the oceanic input of Ba is dominated by the high Ba content of rivers; as a result, marginal basins like the Mediterranean have enriched Ba contents and a distinct Ba signature that can be used as a tracer of temporal change in the input of Mediterranean water to the Atlantic.

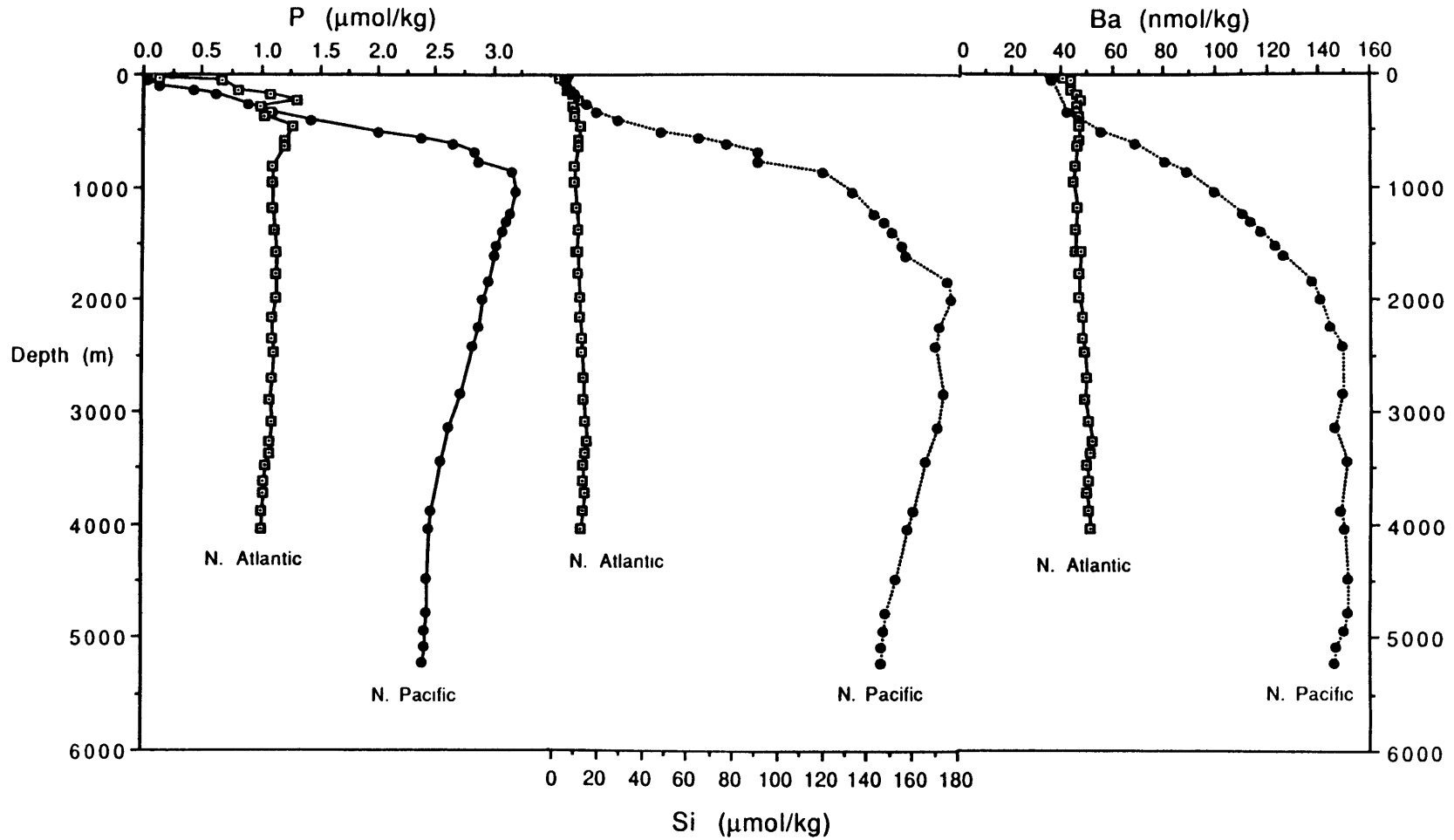


Figure 1.1 Phosphate, silica and barium profiles from GEOSECS stations in the North Atlantic (St. 3: 54°5'N, 42°57'W) and North Pacific (St. 204: 31°22'N, 150°2'W). Data from Bainbridge *et al.*, 1981, Broecker *et al.*, 1982 and Ostlund *et al.*, 1987.

1.3 Records of Barium in ancient oceans

The best candidates for continuous historical oceanic records of dissolved Ba are massive coral reefs and the biogenic components of marine sediments. Each has its advantages: the corals can record high resolution (<1 year), continuous records of surface water chemistry, but long continuous records (>1000 years) are generally not available. Marine sediments, on the other hand, contain continuous long records (>100 kyr) of both surface and deep water chemistry but at the price of low resolution (>1 kyr).

Analysis of corals is the optimal way to recover recent historical records of dissolved Ba. Ba is a large ion which fits well into the open structure of coralline aragonitic CaCO₃. Corals, which are not buried in sediments, have fewer cleaning artifacts. Large samples (>10 mg) are easily obtainable.

Recovering Ba records from marine sediments is more complicated. Among the biogenic components the most ubiquitous are the calcite remains of planktonic and benthic foraminifera. Since foraminifera live in both surface and bottom waters, they are ideal for mapping a complete distribution of a tracer in both vertical and horizontal space. Their small size (<0.1 mg), however, makes measurement difficult and contamination a greater hazard.

Foraminifera have been used to record temporal change in the isotopic content of seawater since the mid-1950's, but successful attempts to recover trace element records from foraminifera have only been undertaken since the early 1980's (Boyle, 1981; Boyle and Keigwin, 1982). Cleaning of trace element rich residual sedimentary coatings and phases from foraminifera shells ranks as the principal obstacle in foraminiferal paleochemistry (Boyle, 1981). This problem is unique for each element studied, and so far has only been solved for foraminiferal Cd (Boyle, 1988; Boyle *et al.*, 1981; Boyle and Keigwin, 1982; Boyle and Keigwin, 1985). Boyle (1981) measured Ba in the shells of a

planktonic foraminifera, but the large scatter and range in the values suggested at that time that cleaning artifacts dominated any paleoceanographic signal.

1.4 Content of the thesis

Chapter 2 describes the final analytical and cleaning methods used in the determination of Ba/Ca ratios in both corals and foraminifera. Chapter 3 documents high resolution records of Ba/Ca in a Galapagos coral, which reflect temporal variations in Equatorial Pacific upwelling. Chapter 4 includes the development and application of cleaning methods to planktonic foraminifera as well as a survey of the Ba content of various species of foraminifera. Chapter 5 demonstrates that Ba/Ca ratios in core-top benthic foraminifera reflect bottom water Ba. Chapter 6 discusses reconstruction of Ba in the glacial oceans and the implications of these distributions to oceanic change. Chapter 7 presents a 212 kyr record of Ba in the deep North Atlantic, including spectral analysis of the Ba time series. Chapter 8 summarizes the general conclusions of the thesis. Appendix 1 lists analyses of Ba in Mediterranean seawater; the "blueprints" of the model developed in Chapter 6 appear in Appendix 2.

References--Chapter 1

- Bacon, M. P. and Edmond, J. M. (1972) Barium at GEOSECS III in the Southwest Pacific. *Earth Planet. Sci. Lett.* **16**, 66-74.
- Bainbridge, A. E. (1981) *GEOSECS Atlantic Expedition, Vol.1, Hydrographic Data*. National Science Foundation, Washington, DC, 121p.
- Bender, M., Snead, T., Chan, L. H., Bacon, M. P. and Edmond, J. M. (1972) Barium intercalibration at GEOSECS I and III. *Earth Planet. Sci. Lett.* **16**, 81-83.
- Bishop, J. K. B. (1988) The barite-opal-organic carbon association in oceanic particulate matter. *Nature* **332**, 341-343.
- Boyle, E. A. (1976) On the marine geochemistry of cadmium. *Nature* **263**, 42-44.
- Boyle, E. A. (1981) Cadmium, zinc, copper, and barium in foraminifera tests. *Earth Planet. Sci. Lett.* **53**, 11-35.
- Boyle, E. A. (1988) Cadmium: chemical tracer of deepwater paleoceanography. *Paleoceanography* **3**, 471-489.
- Boyle, E. A., Husted, S. S. and Jones, S. P. (1981) On the distribution of copper, nickel and cadmium in the surface waters of the North Atlantic and North Pacific Ocean. *J. Geophys. Res.* **86**, 8048-8066.
- Boyle, E. A. and Keigwin, L. D. (1982) Deep circulation of the North Atlantic over the last 200,000 years: Geochemical evidence. *Science* **218**, 784-787.
- Boyle, E. A. and Keigwin, L. D. (1985) Comparison of Atlantic and Pacific paleochemical records for the last 215,000 years: changes in deep ocean circulation and chemical inventories. *Earth planet Sci. Lett.* **76**, 135-150.
- Broecker, W. S., Spence, D. W. and Craig, H. (1982) *GEOSECS Pacific Expedition Vol. 3, Hydrographic Data*. NSF, Washington, D.C.,
- Bruland, K. W. (1983) Trace elements in sea-water. In *Chemical Oceanography, Vol. 8* (ed. J. P. Riley and R. Chester), pp. 157-220, Academic Press, London.
- Chan, L. H., Drummond, D., Edmond, J. M. and Grant, B. (1977) On the barium data from the Atlantic GEOSECS Expedition. *Deep-Sea Res.* **24**, 613-649.
- Chan, L. H., Edmond, J. M., Stallard, R. F., Broecker, W. S., Chung, Y. C., Weiss, R. F. and Ku, T. L. (1976) Radium and barium at GEOSECS stations in the Atlantic and Pacific. *Earth Planet. Sci. Lett.* **32**, 258-267.
- Chow, T. J. and Goldberg, E. D. (1960) On the marine geochemistry of barium. *Geochim. Cosmochim. Acta.* **20**, 192-198.

Church, T. M. and Wolgemuth, K. (1972) Marine barite saturation. *Earth Planet. Sci. Lett.* **15**, 35-44.

Dehairs, F., Chesselet, R. and Jedwab, J. (1980) Discrete suspended particles of barite and the barium cycle in the open ocean. *Earth Planet. Sci. Lett.* **49**, 528-550.

Ostlund, H. G., Craig, H., Broecker, W. S. and Spencer, D. W. (1987) *GEOSECS Atlantic, Pacific, and Indian Ocean Expeditions, Vol. 7, Shorebased Data and Graphics*. National Science Foundation, Washington, DC, 200p.

Shen, G. T., Boyle, E. A. and Lea, D. W. (1987) Cadmium in corals as a tracer of historical upwelling and industrial fallout. *Nature* **328**(6133), 794-796.

Turekian, K. K. and Johnson, D. G. (1966) The barium distribution in sea water. *Geochim. et Cosmochim. Acta.* **30**, 1153-1174.

Wolgemuth, K. (1970) Barium analyses from the first Geosecs test cruise. *J. Geophysic. Res.* **75**, 7686-7687.

Wolgemuth, K. and Broecker, W. S. (1970) Barium in sea water. *Earth Planet. Sci. Lett.* **8**, 372.

Chapter 2: Methods

2.1 Introduction

This chapter details the analytical methods used in this work. Development of the barite cleaning step for planktonic foraminifera is documented in Chapter 4. Chapter 4 also describes the Ta-GFAAS Ba method used for planktonic-Ba determinations, since replaced by the ICP-MS isotope dilution method discussed below.

2.2 Purification of benthic foraminifera shells for Ba/Ca analysis

Ba can reside in a number of extraneous phases associated with shells: detrital grains, fine-grained CaCO_3 , organic matter, Mn and Fe oxides, and barite (BaSO_4). Purification of benthic foraminifera shells presents less of an obstacle than that required for the shells of planktonic foraminifera (Chapter 4). Benthic shells contain on average 3-7 times more lattice-bound Ba than planktonic shells (Lea and Boyle, 1989; Chapter 5, this work), reducing the ratio of spurious sedimentary Ba to lattice-bound Ba. In addition, benthic foraminifera have less surface area, diminishing the incidence of contamination resulting from surface-bound phases.

Initial cleaning follows methods developed for foraminiferal Cd (Boyle, 1981; Boyle and Keigwin, 1985); the detrital grains and fine grained material are removed by physical agitation in distilled water and methanol, the organic matter by oxidation in hydrogen peroxide-sodium hydroxide, and ferromanganese oxide coatings by reduction in hydrazine-ammonium citrate. The technique of barite dissolution developed for planktonic shells is applied to benthic shells. The strategy is to clean all samples with the full set of cleaning measures rather than try to predict which samples require extra cleaning. Use

of the alkaline-diethylene-triaminepentaacetic acid (DTPA) reagent on the smaller samples typical for benthic foraminifera requires extreme care since calcite dissolves very rapidly in the cleaning reagent. 50 μl of ~ 0.1 M DTPA is used for samples greater than 0.5 mg before cleaning, and 25 μl of ~ 0.1 M DTPA is used for smaller samples. Sample vials are placed in boiling water for 5 minutes; during the cleaning time vials are ultrasonicated and turned over every minute. Immediately after the 5 minutes of treatment 3 to 5 rinses of full strength ammonium hydroxide are applied to rapidly remove the alkaline-DTPA. 3 to 5 water rinses follow to remove the ammonium hydroxide.

Comparisons of benthic foraminifera samples cleaned with and without the alkaline-DTPA step reveal that a barite dissolution step does make a significant difference for many samples. The first comparison was made on samples of *Uvigerina spp.* from Equatorial Pacific core TR163-31B (water depth = 3210 m). One set of samples was cleaned for Cd assay (Boyle, 1988), which does not include the barite dissolution step. The second set of samples originate from a re-sampling of the core and were cleaned with the addition of the barite dissolution step. Fig. 2.1 shows the results obtained for this cleaning comparison over the top 100 cm of the core, corresponding to the last 15 kyr. Fig. 2.2 is an x-y plot of the same data; since the results are from two different samplings of the core, analyses within less than 2 cm depth interval were paired. The data demonstrate that Ba can be significantly higher in the samples not subjected to the alkaline-DTPA barite dissolution step. This core underlies the equatorial high productivity belt and has a total Ba content of greater than 0.1% in the sediment (T. Pedersen, unpublished data), suggesting that barite is present in significant amounts (Church, 1979).

Results for a comparison of core-top benthic foraminifera cleaned with and without the barite dissolution step are plotted in Fig. 2.3. Many samples not

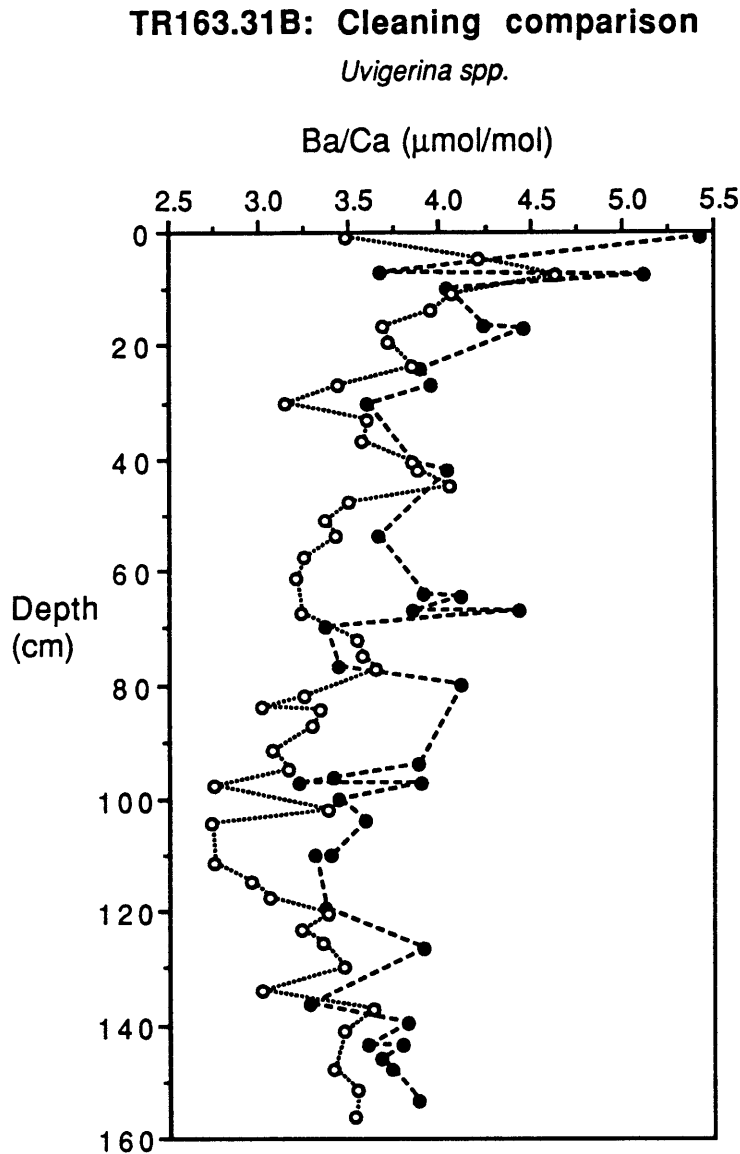


Figure 2.1 *Uvigerina spp.* Ba/Ca plotted as a function of depth in core TR163-31B. Two sets of samples are plotted: the first set is cleaned without the DTPA treatment (closed circles-dashed line), the second with the DTPA treatment (open circles-dotted line).

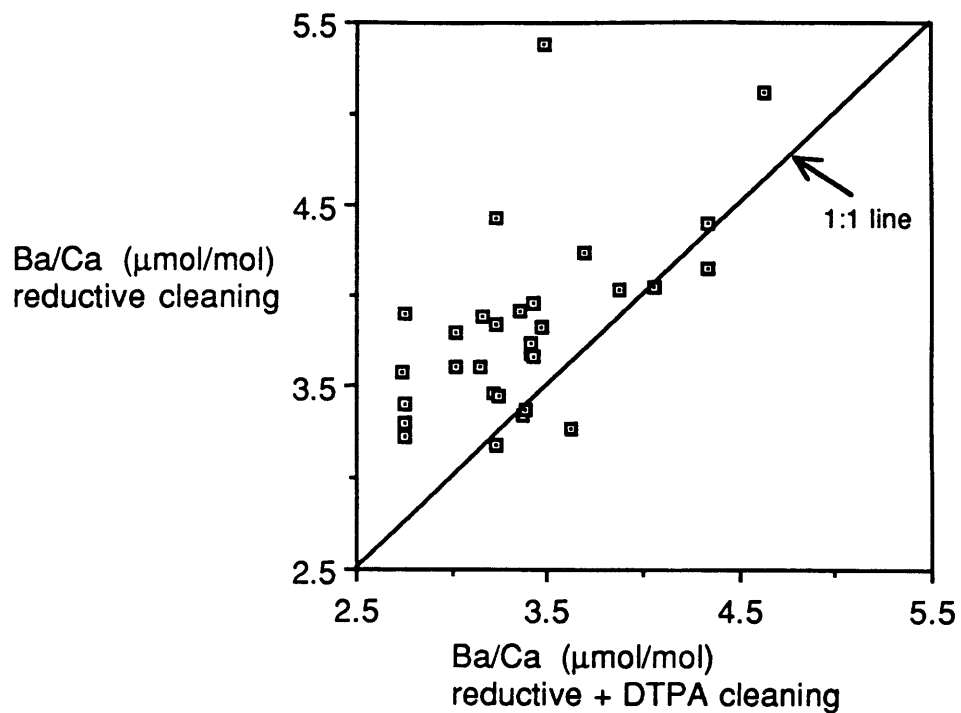


Figure 2.2 Plot of paired TR163-31B *Uvigerina* Ba/Ca for samples cleaned with and without the alkaline-DTPA treatment. Samples that fall above the 1:1 line had higher Ba/Ca when the DTPA step was omitted.

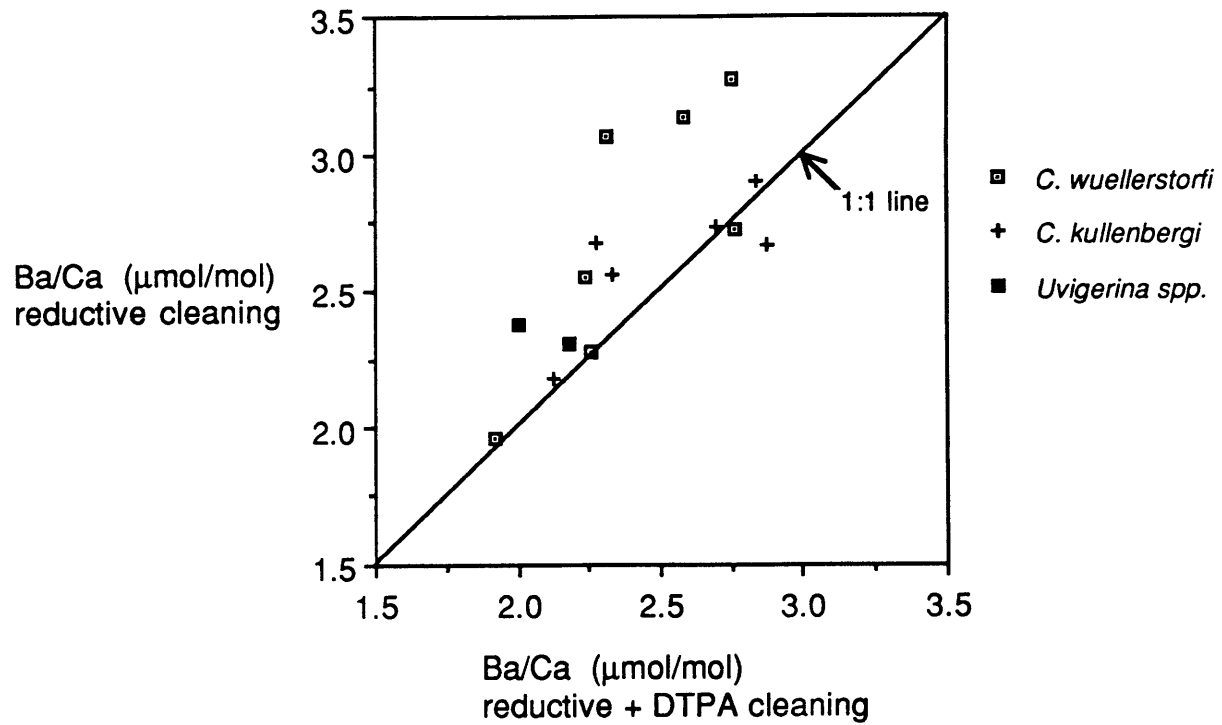


Figure 2.3 Plot of paired Atlantic core-top benthic foraminiferal Ba/Ca for samples cleaned with and without the alkaline-DTPA treatment. Samples that fall above the 1:1 line had higher Ba/Ca when the DTPA step was omitted.

subject to the barite dissolution step have higher Ba, although for some samples the addition of the barite dissolution step does not make a significant difference. Variability in barite content from core to core presumably causes variation in the degree of difference the alkaline-DTPA step makes. This result validates the general strategy of cleaning **all** samples with all steps, because there is no simple way to predict what degree of cleaning is required. The major drawback to this strategy is that harsher cleaning increases sample size requirement.

One uncertainty in the cleaning procedure is that alkaline-DTPA solution, because it has an affinity for both Ba and Ca (Ringbom, 1963), dissolves both barite and calcite. Therefore lower values found for samples treated with this procedure could result from removal of calcite layers containing higher Ba/Ca ratios. Evidence drawn from acid leaches and partial acid dissolutions of foraminifera samples suggests that this is not the case. However, a cleaning agent that attacks barite exclusive of calcite would be preferable, and it would also reduce the sample size requirement.

Further assessment of the cleaning method was accomplished by performing a series of partial dissolutions on large samples of benthic shells. These partial dissolutions can also reveal heterogeneities in the distribution of Ba in the calcite shells. Samples were picked from depth intervals where a single species was relatively abundant; these included *C. wuellerstorfi* from the Norwegian Sea (V27-60), *Uvigerina spp.* from the North-West Atlantic (CHN82-11PC), and *Oridisalis spp.* from the Equatorial Pacific (TR163-31B). Initial sample weights were 2 to 4 mg. Samples were cleaned with the standard procedure. After the final cleaning step, 100 μ L aliquots of 0.072N HNO₃ were added to the sample and the samples were ultrasonicated for about 30-60 seconds. This was sufficient time for dissolution to take place but a short

enough time that pH remained acidic (≤ 2.5). 100 μL was removed and transferred to a new vial. This procedure was repeated 2 to 4 times, depending on the size of the sample. The Ba and Ca contents were determined on the leachates. In Figure 2.4 the Ba/Ca ratio of each dissolution fraction is plotted versus per cent sample dissolved, calculated from the Ca content of each leachate. The data show relatively uniform values, the variability only slightly exceeding analytical reproducibility. The fractions within each dissolution experiment were reproducible to about 5% (1 SD) compared to analytical reproducibility of 3% for consistency standards (see below). This difference might indicate some limit to foraminifera as recorders of seawater Ba, or alternatively it might reflect heterogeneity among the shells that were used for the partial dissolution. This 5% error is one measure of the inherent variability of a sample pick from a given depth interval in a core.

2.3 Analysis of benthic foraminiferal Ba/Ca ratios

Upon completion of the barite dissolution step, samples are transferred to acid-leached 0.5 mL centrifuge vials and then subjected to a series of final acid leaches (1-5x) in 0.001N HNO_3 to remove any remaining surface contamination. These acid leaches also make the sample size more uniform since larger samples can be leached several times. The acid is removed via several water rinses, and a pipet is used to remove the last portion of water. At this stage each vial consists of the purified shell material and about 5 μL of distilled Ba-free water. Each sample is dissolved in 100 μl of 0.072N HNO_3 , with dissolution encouraged by ultrasonication. Samples are checked visually for complete dissolution, and extra acid is added where needed. A tiny portion (1-2 μL) of each sample is used to check for pH on 0-2.5 pH paper. This serves two purposes: First, it insures complete dissolution of the samples since

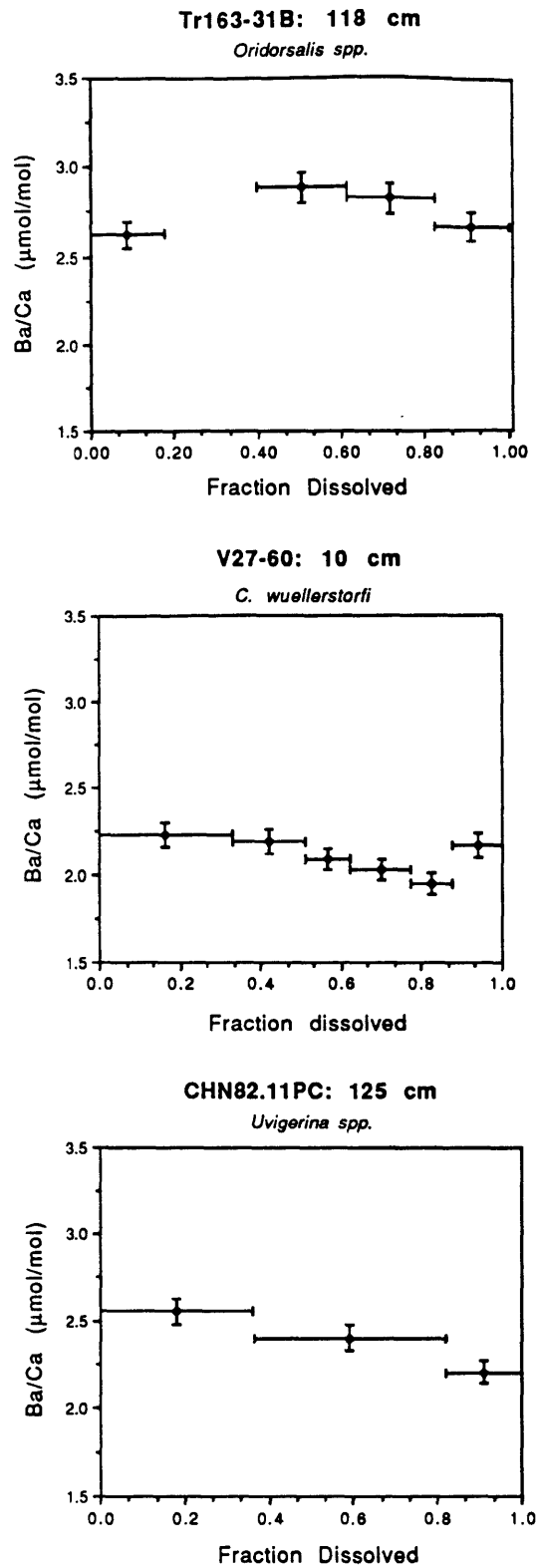


Figure 2.4 Partial dissolutions of three species of benthic foraminifera. The second leachate from TR163-31B experiment was lost. See text for explanation.

undissolved calcite will buffer the pH to high values; and finally, by titrating all samples to a narrow pH range uniform calcium concentrations are ensured. For example, since all samples are dissolved in 72 mequiv/L acid, a final Ca concentration of 11 mmol/l is achieved if the pH of the samples is titrated to 1.3. A pH of 1.3 is equivalent to an acid concentration of 50 mequiv/l, which means 22 mequiv/l of acid have been consumed by reaction with 11 mmol/l or 22 mequiv/l of calcite.

After dissolution 100 μL of each sample is transferred to an acid leached, dry vial. Samples are spiked with 1 or 2 100 μL aliquots of ^{135}Ba enriched spike for determination of total Ba by isotope dilution mass spectrometry (Table 2.1). The ratio of spike to sample chosen depends on the analyst's judgement of the sample size and the expected Ba/Ca ratio. Those samples that require only 100 μl of spike solution get an additional 100 μL of 0.072N HNO_3 acid, so that all samples have a final volume of 300 μl . Generally larger samples (which are titrated to uniform Ca concentration) receive 1 spike aliquot for Atlantic samples and 2 spike aliquots for Pacific samples. Small samples always received 1 spike aliquot. Using this method one can routinely achieve $^{135}\text{Ba}/^{138}\text{Ba}$ ratios within a factor of 2 of the target ratio, which is 1.55 (Table 2.1).

At this stage one-fourth of the sample (75 μL) is removed for Ca analysis. This 75 μL is diluted with 5 mLs of La solution (0.4 ppt La in a solution of 0.05N HCL and 0.002N HNO_3) to eliminate suppression of the Ca signal due to phosphine in the acetylene. These solutions are then quantified for Ca by comparison to standards on a Perkin-Elmer 403 flame atomic absorption spectrophotometer.

The remaining 225 μL is used for quantification of Ba. A 200 μl flow injection loop is used to inject the sample into a 0.85 mL/min eluant flow (also

	<u>135/138</u>
Spike S-6-STK (6th GEOSECS Spike, Nov. 1976): 93.6% ¹³⁵ Ba:	26.29
Natural Ba: 0.06592% ¹³⁵ Ba	0.09194
Target ratio (geometric mean of spike and natural ratio):	1.55

Table 2.1 Ba isotopic ratios of ¹³⁵Ba-enriched spike and natural Ba.

	CN2 Ba/Ca μmol/mol	CN2 Ba nM	CN2 Ca mM	CN3 Ba/Ca μmol/mol	CN3 Ba nM	CN3 Ca mM
Mean	2.36	28.86	12.24	3.12	58.28	18.68
SD (1 sigma)	0.07	0.75	0.21	0.08	1.30	0.29
SD in %	3.1	2.6	1.7	2.6	2.2	1.6
Number	89	96	98	96	104	98

Table 2.2 Concentrations and analytical precision of foram consistency standards CN2 and CN3. Concentrations were determined on 100 μL aliquots of each solution.

0.08N HNO₃). ¹³⁵/¹³⁸ ratios are determined on a VG inductively coupled plasma mass spectrometer. Each injection is scanned 440 times from mass 135 to 138 with a 100 μs dwell time on each of 512 channels (total scan time = 23 s). Optimal samples (about 10 nmol/L Ba) yield about 2500 total counts per peak for a relative error (one standard deviation) of 2% based on counting statistics. A typical blank yields 20 to 30 total counts, so a signal to noise ratio of greater than 100 is usual for most samples, with even the smallest samples achieving signal to noise ratios of better than 50. Samples with very low Ca contents (<1 mM Ca in the final 300 μl) are regarded as questionable and are always re-determined if sufficient foraminifera remain.

To ensure overall accuracy and reproducibility between runs the ¹³⁵Ba-enriched spike is repeatedly calibrated to a gravimetric standard. This eliminates the requirement for calibration of any isotope fractionation inherent in the plasma-quad system. This calibration is repeated at least 4 times per run to check for possible machine drift. The ¹³⁵/¹³⁸ ratio of these spiked gravimetric standards (SGS) are always reproducible to better than 1% over the course of a run. The gravimetric standard used for the calibration was made from reagent grade BaCl₂•2H₂O. Another standard was made from SPEX ultrapure assayed BaCO₃. The Ba concentration of these two standards was intercalibrated by the isotope dilution method; within a 0.5% analytical error there was no significant difference between the two standards.

The Ba concentration of each sample is calculated from the following formula:

$$[\text{Ba}]_{\text{sample}} = \frac{0.0356}{0.717} [\text{Ba}]_{\text{spike}} \left(\frac{\text{spike}}{\text{sample}} \right)_{\text{volume}} \left(\frac{R_{\text{mix}} - 26.29}{0.09194 - R_{\text{mix}}} \right)$$

where R_{mix} is the ratio found for the mixture of sample and spike, 0.0356 is the per cent ¹³⁵Ba in the spike (Oak Ridge value), 0.717 is the per cent ¹³⁸Ba in

natural Ba, 26.29 is the ratio of $^{135}/^{138}\text{Ba}$ in the spike (Oak Ridge value), and 0.09194 is the natural $^{135}/^{138}\text{Ba}$ ratio. This expression is evaluated for both the unknown sample and the known standard-spike mixture. The sample is then adjusted by the deviation of the calculated concentration of the standard from the true value. This correction is generally of order 1 to 2 % and has never been more than 3.5%.

Two consistency standards analyzed three times in each run are used as a final check on the precision of the method. These consistency standards were made by adding known amounts of Ba to ion-exchanged $\text{Ca}(\text{NO}_3)_2$ solutions. Ion exchange was used to remove Ba associated with the reagent grade calcite used to make up the $\text{Ca}(\text{NO}_3)_2$ solutions. The concentration and statistical reproducibility of these solutions is given in Table 2.2. The Ba/Ca ratio of CN2, the consistency standard with the lower Ba content, is reproducible to about 3% over more than 80 analyses.

The reproducibility of these consistency standards is a good measure of the ultimate precision of the method. However, the analytical precision of real samples might be less favorable. While the Ba content of consistency standards is always known and therefore spiked to an optimum $^{135}/^{138}$ ratio, there is uncertainty associated with choosing the correct spike amount for real samples. As mentioned previously, this uncertainty is reduced by keeping the Ca concentrations relatively uniform. To ascertain how much of a problem this might be Ba was determined in a solution spiked with different ratios of spike to solution to yield a range of $^{135}/^{138}$ ratios (Table 2.3). Sufficient counts were collected for counting statistic of about 0.5%. $^{135}/^{138}$ ratios of 0.7 to 4.8 encompasses the range of ratios obtained over 99% of the time for foraminifera samples. The Ba content was reproducible to 1.5%, with a slight trend towards higher Ba values at higher $^{135}/^{138}$ ratios. Over 90% of the samples analyzed

ID	Spk/Std Ratio	¹³⁵ CPS	¹³⁸ CPS	¹³⁵ / ¹³⁸ Ratio	{Ba} nM
1	0.39	2194	3281	0.67	203
2	0.77	3429	2836	1.21	206
3	1.55	6468	2900	2.23	206
4	1.55	6438	2908	2.21	208
5	2.32	5143	1601	3.21	203
6	3.10	11875	2965	4.01	209
7	3.48	12723	2873	4.43	208
8	3.87	12944	2713	4.77	211
mean					207 ±3

Table 2.3 Ba determination as a function of the ¹³⁵/¹³⁸Ba ratio of spiked solutions. 95% of the foram samples were spiked between a ratio of 0.8 and 3.1 Over this interval there is no significant dependence of measured Ba on the solution ratio.

Ca content mM	Ba added μM	Ba found μM	Deviation
0	2.00	1.99	-0.6%
1	2.02	2.01	-0.8%
2	2.04	2.01	-1.7%
3	2.06	2.04	-0.6%
4	2.08	2.06	-1.0%
5	2.10	2.08	-1.1%

Note: the actual Ba contents of aspirated solutions after dilution was 20-25 nM

Table 2.4 Ba determination in solutions of varying Ca concentration. Measured Ba shows no dependence on solution Ca content.

have 135/138 ratios between 0.7 and 3.2; over this range the Ba content of the solution in this experiment was reproducible to 1.1%. One can conclude that the error associated with the range of isotope ratios used in this study is small relative to the overall analytical precision.

To ascertain that variability in the Ca contents of the injected solutions has no effect on the isotope ratio, a series of solutions with similar Ba contents and differing Ca contents was made up (Table 2.4). There was no significant bias on the measured Ba content with differing Ca contents. The average deviation between measured Ba and expected Ba was about 1%.

A factor that will clearly degrade the reproducibility of real samples is reduced count totals for the smaller samples. The mean Ba content of all samples thru run BZ is 12 nM, 20% more Ba than is in CN2. About 8% of the samples have Ba contents less than one-quarter that of CN2; counting statistics would suggest that these smallest samples have precisions a factor of 2 poorer than CN2. Therefore a rough estimate of the reproducibility of the least favorable 8% of determinations is a relative error of 6% (1 standard deviation). Most of these small samples have Ca contents less than 3 mM and therefore are replicated if sufficient foraminifera remain.

Reproducibility of splits of benthic foraminifera from the same depth in a core are seldom as good as the analytical precision (Chapters 5-7). The pooled standard deviation of replicates was 7-10% for three cores for which many replicates were determined. The decrease in precision associated with real samples is presumably related to bioturbation which mixes together individuals that lived at different times when Ba contents might have been different (Boyle, 1984). However, some portion of this variability might be due to imperfect cleaning and/or imperfect nature of the foraminifera as chemical recorders of

bottom water Ba. For this reason no single data point on its own should be taken as conclusive.

2.4 Determination of Ba/Ca ratios in coral aragonite

The method for determination of Ba/Ca in the aragonite skeletons of corals is essentially the same as that employed for foraminifera. The cleaning procedure for corals is outlined in Shen and Boyle (1988); it does not include a barite dissolution step. Because corals are far more massive than foraminifera larger samples can be employed for analysis. Therefore, flow injection for Ba is not necessary, although it can be used for corals where sample is limited. For these coral samples flow injection is the preferred method since one achieves higher signal to noise ratios for the same number of total counts.

Corraline Ba is relatively uniform (see below and Chapter 3) and therefore coral solutions can be spiked quite easily to an optimum $^{135}/^{138}\text{Ba}$ ratio; for this study the ratio employed was generally between 0.9 and 1.5. Counting times and dilutions were adjusted to yield total counts > 10,000 for each Ba peak. For coral samples, where signal to noise on the ICP-MS is always greater than 100, the reproducibility of the ratios is very close to that expected from counting statistics. Therefore 10,000 total counts on each peak generally yields precisions on the ratios near 1% (1 relative standard deviation).

Typical Ba concentrations after spiking and dilution were between 15-45 nmoles/L, equivalent for corals to 3-10 mmol/L of Ca or 0.3-1 mg of coral aragonite per mL of solution. Typical volumes of solutions were 0.8-3 mL, with counting times of 1 to 3 minutes.

Reproducibility of coral Ba/Ca ratios based on replicates of the same coral solutions run on different days is about 2% (1 relative standard deviation). Replicates for a coral time series (1950-1960) from Punta Pitt in the Galapagos

Islands for which replicates were run over 5 separate runs are detailed in Table 2.5 and plotted with error bars in Figure 2.5. A more detailed coral record from 1965-1978 was obtained by analysis in a single day's run; consistency standards had a reproducibility of 1.0% for the Ba/Ca over the course of this run (see Chapter 3).

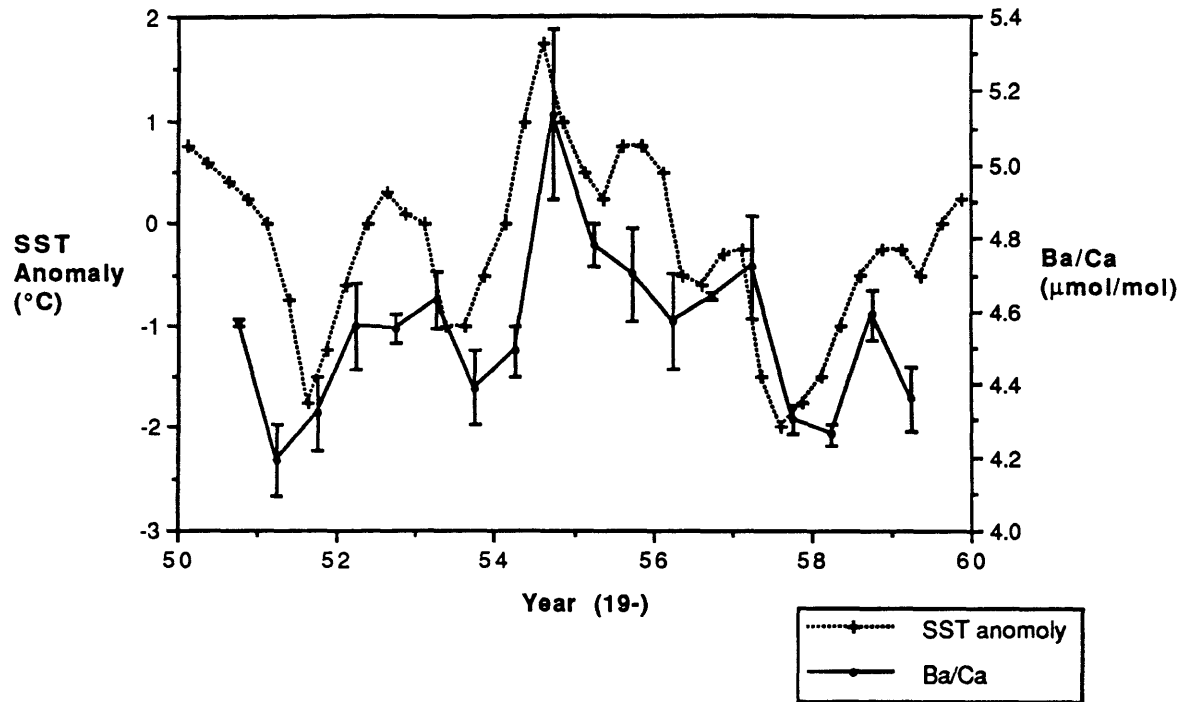


Figure 2.5 Plot of Ba/Ca determined on semi-annual bands of the coral *Pavona clavus* from Punta Pitt (San Christobal Island, Galapagos Islands) compared with sea surface temperature (SST) anomalies (E. Rasmusson, pers. comm.). See text and Chapter 3 for further explanation.

Coral Year-section	Date of Analysis (1988):						MEAN	Std Dev		n
	16-Mar	25-Mar	28-Apr	1-May	19-May	22-May				
1950-2	4.58	4.56			4.56		4.57	0.01	0.3%	3
1951-1	4.26	4.05					4.19	0.10	2.5%	4
1951-1			4.16		4.27					
1951-2	4.28	4.21			4.44	4.35	4.32	0.10	2.3%	4
1952-1	4.49	4.7				4.49	4.56	0.12	2.7%	3
1952-2	4.58	4.51			4.55		4.55	0.04	0.8%	3
1953-1	4.62	4.52			4.71	4.65	4.63	0.08	1.7%	4
1953-2			4.35	4.5		4.32	4.39	0.10	2.2%	3
1954-1				4.42		4.55	4.49	0.07	1.6%	2
1954-2	4.93	5.12					5.14	0.23	4.4%	3
1955-1			4.83	4.71		4.81	4.78	0.06	1.3%	3
1955-2		4.62	4.62				4.85	0.13	2.8%	3
1956-1			4.43	4.62		4.67	4.57	0.13	2.8%	3
1956-2			4.64		4.63		4.64	0.01	0.1%	3
1957-1	4.69		4.6			4.87	4.72	0.14	2.9%	3
1957-2			4.28			4.28	4.30	0.04	0.9%	3
1958-1	4.26	4.22					4.26	0.03	0.6%	4
1958-1			4.28		4.27					
1958-2	4.65		4.52	4.61			4.59	0.07	1.4%	3
1959-1			4.28		4.45		4.34	0.09	2.0%	3

Note 1: Two entries occur for 1951-1 and 1958-1 because 2 different coral pieces from the same band were analyzed.

Note 2: 1 value each from 54-1,55-2,57-2 and 59-1 was rejected due to a mixing problem for Ca.

Table 2.5 Ba/Ca averages for semi-annual coral bands from Punta Pitt, Galapagos Islands (1950-1959).

References--Chapter 2

Boyle, E. A. (1981) Cadmium, zinc, copper, and barium in foraminifera tests. *Earth Planet. Sci. Lett.* **53**, 11-35.

Boyle, E. A. (1984) Sampling statistic limitations on benthic foraminifera chemical and isotopic data. *Mar. Geol.* **58**, 213-224.

Boyle, E. A. and Keigwin, L. D. (1985) Comparison of Atlantic and Pacific paleochemical records for the last 215,000 years: changes in deep ocean circulation and chemical inventories. *Earth planet Sci. Lett.* **76**, 135-150.

Boyle, E. A. (1988) Cadmium: chemical tracer of deepwater paleoceanography. *Paleoceanography* **3**, 471-489.

Church, T. M. (1979) Marine Barite. In *Marine Minerals* (ed. R. G. Burns), pp. 175-209, Mineralogical Society of America, Washington, D.C.

Lea, D. and Boyle, E. (1989) Barium content of benthic foraminifera controlled by bottom water composition. *Nature* **338**, 751-753.

Ringbom, A. (1963) *Complexation in Analytical Chemistry*. Interscience Publishers, 361p.

Chapter 3: Coralline Ba reflects variations in equatorial Pacific upwelling

Lattice-bound cadmium in scleractinian corals has been shown to be a sensitive tracer of historical changes in the nutrient content of surface waters (Shen *et al.*, 1987; Shen and Sanford, in press). Barium also substitutes into the lattice of aragonite reef-building corals, because there is solid solution between orthorhombic BaCO_3 (witherite) and CaCO_3 (aragonite) (Speer, 1983). It is expected that the substitution should be proportional to the Ba content of seawater, which increases from low values in warm surface waters to higher values in cold deep waters. Here the first high resolution coralline Ba record spanning the period 1965 to 1978 from the Galapagos Islands is presented. Coralline Ba/Ca tracks historical sea surface temperatures, reflecting the vertical displacement of warm nutrient-poor surface waters by cold, nutrient-rich source waters. Differences between coralline Ba and Cd records may be due to preferential uptake of Cd by phytoplankton during times of lower surface nutrients.

A Ba/Ca record was recovered from a cored sample of the reef-building coral *Pavona clavus* collected at Punta Pitt on San Cristobal Island, Galapagos Islands (McConnaughey, 1989) (Fig. 3.1; Table 3.1). The coral was sampled at approximate 3-month increments over the period 1965-1978. Coral samples were cut into 4 divisions of a single year of growth; annual band widths averaged about 11 mm. Narrow high density bands were used as marker points for yearly increments. Corals were cleaned by a series of oxidizing and reducing steps designed for Pb and Cd assay (Shen and Boyle, 1988), elements which are considerably more prone to contamination than Ba. After dissolution in vycor-distilled 2N HNO_3 the samples were spiked with a known

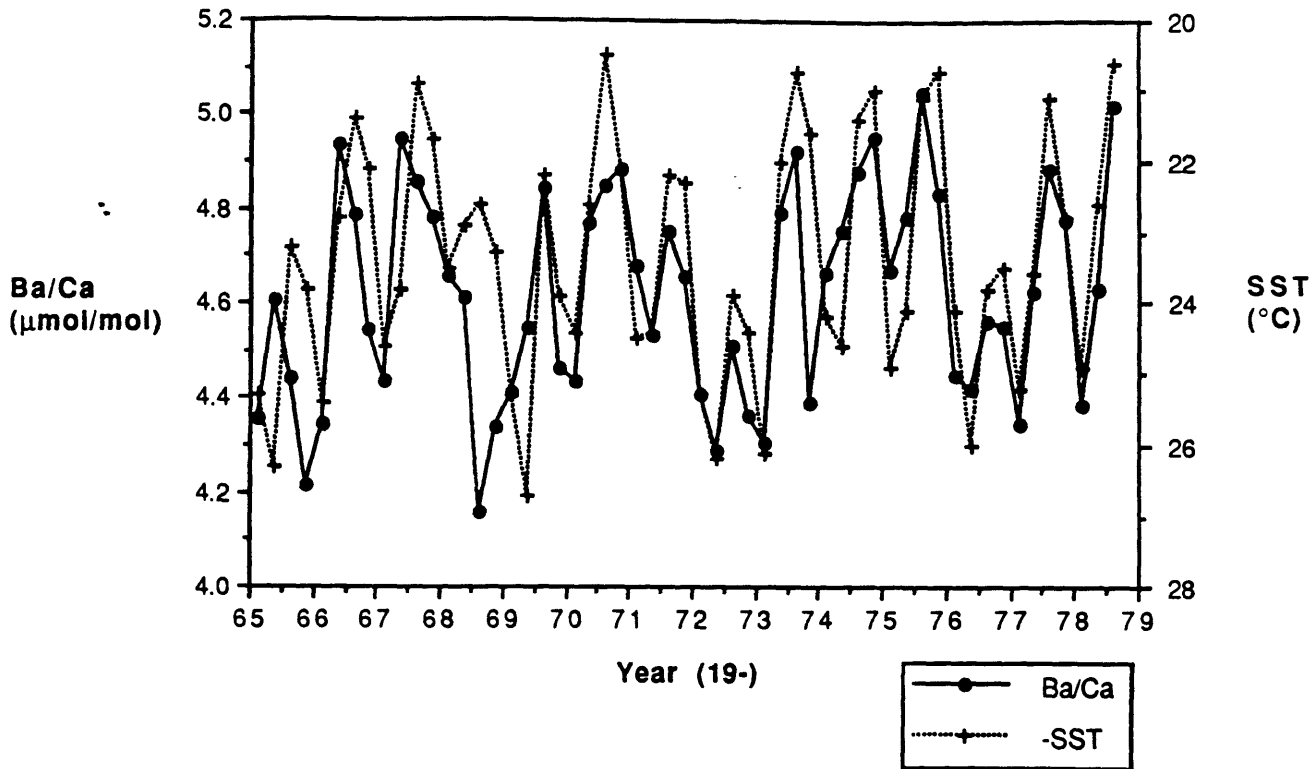


Figure 3.1 Ba/Ca measured in quarter-annual bands of the coral *P. clavus* (Punta Pitt, San Cristobal Is., Galapagos Is.) compared with sea surface temperature recorded at Academy Bay, Santa Cruz Island, Galapagos Is. (Charles Darwin Research Station, 1988) over the time period 1965-1978. Sea surface temperatures are averaged over 3 month intervals.

Year	Quarter	Ba/Ca ($\mu\text{mol/mol}$)	Sr/Ca (mmol/mol)
1965	1	4.36	9.33
	2	4.60	9.46
	3	4.44	9.42
	4	4.22	9.21
1966	1	4.34	9.34
	2	4.94	9.61
	3	4.79	9.52
	4	4.54	9.49
1967	1	4.44	9.52
	2	4.94	9.60
	3	4.85	9.65
	4	4.78	9.62
1968	1	4.66	9.61
	2	4.61	9.59
	3	4.16	9.24
	4	4.34	9.22
1969	1	4.41	9.44
	2	4.55	9.54
	3	4.84	9.54
	4	4.46	9.41
1970	1	4.43	9.26
	2	4.77	9.49
	3	4.85	9.70
	4	4.88	9.80
1971	1	4.68	9.55
	2	4.53	9.27
	3	4.75	9.63
	4	4.66	9.11
1972	1	4.41	9.13
	2	4.29	9.39
	3	4.51	9.44
	4	4.36	9.48
1973	1	4.31	9.44
	2	4.79	9.86
	3	4.92	9.74
	4	4.39	8.93
1974	1	4.66	9.57
	2	4.75	9.46
	3	4.88	9.64
	4	4.95	9.71
1975	1	4.67	9.55
	2	4.78	9.60
	3	5.05	9.84
	4	4.83	9.54
1976	1	4.45	9.55
	2	4.42	9.66
	3	4.56	9.48
	4	4.55	9.52
1977	1	4.34	9.56
	2	4.62	9.55
	3	4.89	9.75
	4	4.77	9.66
1978	1	4.39	9.32
	2	4.63	9.33
	3	5.02	9.35

Table 3.1 Ba/Ca and Sr/Ca values for the Punta Pitt section

quantity of ^{135}Ba for determination by isotope dilution. Measurement of the $^{135}\text{Ba}/^{138}\text{Ba}$ ratio was made on a VG PlasmaQuad inductively coupled plasma-mass spectrometer (ICP-MS). Accuracy was controlled by calibration of isotope dilution determinations relative to a gravimetric standard. The barium detection limit is 0.1 nmol/L; for coral samples signal to noise was always greater than 100:1. Typical sample size corresponded to 1 mg of dissolved coral. Ca was quantified by flame atomic absorption. Replicates of Ba/Ca ratios of individual coral samples were reproducible to 2% on different days; however, to optimize the internal precision of the data set the 1965 thru 1978 record was run on a single day. On that day, eight replicate determinations of 0.5 mL consistency standard containing 95.7 nmol/L Ba and 18.2 mmol/L Ca yielded a reproducibility (1 standard deviation) of 0.9% for Ba, 1.0% for Ca, and 1.0% for Ba/Ca over the course of this run. Samples for Sr were spiked with ^{87}Sr and concentrations determined by the isotope dilution measurement of the $^{87}\text{Sr}/^{88}\text{Sr}$ ratio on the ICPMS. Precision of the Sr/Ca ratios is about 1%.

The Ba/Ca ratio measured on the Galapagos coral ranges from 4.1 to 5.1 $\mu\text{mol}/\text{mol}$; this natural variation of 1 $\mu\text{mol}/\text{mol}$ is about 10 times greater than the inter-run precision of ± 0.1 $\mu\text{mol}/\text{mol}$ and 20 times greater than the within-run precision of ± 0.05 $\mu\text{mol}/\text{mol}$. Our values generally agree with recent determinations of Ba in corals (Buddemeier *et al.*, 1981; Ohde *et al.*, 1978; Shen, 1986; Shen and Sanford, in press). Some older studies give values up to 10 times higher than our values (Flor and Moore, 1977; Livingston and Thompson, 1971); this might be due to insufficient cleaning of these coral samples to remove residual non lattice-bound Ba such as that associated with organic tissues, which can contain several orders of magnitude more Ba than is present in the coral skeleton (Buddemeier *et al.*, 1981).

Variability in Ba values recorded by *Pavona clavus* at Punta Pitt in the Galapagos Islands results from changes in the intensity of upwelling of cold, nutrient-rich source waters to the surface ocean. Cold deep waters contain more Ba; shoaling of the thermocline in the Eastern Equatorial Pacific allows Ba-rich waters to mix into the surface layer. Upwelling variability is documented for the Eastern Equatorial Pacific in the form of historical sea surface temperature (SST) records (Rasmusson and Carpenter, 1982). A SST record is available from Academy Bay on Santa Cruz Island (Charles Darwin Research Station, 1988); although Academy Bay averages 1 to 2°C warmer than Punta Pitt during normal climatic conditions, records of temperature variability at the two sites are very similar (McConnaughey, 1989). Comparison of the Academy Bay SST record with our coral record of Ba/Ca indicates coherent variability between these two records (Fig. 3.1). Cold peaks in the temperature record line up with relative maxima in the Ba record, and warm peaks in the temperature record align with relative minima. The correspondence is not perfect; the largest discrepancies arise in the precise temporal location of the peaks (1965-66; 1968-1969; 1973-1974). These differences are primarily attributed to inability to sample the coral perfectly; sectioning of single year growth increments into 4 even sections does not guarantee that that section actually represents 3 months of growth. In addition, there is always some difficulty in assigning a single year of growth to a band width. These sectioning limitations will also affect the magnitude of the Ba peaks that are measured. Seasonal averaging of the signals truncates the extremities of the record. This bias is alleviated by comparing the Ba record to a SST record for which points are averaged over 3 months, but the aforementioned difficulties should be kept in mind when comparing the two records.

Relatively cool temperatures in the Eastern Equatorial Pacific are maintained in part by the entrainment of colder, upper thermocline waters which lie close to the base of a very shallow mixed layer (Wyrski, 1981). Depression of the usually shallow thermocline due to atmospheric forcing by the trade winds (Wyrski, 1975) causes large positive excursions in temperature which are classified as El Niño-Southern Oscillation (ENSO) events. Such events show up best on SST anomaly plots; Figure 3.2 compares SST anomalies with Ba anomalies. The El Niño events of 1965, 1969, 1972-73 and 1976 (Rasmusson, 1984) are accompanied by positive excursions in temperature and negative excursions in Ba/Ca. Depression of the thermocline during El Niño events reduces the entrainment of cold, Ba-rich waters, resulting in the coincidence of positive temperature anomalies and negative Ba/Ca anomalies.

Since both Cd and Ba are enriched in the upwelled cold source waters, they show a strong correspondence in the coral records (Fig. 3.3). However, because the Cd-depth gradient is much greater than the gradient for Ba, Cd is more sensitive to changes in the vertical restructuring of source waters: compare the 4-fold variation in Cd/Ca ratios to the 20% variation in Ba/Ca ratios. Another strong difference that emerges when comparing the records is that Ba appears to be more responsive to weak upwelling events (Fig. 3.3: 1969, 1971, 1972, 1977 and 1978). Fundamental differences in the oceanographic controls on Cd and Ba may account for this behavior. Cd is more bio-active than Ba in surface waters and hence stripped out more rapidly by biological activity. One can speculate that during periods of lower upwelling, Cd may be scavenged almost as fast as it is supplied; only during periods of more intense upwelling does supply exceed removal.

Conversion of the coral-Ba values to seawater Ba contents requires estimation of a distribution coefficient for Ba in coral

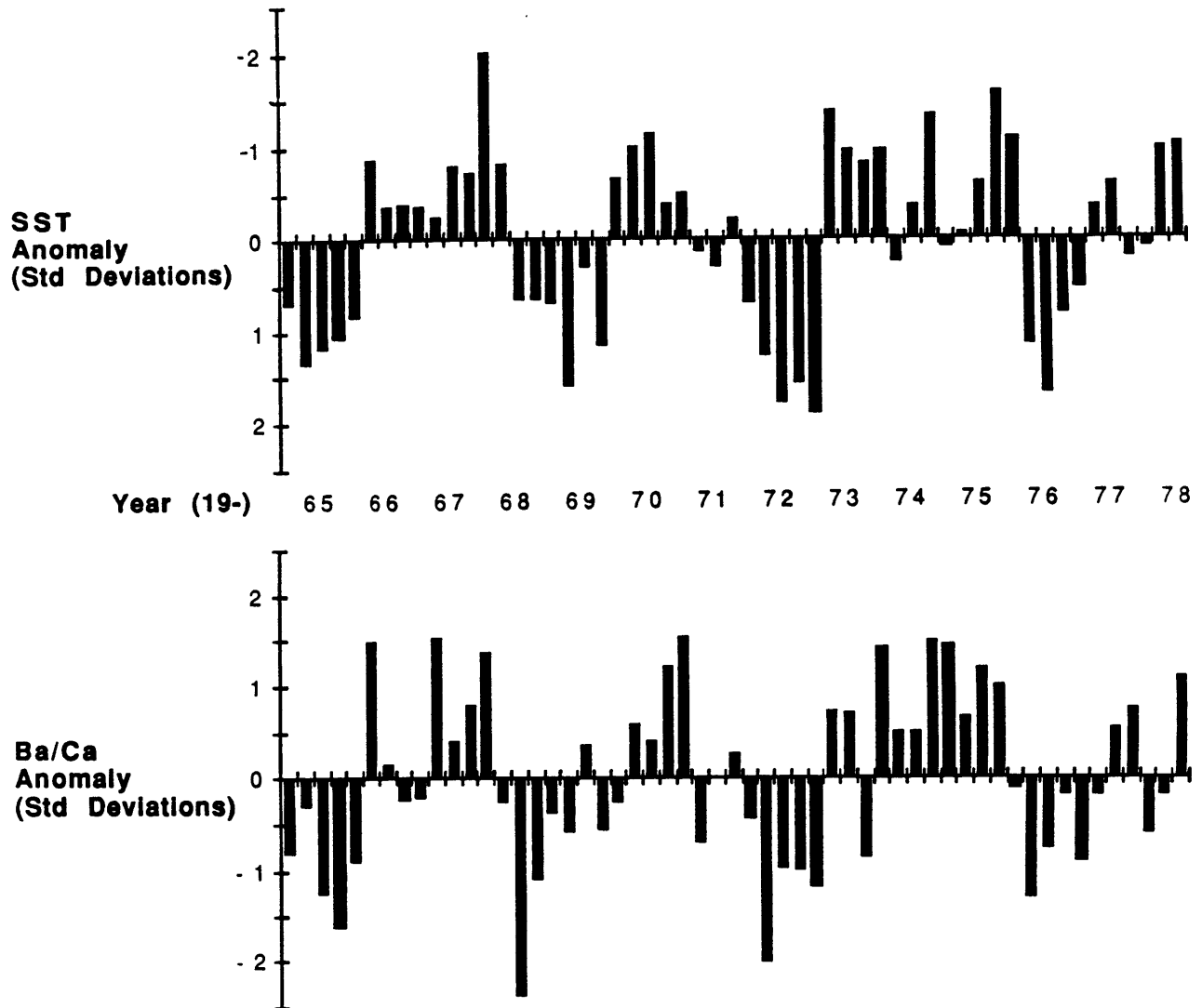


Figure 3.2 Quarterly anomalies of Ba/Ca in the Punta Pitt coral record compared with quarterly anomalies in sea surface temperature at Academy Bay over the time period 1965-1978. Anomalies were calculated by normalizing the difference from the mean for each quarter to the standard deviation of the mean for each quarter.

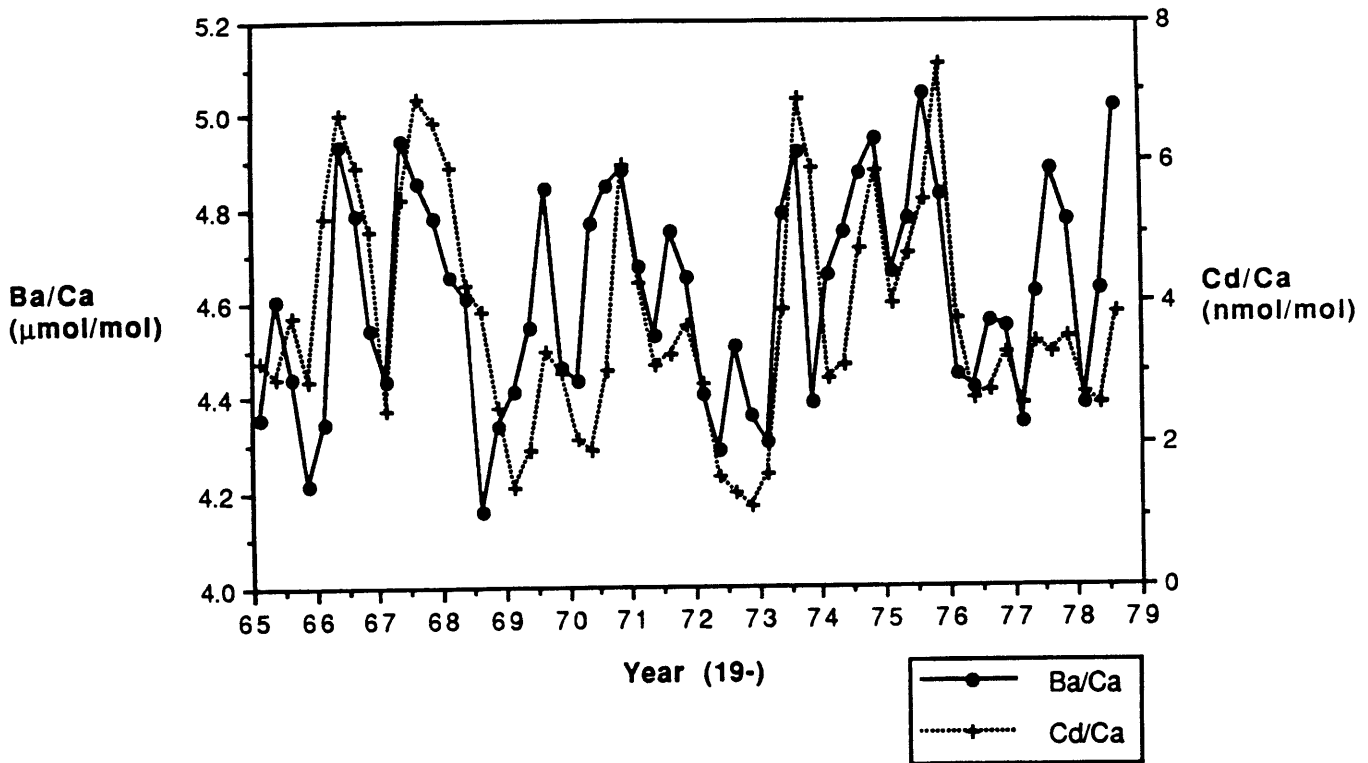


Figure 3.3. Comparison of Ba/Ca and Cd/Ca (Shen and Sanford, in press) in the Punta Pitt coral record over the time period 1965-1978.

($D_{Ba} = \{Ba/Ca\}_{coral} / \{Ba/Ca\}_{seawater}$). $D_{Ba} = 1.41 \pm 0.14$ based on the Punta Pitt Ba/Ca data and the Ba content of surface seawater at the nearest GEOSECS station (St. 331: 125°W, 5°S) (Ostlund *et al.*, 1987). A better determination of D_{coral} can be made for corals from areas where variability in surface Ba due to upwelling is minimal; therefore Ba/Ca ratios were measured in 2 species of coral collected from North Rock off Bermuda Island. Two samples of *Diploria labyrinthiformis* yield Ba/Ca = 5.21, and two samples of *Montastrea annularis* yield Ba/Ca = 5.32 ± 0.08 . The Bermuda coral measurements give $D_{Ba} = 1.27 \pm 0.03$, based on the Ba content of surface water at the nearest GEOSECS station (St. 29: 36°N, 47°W) (Ostlund *et al.*, 1987). Both estimates agree within error; a more precise determination of D cannot be done without simultaneous coral and seawater Ba determinations. In addition, there might be differences in D_{coral} for the various species, although our measurements of Ba/Ca ratios in the three species studied so far seem to rule out large differences. Corals take up several metals with a distribution coefficient near 1 (Shen, 1986; Shen and Sanford, in press). The calculated thermodynamic distribution coefficient for Ba in aragonite is 1.3 (Shen and Sanford, in press), so our values are in agreement with the thermodynamically predicted value.

Converting coralline Ba/Ca at the Punta Pitt site to seawater Ba values using $D_{Ba} = 1.3$ yields a range of 33 nmol/kg during the warmest quarters to 40 nmol/kg during the coolest quarters. The lower range is typical of values for nutrient depleted Pacific surface water (34 ± 1 nmol/kg) (Ostlund *et al.*, 1987); although a lack of data for Ba-depth gradients in Galapagos region makes an estimation difficult, the upper range can be reconciled with previous estimates of the maximum depth of source waters to the Eastern Equatorial Pacific, which are in the range 135 to 225 m (Bryden and Brady, 1985; Fine *et al.*, 1987; Ostlund *et al.*, 1987; Quay *et al.*, 1983).

A complication in calculating source water depths from coral Ba/Ca values is the possibility that coral uptake of Ba is influenced by temperature or biologically mediated factors. To test this hypothesis a record of chemically similar Sr was recovered for the Punta Pitt coral (Fig. 3.4; Table 3.1). In contrast to Ba, seawater Sr/Ca is essentially conservative in seawater, with a slight upper ocean depletion of about 1% (Brass and Turekian, 1974). Variation in coralline Sr has generally been ascribed to a temperature effect on incorporation, but taxonomy, metabolism and growth rate have also been cited as possible controlling factors (Smith *et al.*, 1979; Weber, 1973). Figure 3.4 indicates distinct similarities between the Sr/Ca and Ba/Ca records. While one cannot be sure that a temperature effect on incorporation is causing this covariance, the similarity between the two records suggests that some of the Ba signal is due to factors other than variations in the upwelling of source waters with different chemical signatures. The 17% average difference in Ba/Ca between warm and cold quarters is reduced to about 12% when the Ba signal is normalized to Sr rather than Ca, suggesting that up to 1/3rd of the Ba/Ca signal might be due to a temperature effect on incorporation. If incorporation of Sr and Ba in this coral is temperature-dependent, Ba/Sr ratios might be a better indicator of changes in the Ba concentration of surface waters.

In conclusion, Ba/Ca ratios can be a powerful tracer of historical variability in upwelling and entrainment of nutrient rich deep waters into the surface ocean. Comparison of Ba records with coral records of more bio-active metals like Cd can lead to insight into the relative behavior of the metals in the surface ocean. Finally, long coral records could be employed to reconstruct changes in upwelling of cold source waters to prehistoric oceans.

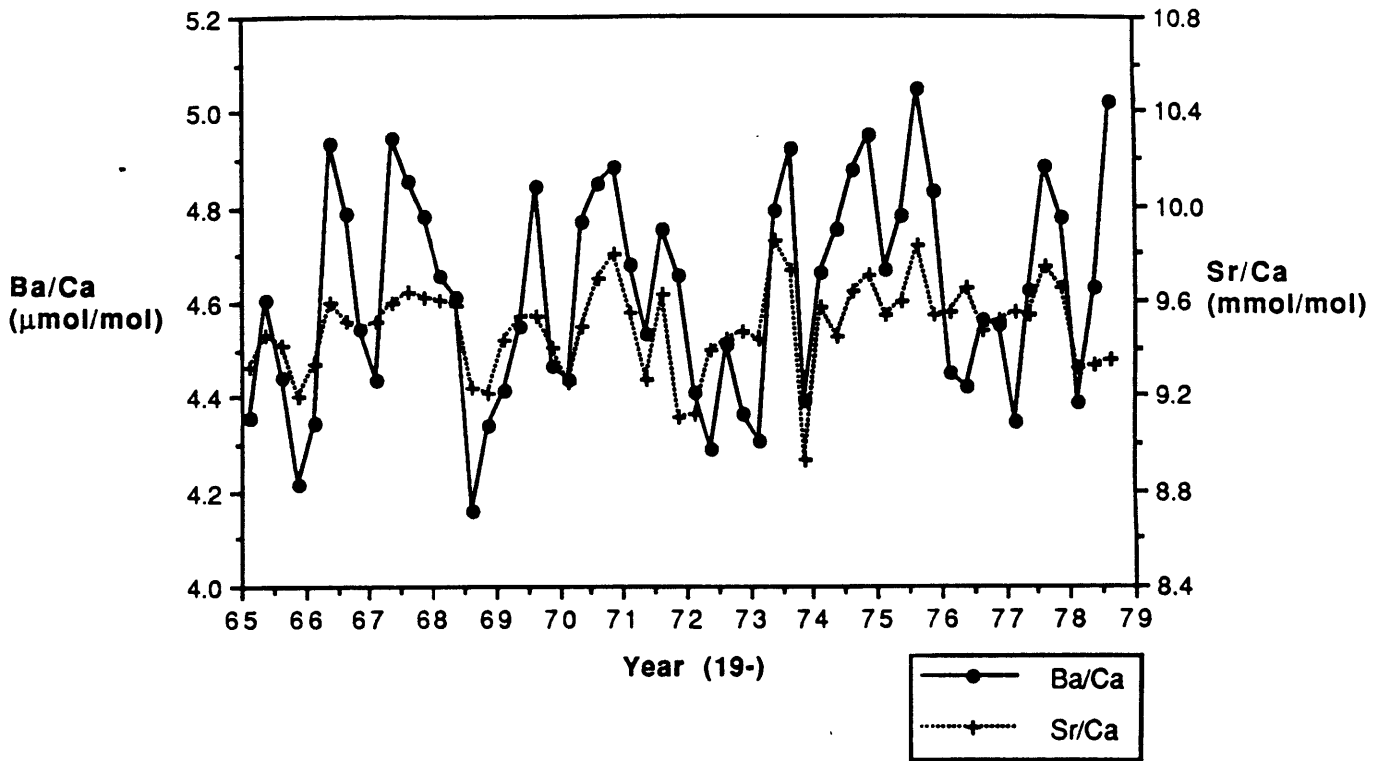


Figure 3.4 Comparison of Ba/Ca and Sr/Ca in the Punta Pitt coral record over the time period 1965-1978. The plot is scaled so that approximately the same amount of variance is shown for each ratio.

References--Chapter 3

- Brass, G. W. and Turekian, K. K. (1974) Strontium distribution in GEOSECS oceanic profiles. *Earth Planet. Sci. Lett.* **23**, 141-148.
- Bryden, H. L. and Brady, E. C. (1985) Diagnostic model of the three-dimensional circulation in the upper Equatorial Pacific Ocean. *J. Phys. Oceanogr.* **15**, 1255-1273.
- Buddemeier, R. W., Schneider, R. C. and Smith, S. V. (1981) The alkaline earth chemistry of corals. In *Proc. 4th Int. Coral Reef Symposium*, pp. 81-85, Manila.
- Fine, R. A., Peterson, W. H. and Ostlund, H. (1987) The penetration of Tritium into the Tropical Pacific. *J. Phys. Oceanogr.* **17**, 553-564.
- Flor, T. H. and Moore, W. S. (1977) Radium/Calcium and Uranium/Calcium determinations for Western Atlantic reef corals. In *Proc. 3rd Int. Coral Reef Symposium*, pp. 555-561, Miami.
- Livingston, H. D. and Thompson, G. (1971) Trace element concentrations in some modern corals. *Limnol. Oceanogr.* **16**, 786-796.
- McConnaughey, T. (1989) ^{13}C and ^{18}O isotopic disequilibrium in biological carbonates: I. Patterns. *Geochim. Cosmochim. Acta.* **53**, 151-162.
- Ohde, S., Ohta, N. and Tomura, K. (1978) Determination of trace elements in carbonates by instrumental neutron activation analysis. *J. Radioanal. Chem.* **42**, 159-167.
- Ostlund, H. G., Craig, H., Broecker, W. S. and Spencer, D. W. (1987) *GEOSECS Atlantic, Pacific, and Indian Ocean Expeditions, Shorebased Data and Graphics*. National Science Foundation, Washinton D.C., 200p.
- Quay, P. D., Stuiver, M. and Broecker, W. S. (1983) Upwelling rates for the equatorial Pacific Ocean derived from the bomb ^{14}C distribution. *J. Mar. Res.* **41**, 769-792.
- Rasmusson, E. M. (1984) El Niño: The ocean/atmosphere connection. *Oceanus.* **27**(2), 5-12.
- Rasmusson, E. M. and Carpenter, T. H. (1982) Variations in tropical sea surface temperature and surface wind fields associated with the Southern Oscillation/El Niño. *Monthly Weath. Rev.* **110**, 354-384.
- Shen, G. T. (1986) *Lead and Cadmium Geochemistry of Corals: Reconstruction of historic perturbations in the upper ocean*. PHD/Thesis. MIT/WHOI, WHOI-86-37, 233p.

Shen, G. T. and Boyle, E. A. (1988) Determination of lead, cadmium and other trace metals in annually-banded corals. *Chem. Geol.* **67**, 47-62.

Shen, G. T., Boyle, E. A. and Lea, D. W. (1987) Cadmium in corals as a tracer of historical upwelling and industrial fallout. *Nature* **328**, 794-796.

Shen, G. T. and Sanford, C. L. (in press) Trace element indicators of climate variability in reef-building corals. In *Global ecological consequences of the 1982-1983 El Niño*. (ed. P. W. Glynn), Elsevier, New York.

Smith, S. V., Buddemeier, R. W., Redalje, R. C. and Houck, J. E. (1979) Strontium-Calcium Thermometry in Coral Skeletons. *Science* **204**, 404-407.

Speer, J. A. (1983) Carbonates: Mineralogy and Chemistry. In *Reviews in Mineralogy* (ed. P. H. Ribbe), pp. 145-190, Mineralogical society of America, Washington.

Weber, J. N. (1973) Incorporation of strontium into reef coral skeletal carbonates. *Geochim. et Cosmochim. Acta.* **37**, 2173-2190.

Wyrtki, K. (1975) El Niño--The dynamic response of the Equatorial Pacific Ocean to Atmospheric forcing. *J. Phys. Oceanogr.* **5**, 572-584.

Wyrtki, K. (1981) An estimate of equatorial upwelling in the Pacific. *J. Phys. Oceanogr.* **11**, 1205-1214.

Chapter 4: Ba in planktonic foraminifera

4.1 Introduction

The distribution of barium in the oceans reflects Ba's involvement in the biological cycle of uptake in surface waters and regeneration in deep waters (Bishop, 1988; Chan *et al.*, 1977; Chow and Goldberg, 1960). Ba is depleted in tropical and sub-tropical surface waters; removal of dissolved Ba from surface waters appears to be controlled by precipitation of barite (BaSO_4) in decaying marine particulate matter (Chow and Goldberg, 1960; Dehairs *et al.*, 1980; Bishop, 1988). The barite in the sinking particulates dissolves deep in the water column and/or in the sediments, creating deep water maxima throughout the oceans (Chan *et al.*, 1977).

The concentration of Ba in oceanic surface waters (excluding high latitudes) is quite uniform, about 34 nmol/kg in the Pacific and 41 nmol/kg in the Atlantic (Chan *et al.*, 1977; Ostlund *et al.*, 1987). Higher Ba values in Atlantic surface waters might be due to the majority of river input draining into the Atlantic (J. Edmond, pers. comm.). The magnitude of depletion of Ba in surface waters (as low as 20% of the highest deep water values) is much smaller than is observed for elements like P, NO_3 , Si and Cd, which are highly depleted in surface waters. Unlike these bio-limiting elements, the concentration of Ba in surface waters must in part reflect the mean Ba concentration of the ocean; if mean oceanic Ba was higher in the past, surface Ba is likely to have been higher as well (see appendix to Chapter 4). Oceanic Ba content is primarily controlled by riverine input of Ba, although Ba from deep ocean hydrothermal vents might account for 20% of the Ba input to the oceans (Von Damm *et al.*, 1985).

Temporal reconstructions of Ba in oceanic surface waters would provide information on the geochemical history of Ba as well as insight into change in the

physical and chemical factors that affect the distribution and behavior of Ba in the oceans. Although Ba is a large ion relative to Ca (1.35 vs. 1.00 Å in 6-fold coordination (Shannon, 1976)), it substitutes into calcite (Kitano *et al.*, 1971). The Ba content of calcitic planktonic foraminifera could be used as a means of reconstructing surface water Ba concentrations in past oceans if Ba is substituted into the lattice of the calcite shell in proportion to its dissolved concentration in seawater. A previous study (Boyle, 1981) found high and variable Ba contents for planktonic foraminifera, suggesting that a careful evaluation of cleaning procedures is required to insure that lattice-bound foraminiferal Ba is not obscured by extraneous Ba-rich sedimentary phases. This study details an assessment of cleaning methods for determination of Ba/Ca in various species of planktonic foraminifera from a number of sediment cores, plankton tows and sediment traps. Results indicate that Ba/Ca in species of *Globigerinoides* can be used as a means of reconstructing historical surface water Ba concentrations.

4.2 Analytical Methods

Samples were analyzed for Ba by a modification of the graphite furnace atomic absorption technique. Graphite tubes were modified by insertion of a 0.127 mm thick rolled tantalum liner (Sen Gupta, 1984). These Ta liners increase sensitivity for Ba by a factor of 12 and reduce the tube blank characteristic of carbide forming elements like Ba. Ta-lined graphite tubes require atomization temperatures of only 2500°C compared to >2700°C required for conventional graphite tubes. Although the Ta-lined tubes often performed well for ~50 injections, it was impossible to predict when the liners would fail, at which point the precision would become intolerably poor. In addition, it was very difficult to produce consistent lined tubes; typically only a quarter of a prepared batch worked effectively.

Ba was quantified by comparison to standards prepared in a $\text{Ca}(\text{NO}_3)_2$ matrix matched to the average sample Ca content. Ca was analyzed by flame atomic absorption with inter-run reproducibility of 2%. Inter-run precision of the Ba/Ca ratio was about 6% for consistency standards with optimal Ba concentrations; however, smaller samples with low Ba, typical for *Globigerinoides* samples, have precisions no better than 10%.

4.3 Cleaning Method

A number of cleaning methods were evaluated in this study to determine which would be effective over a large range of cores and foraminiferal species. Ba can reside in a number of extraneous phases associated with shells: detrital grains, fine-grained CaCO_3 , organic matter, Mn and Fe oxides, and barite (BaSO_4). Relative concentrations of Ba in these phases and details of the stepwise cleaning method employed are given in Table 4.1. Initial cleaning follows methods developed for foraminiferal Cd (Boyle, 1981), the detrital grains and fine grained material are removed by physical agitation in distilled water and methanol, the organic matter by oxidation in hydrogen peroxide-sodium hydroxide, and ferromanganese oxide coatings by reduction in hydrazine-ammonium citrate. A unique cleaning problem for foraminiferal Ba is the presence of barite (BaSO_4) in marine sediments. Barite is present in marine sediments over a range of about 10 to 10,000 ppm (Church, 1979), with highest concentrations occurring in sediments underlying oceanic high productivity belts. SEM examination of sediment samples from the Panama Basin indicates that spheres of barite approximately 1 micron in diameter occur in conjunction with diatom debris coating foraminifera shells (Figure 4.1). These barite crystals are a potential source of contamination to determinations of Ba in the calcite shells of foraminifera. The barite is found in samples from both sediment cores and sediment traps, so at least some portion of

Phase(s)	Ba content	Cleaning step
detrital clays & fine grained CaCO ₃	10-1000 ppm	ultrasonication in distilled water methanol
organic matter	~500 ppm	boiling H ₂ O ₂ /NaOH
Mn and Fe oxides	~1000 ppm	boiling hydrazine/NH ₄ OH/citrate
barite (BaSO ₄)	60%	boiling NaOH/DTPA
surface adsorption	(minor)	leach with 0.001N HNO ₃

Table 4.1 Cleaning steps used to remove specific Ba-bearing phases. Ba contents from Fischer and Puchelt (1978), Collier (1981) and Bishop (1988).

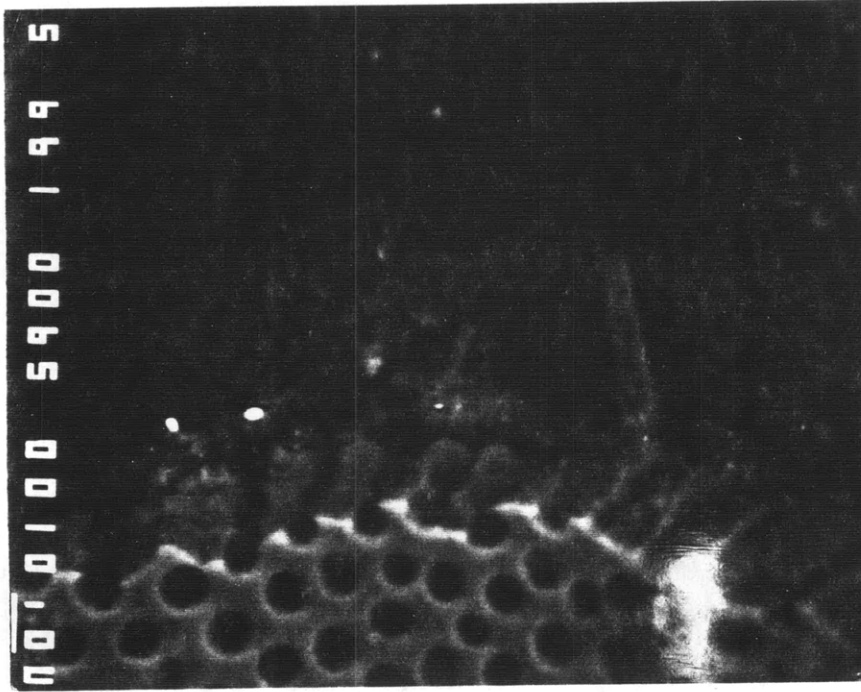


Figure 4.1 Scanning electron microscope image of a separated and rinsed specimen of *N. dutertrei* from box core WH482-483 in the Panama Basin. 10 μm scale bar is indicated in bottom left corner. Image is in back-scattered electron mode. The bright 1 μm spheres are barite occurring in association with diatom debris that coats the foraminifera shells.

the barite must be formed in the water column (or in the trap). The amount of barite present in samples of separated shells is up to tens of ppm, while Ba in cleaned planktonic shells is generally a ppm or less.

Barite is removed by cleaning the separated shells in a solution of alkaline diethylenetriamine-pentaacetic acid (DTPA). DTPA forms strong complexes with Ba under alkaline conditions (Ringbom, 1963), so DTPA concentrations many orders of magnitudes in excess of the barite present causes rapid dissolution of the barite (Sill and Willis, 1964). Since the DTPA has a strong affinity for Ca, an unavoidable side-effect of the alkaline-DTPA treatment is that some foraminiferal calcite is lost. For this reason the concentration of DTPA and length of cleaning time must be carefully balanced to ensure dissolution of the barite without excessive loss of foraminifera. Alkaline-DTPA (~ 0.2 mol/l) is added to the centrifuge vials containing the shell material. The vials are then placed in boiling water for 5 to 15 minutes, depending on sample size. Samples are repeatedly ultrasonicated throughout the treatment. Upon completion of the cleaning ammonium hydroxide is used to rinse out the DTPA followed by distilled water to rinse out the ammonium hydroxide.

A series of measurements has been made to assess the Ba in various phases (Fig. 4.2, 4.3; data compiled in Table 4.2). Planktonic foraminifera treated with ultrasonication to remove loosely adhering sedimentary particles have between 2 -8 $\mu\text{mol/mol}$ Ba/Ca (1 $\mu\text{mol/mol}$ Ba/Ca = 1.37 ppm). Those subject to oxidative cleaning for organically-bound Ba, reductive cleaning to remove oxide coatings and alkaline DTPA to remove barite have Ba/Ca ratios of only 0.8 ± 0.1 $\mu\text{mol/mol}$ (an exception are the *Globorotalia*--see below). Comparison of samples cleaned with and without both the reductive step and the DTPA step indicates that the proportion of Ba these cleaning steps remove depends strongly on the sediment type, with the cleaning steps becoming increasingly more important in

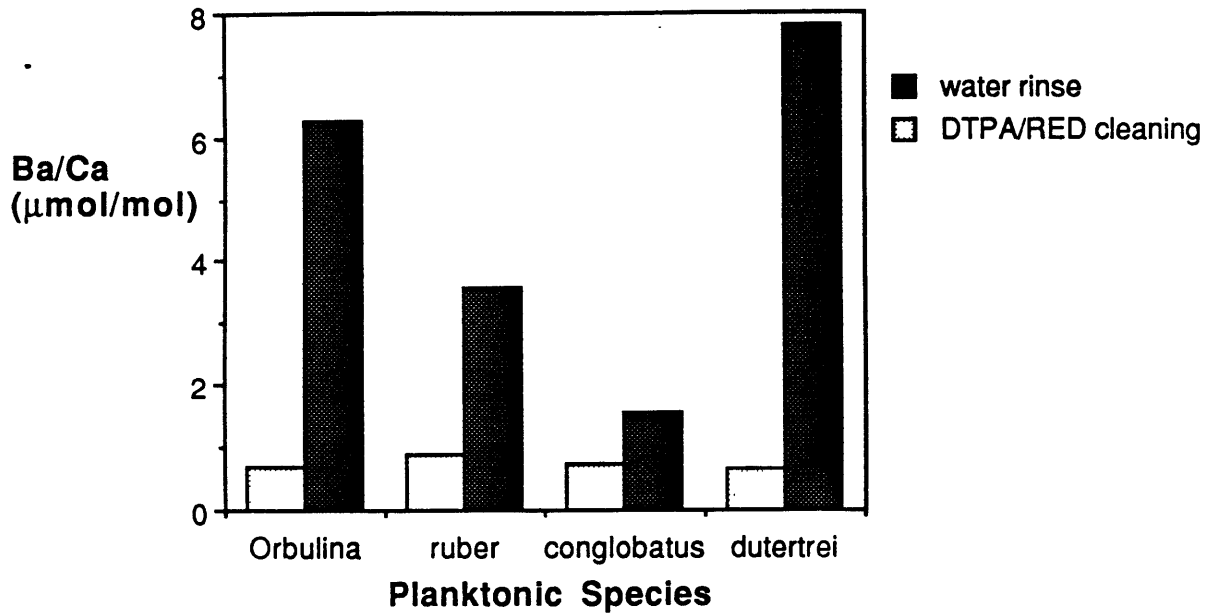


Figure 4.2 Comparison of Holocene planktonic foraminifera cleaned with ultrasonication in distilled water versus full reductive/alkaline-DTPA cleaning. Values represent averages of many analyses (Table 4.2).

Species	Core	Depth cm	Ba/Ca $\mu\text{mol/mol}$	SD	n	r	Cleaning Notes
<i>Globigerinoides conglobatus</i>	All107.65GGC	6	0.82	0.11	2		reductive + DTPA
	All107.67GGC	2	0.82	0.05	2		reductive + DTPA
	All107.71GGC	2	0.82		1		reductive + DTPA
	CHN82.4PC	5	0.60		1		reductive + DTPA
	CHN82.11PC	15	1.35		1		reductive + DTPA
	EN120.GGC1	5 - 7	0.73	0.11	5		reductive + DTPA
	OC173-4.G	5	0.72	0.08	11		reductive + DTPA
	OC173-4.G	5	0.77	0.08	2		std reductive cleaning
	OC173-4.G	5	1.53	0.89	4		no reductive step
<i>Globoquadrina dutertrei</i>	EN66.10GGC	2	4.1	1.0	3		reductive + DTPA
	K73.4.3PC	12	0.46	0.03	3		reductive + DTPA
	K73.4.3PC	12	0.71	0.17	2		std reductive cleaning
	TR163.27	15	0.61	0.05	3		reductive + DTPA
	TR163.28	2	0.55	0.05	2		reductive + DTPA
	TR163.28	2	0.77		1		std reductive cleaning
	TR163.31B	2	0.64	0.14	18	3	reductive + DTPA
	TR163.31B	2	0.87		1		std reductive cleaning
	TR163.32	4	0.57		1		reductive + DTPA
	WH411	ST	0.86	0.11	5		reductive + DTPA
	WH411	ST	2.0	0.9	3		std reductive cleaning
	WH411	ST	4.7	1.5	3		no reductive step
	WH482-483	1 - 6	1.29	0.05	2		reductive + DTPA
	WH482-483	1 - 6	7.8	2.2	3		no reductive step
<i>Globorotalia hirsuta</i>	OC173-4.G	5	4.8	0.9	7	1	std reductive cleaning
	OC173-4.G	5	4.5	2.6	4		reductive + DTPA
<i>Globorotalia menardii</i>	OC173-4.G	5	13.1	6.2	3		std reductive cleaning
	OC52-2	PT	6.5	2.2	2		std reductive cleaning
<i>Orbulina universa</i>	CHN82.4PC	5	0.63	0.06	2		reductive + DTPA
	CHN82.11PC	13	0.96	0.04	2		no reductive step
	EN120.GGC1	5 - 55	0.66	0.24	15	1	reductive + DTPA
	EN66.10GGC	2	0.98	0.26	2	1	reductive + DTPA
	OC173-4.G	5	0.73		1		reductive + DTPA
	OC173-4.G	5	0.86	0.12	4		std reductive cleaning
	OC173-4.G	5	0.87	0.05	2		acid leach only
	OC173-4.G	5	6.3	0.9	2		water rinse only
	OC52-2	PT	0.50		1		std reductive cleaning
	RC13.228	7	2.2	1.6	3	1	reductive + DTPA
	RC13.228	7	3.4	1.5	8		std reductive cleaning
	SCIFF	ST	0.83	0.02	2		std reductive cleaning
	TR163.31B	2	1.40		1		no reductive step

Table 4.2 Ba/Ca in Holocene Planktonic Foraminifera. SD = standard deviation; n = number of samples; r = number of rejected samples; ST = sediment trap; PT = plankton tow.

Species	Core	Depth	Ba/Ca	SD	n	r	Cleaning Notes
<i>Globigerinoides ruber</i>	EN120.GGC1	45-51	0.85	0.18	3		reductive + DTPA
	EN66.10GGC	2	0.95	0.01	2		reductive + DTPA
	OC173-4.G	5	0.73		1		reductive + DTPA
	OC173-4.G	5	1.18	0.13	4		std reductive cleaning
	OC173-4.G	5	1.14	0.03	2		acid leach only
	OC173-4.G	5	3.52	0.16	2		water rinse only
	OC52-2	PT	1.01	0.12	5		std reductive cleaning
	WH411	ST	1.96	0.42	2		no reductive step
	WH482-483	1 - 6	6.10		1		no reductive step
<i>Globigerinoides sacculifera</i>	EN120.GGC1	21-65	0.64	0.01	6	1	reductive + DTPA
	EN66.10GGC	2	0.94	0.21	4		reductive + DTPA
	OC173-4.G	5	0.85	0.06	2		std reductive cleaning
	OC52-2	PT	0.66	0.02	2		std reductive cleaning
	TR163.28	2	0.80		1		std reductive cleaning
	TR163.31B	2	1.76		1		no reductive step
	V22-174	5	0.55		1		reductive + DTPA
	V22-174	56	22.5		1		reductive + DTPA
	V22-174	96	46.5	9.7	3		reductive + DTPA
	WH411	ST	1.59		1		std reductive cleaning
	WH482-483	1 - 6	0.58		1		std reductive cleaning
	WH482-483	1 - 6	2.33		1		no reductive step
	<i>Globorotalia truncatulinoides</i>	EN120.GGC1	5	4.2	0.3	3	
OC173-4.G		5	2.7	1.4	24		reductive + DTPA
OC173-4.G		5	6.1	1.2	19	1	std reductive cleaning
SCIFF		ST	3.3	2.5	3		reductive + DTPA
SCIFF		ST	2.4	0.4	2		std reductive cleaning

Table 4.2 Ba/Ca in Holocene Planktonic Foraminifera (cont.)

sediments from more productive regions of the ocean where barite abundances (and possibly the proportion of oxide coatings) are greater. Samples of both sediment and sediment trap material from the Panama Basin indicate the importance of the DTPA step for removing adhering barite (Fig. 4.3). The final strategy has been to use the most rigorous cleaning method on all samples under the assumption that one can not predict how sediment properties might change throughout the length of a core.

4.4 Additional notes on cleaning

During the course of this study two unique cases particular to two cores arose:

1) Foraminifera from a sediment core treated with kalgon during disaggregation yield Ba/Ca ratios 2 to 12 times higher than normal, even after prolonged cleaning (see data for core RC13-228: Table 4.2). This is presumably due to precipitation of an insoluble PO_4 phase (BaHPO_4). All other Ba/Ca determinations were made on cores that were dissagregated in de-ionized water.

2) Planktonic foraminifera from 56 and 96 cm in Core V22-174 yielded Ba/Ca ratios 10 to 100 times higher than those from 5 cm, even after protracted cleaning with alkaline-DTPA (Table 4.2). Similar results were found for foraminifera from this core in an earlier effort to quantify Ba in planktonic foraminifera (Boyle, 1981). Examination of specimens of these individuals by SEM indicates that the sediment in the high-Ba intervals was subject to a hydrothermal event which caused occlusion of pore spaces and precipitation of hydrothermal barites. Although the cleaning method employed can **not** remove the (hydrothermally) precipitated barite from the foraminifera in this core, this was the only such instance encountered in this study, as well as in determination of Ba contents of benthic foraminifera in over 40 Quaternary cores (Lea and Boyle, 1989;

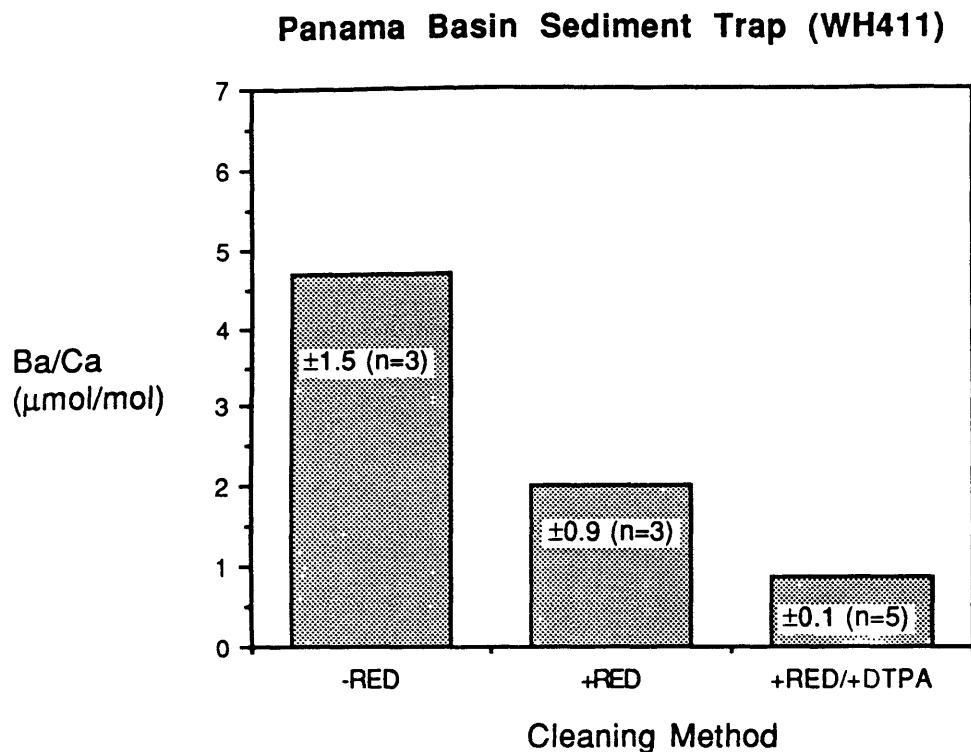


Figure 4.3 Comparative cleaning of *N. dutertrei* shells from a sediment trap sample collected in the Panama Basin (WH411). Key: -RED = cleaning steps outlined in Table 4.1 with omission of the hydrazine reductive step and alkaline-DTPA step. +RED = cleaning steps outlined in Table 4.1 with omission of the alkaline-DTPA step only. +RED/+DTPA = All cleaning steps included.

Chapter 5) and in two DSDP cores of Pliocene age (Lea, unpublished data).

However, diagenesis of sediments might be a more persistent problem in older (>1 MA) sediments where barite precipitation might have occurred more frequently.

4.5 Ba/Ca in Holocene *Globigerinoides*

The range of Ba in the low latitude surface waters of the world's oceans is relatively small. Thirteen GEOSECS stations in the Atlantic north of 33°S had dissolved Ba = 41 ± 2 nmol/kg. Six GEOSECS stations in the Pacific between 30°S and 30°N had dissolved Ba = 34 ± 1 nmol/kg (Ostlund *et al.*, 1987). The surface waters of the Southern Oceans and North Pacific are enriched in Ba due to out-cropping of cold, nutrient-enriched waters.

Ba/Ca in cleaned samples of *Globigerinoides sacculifera*, *G. ruber*, *G. conglobatus*, and *Orbulina universa* recovered from Holocene sediments primarily in the sub-tropical and Equatorial Atlantic have ratios of 0.8 ± 0.1 $\mu\text{mol/mol}$ (Table 4.3). Ba/Ca in *Neogloboquadrina dutertrei* from the Equatorial Pacific have ratios of 0.6 ± 0.1 $\mu\text{mol/mol}$. The uniformity of values in the Atlantic and the lower values for *N. dutertrei* in the Pacific both agree with the distribution of Ba in the surface oceans.

Measurements of Ba/Ca in foraminifera samples from sediment traps and plankton tows can be used to ascertain that Ba present in the foraminifera shells recovered from cores is not an artifact of sediment contamination. Three sets of samples were used (Fig. 4.4): *O. universa* from a North Atlantic Sediment trap placed at 3400 m (31°N, 64°W); *N. dutertrei* from an Equatorial Pacific Sediment trap placed at 3354 m (5°N, 82°W); and, *G. sacculifera* and *G. conglobatus* from a plankton tow in the North-East Atlantic (cruise *Oceanus* 52-2). These samples were cleaned with slightly different procedures, as indicated in Table 4.2. Within the reproducibility of the samples, Ba/Ca of *Globigerinoides* from plankton tows

Basin	Species	No. of cores	Ba/Ca ($\mu\text{mol/mol}$)
Atlantic	<i>G. conglobatus</i>	6 (r=1)	0.75 ± 0.09
	<i>Orbulina spp.</i>	4	0.75 ± 0.16
	<i>G. ruber</i>	3	0.84 ± 0.11
	<i>G. sacculifera</i>	2	0.79 ± 0.15
	All	15	0.77 ± 0.12
Pacific	<i>G. dutertrei</i>	5 (r=1)	0.57 ± 0.07

Table 4.3 Mean Ba/Ca for certain planktonic foraminiferal species.

r = number of rejected samples.

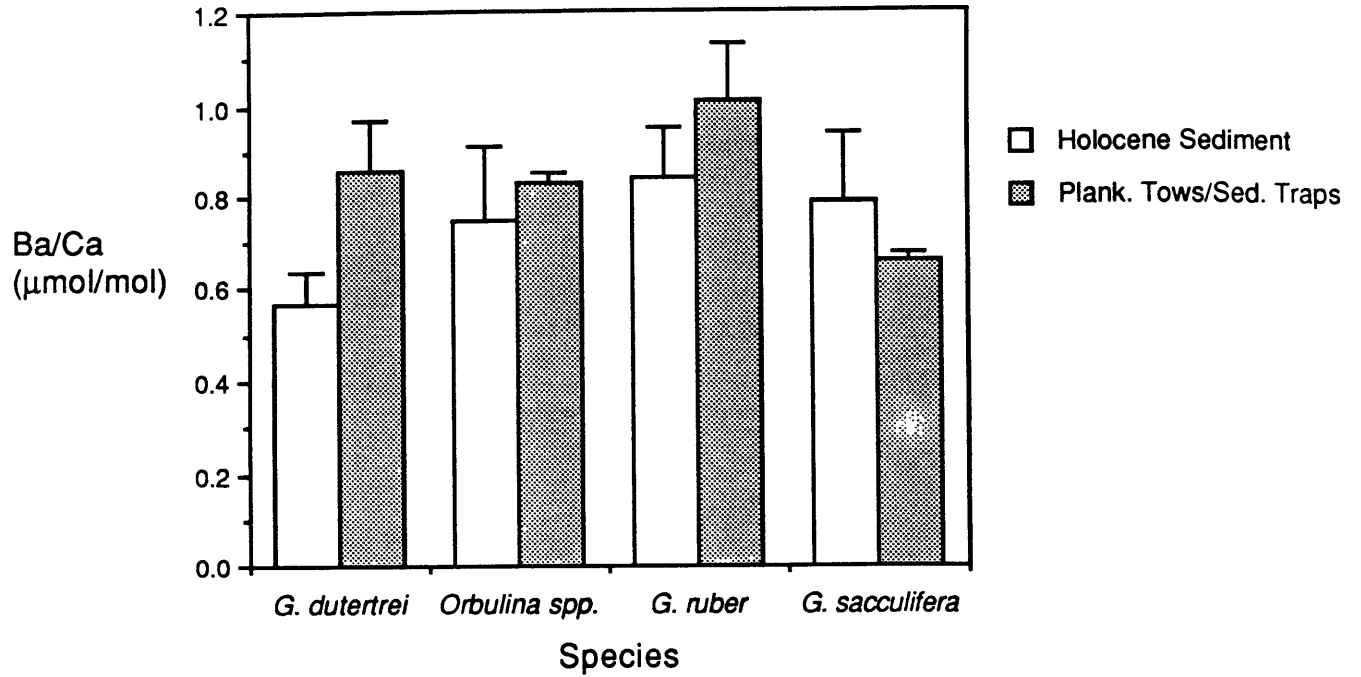


Figure 4.4 Average Ba/Ca for 4 species of planktonic foraminifera from Holocene sediments versus plankton tows and sediment traps. Not all samples were cleaned with the alkaline-DTPA treatment (see Table 4.2). Averages for *N. dutertrei* include Pacific samples only. Values represent averages of many analyses (Table 4.2).

and sediment traps generally agrees with shells recovered from cores (Fig. 4.4). Therefore the Ba content of the shells does not appear to be changed by contact with sediments.

A further test for lattice-bound metals is sequential dissolution of shells accompanied by determination of the metal to calcium ratio in each partial dissolution fraction. Reproducible values that do not change over the course of the dissolution suggest that Ba is in the calcite lattice, while a lack of reproducibility or systematically decreasing values might indicate that Ba is associated with another phase (Boyle, 1981). A 4.5 mg sample of *G. conglobatus* (about 75 individuals) from box core OC173-4.G taken at 4469 m on the Bermuda Rise was cleaned in the normal manner and sequentially dissolved. Ba/Ca was measured on 9 dissolution fractions (Fig. 4.5) Within the error of the measurement there was no change in Ba/Ca of the leachates. The results of this experiment indicate no evidence for contribution of Ba from external phases. Additionally, the relative constancy of the values suggests a homogeneous distribution of the Ba in the calcite lattice of the foraminifera.

Measurements of Ba/Ca in *G. sacculifera* from the core-top of an Eastern Mediterranean core by the ICP-MS method described in Chapter 2 have Ba/Ca = 1.0 ± 0.2 . Measurement of surface water Ba near this site indicates Ba of about 53 nmol/kg (Appendix 1). The averages for planktonic foraminiferal Ba/Ca for Holocene sediments from the Atlantic, Pacific and Mediterranean (excluding *Globorotalia*--see below) are used to calculate a distribution coefficient $D = \{Ba/Ca\}_{\text{foram}} / \{Ba/Ca\}_{\text{seawater}}$ (Table 4.4). For the 5 species of foraminifera from these cores $D = 0.19 \pm 0.05$. Fig. 4.6 indicates the averaged Ba/Ca values plotted as a function of surface water Ba concentration for each basin.

Kitano and co-authors (Kitano *et al.*, 1971) found that under conditions of slow precipitation the distribution coefficient for Ba in inorganic calcite is about 0.1.

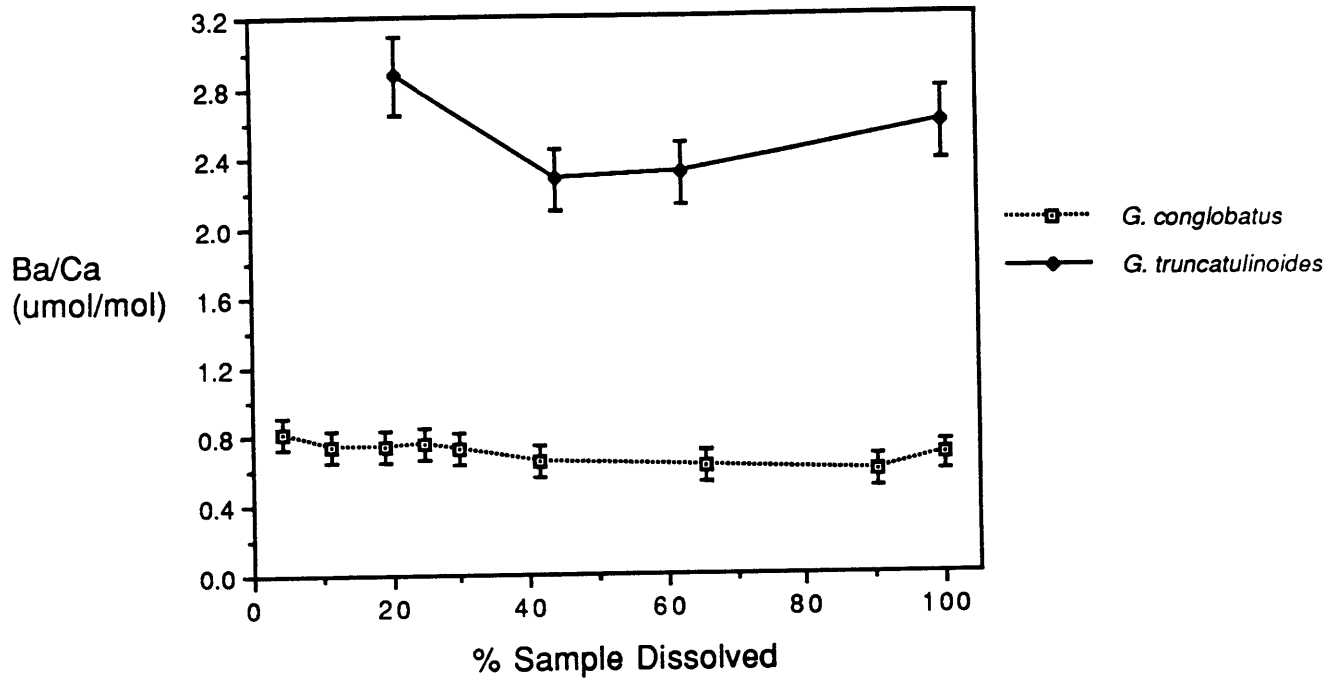


Figure 4.5 Partial dissolutions of ~5 mg samples of cleaned *G. conglobatus* shells and cleaned *G. truncatulinoides* shells. Ba/Ca is plotted vs. the per cent sample dissolved at each stage (see text).

Basin	(Ba/Ca)_{foram} μmol/mol	SW Ba nmol/kg	SW Ca mmol/kg	(Ba/Ca)_{sw} μmol/mol	D_{foram}
Atlantic	0.77±0.12	41±2	10.3	4.0	0.19±0.03
Pacific	0.57±0.07	34±1	10.0	3.4	0.17±0.02
Mediterranean	1.04±0.19	53±1	11.3	4.7	0.22±0.04

Table 4.4 Calculation of foraminiferal distribution coefficients. SW = surface water; foram = planktonic foraminifera. Mediterranean surface seawater Ba from this work (Appendix 1).

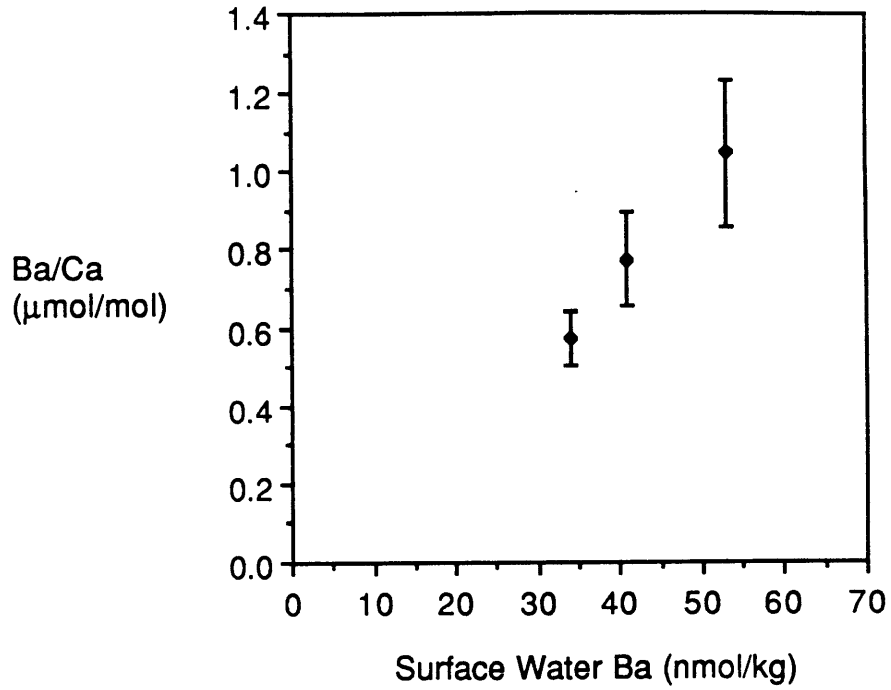


Figure 4.6 Mean Ba/Ca determinations for *N. dutertrei* from the Equatorial Pacific, 4 species of *Globigerinoides* from the Atlantic, and *G. sacculifera* from the Mediterranean (15) plotted vs. surface water Ba in each basin (see Tables 4.3 and 4.4).

However, during rapid precipitation achieved by "vigorous stirring", Ba distribution coefficients were as high as 3 during the early stages of precipitation and never dropped as low as 0.5 during the final stages of precipitation. The calculated distribution coefficient of 0.2 for planktonic foraminifera is about double the value for slow precipitation.

4.6 Ba in *Globorotalia*

Analysis of Ba/Ca in the non-spinose foraminifera *Globorotalia truncatulinoides* and *G. hirsuta* from several cores and a North-West Atlantic sediment trap indicates ratios 3 to 9 times higher than those measured in *Globigerinoides* from the same cores (Table 4.2). A few measurements of Ba/Ca in *G. menardii* and *G. inflata* indicate high values for these *Globorotalia* as well (Table 4.2). Partial dissolution of a *G. truncatulinoides* sample did not result in a reduction of Ba/Ca (Fig. 4.5). Attempts to use more extensive cleaning with alkaline-DTPA did eventually yield lower values, although Ba/Ca is never as low as in *Globigerinoides* (Fig. 4.7). Examination of *G. truncatulinoides* shells by SEM did not reveal the presence of barite particles, although this does not rule out the existence of barite particles smaller than 0.1 μm . The high Ba contents of sediment trap samples of *G. truncatulinoides* suggests that Ba enrichment of *Globorotalia* is not simply related to sediment contamination occurring when shells are deposited on the ocean floor.

The origin of high Ba/Ca in the *Globorotalia* might be related to the unique lifestyle and feeding habitats of this genus. For one, *Globorotalia* live at greater depths than *Globigerinoides* (Deuser *et al.*, 1981), and since Ba increases with depth they would be expected to have more Ba in their shells. However, the increase in Ba in the deep Atlantic is not nearly large enough to account for the observed Ba/Ca ratios. A more likely explanation for enriched Ba might be the

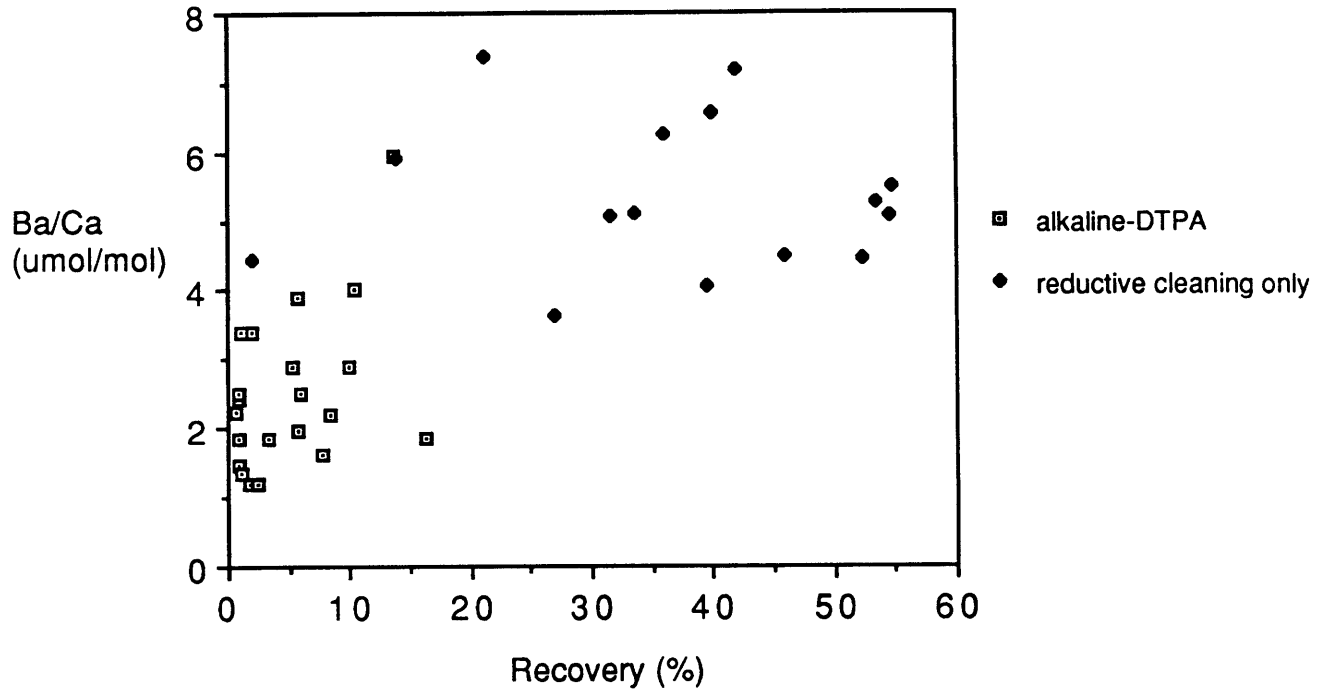


Figure 4.7 Effect of alkaline-DTPA treatment on samples of *G. truncatulinoides*. Ba/Ca of samples is plotted vs. per cent recovery of calcite (i.e. final CaCO_3 after cleaning divided by initial CaCO_3 before cleaning). Per cent recovery is a measure of the DTPA cleaning time.

feeding habits of the *Globorotalia*. Laboratory studies suggest that their main food source may be diatoms (Spindler *et al.*, 1984), and an association between precipitation of barite and the presence of diatom frustules has recently been established (Bishop, 1988). The shells of *Globorotalia* might precipitate in a high Ba (or barite) environment due to the presence of diatom frustules in the feeding cyst. This hypothesis could be tested by culturing *Globorotalia* using food sources with known Ba contents. If Ba-rich food sources are the cause of enriched Ba in the shells of the *Globorotalia*, then the Ba content of the shells might serve as a regional or historical indicator of food sources.

The only non-spinose foraminifera that yielded low Ba/Ca consistent with the *Globigerinoides* is *Neogloboquadrina dutertrei* from Equatorial Pacific cores (Table 4.2). However, *N. dutertrei* shells from a single Equatorial Atlantic core (EN66-10GGC) have Ba contents comparable to the *Globorotalia* (Table 4.2). Ba/Ca of other *Globigerinoides* in this core are not elevated, so the enhanced Ba content of the *N. dutertrei* in this core might indicate a different food source for this species in the Equatorial Atlantic.

4.7 Reconstruction of surface Ba in the Atlantic over the last 14 kyr

Since Ba/Ca of cleaned *Globigerinoides* reflects surface water Ba/Ca, temporal change in surface Ba contents can be reconstructed by recovery of down-core *Globigerinoides* Ba/Ca records. Core EN120-GGC1 from the Bermuda Rise in the North-West Atlantic was raised from 4450 m water depth at 33°40' N, 57°37' W (Boyle and Keigwin, 1987). It contains a high sedimentation record (from 12 cm/kyr in the early Holocene to 200 cm/kyr in the glacial) of the last 15,000 years; the oxygen isotope record indicates heavy glacial values (>3.7‰) from 161 cm to the bottom of the core at 273 cm. Age models based on radiocarbon dates on another Bermuda Rise core (GPC-5) indicate higher sedimentation rates in the

glacial intervals, so that the bottom 100 cm of the core covers less than a 1000 years (L. Keigwin, pers. comm.).

Ba/Ca was analyzed in 4 *Globigerinoides* species over the top 217 cm, corresponding to the last 14 kyrs (Fig. 4.8; Table 4.5). Abundances of the *Globigerinoides* fall off markedly in the glacial intervals, especially below 200 cm. Species analyzed included *G. conglobatus*, *G. ruber*, *G. sacculifera*, and *O. universa*; no obvious differences in Ba/Ca were noted from species to species. As Fig. 4.8 indicates, there is a tendency to higher values during glacial intervals, although the scatter in the data precludes confidence in this trend.

An increase in Atlantic surface water Ba during glacial periods might reflect change in a number of oceanic parameters. The Ba content of oceanic surface waters is principally tied to mean ocean Ba and the mean ocean content of a limiting nutrient like P (see appendix to Chapter 4). Present evidence suggests that mean ocean P was unchanged during the LGM (E. Boyle, pers. comm.). Evidence from benthic and planktonic foraminiferal Ba/Ca records from the Equatorial Pacific indicates that mean ocean Ba might have been 10 to 15% lower during the last glacial period (Chapter 6). Lower mean Ba would lead to lower Ba in surface waters, the opposite trend to what is observed in Core EN120-GGC1. However, the 20% enrichment in Ba in Atlantic surface waters over Pacific surface waters in the present ocean demonstrates that oceanic surface waters can not be modelled as a single box for Ba. The simplest explanation for the difference observed today is that the largest proportion of river input drains into the Atlantic (J. Edmond, pers. comm.). Since the glacial data suggest an even larger Atlantic-Pacific difference in surface water Ba content, the increase in planktonic Ba EN120-GGC1 might be due to enhanced riverine fluxes to the Atlantic at 13-14 kyr.

The scatter in the Ba/Ca data from core EN120.GGC1 is in part attributable to analytical scatter. A consistency standard of comparable concentration to

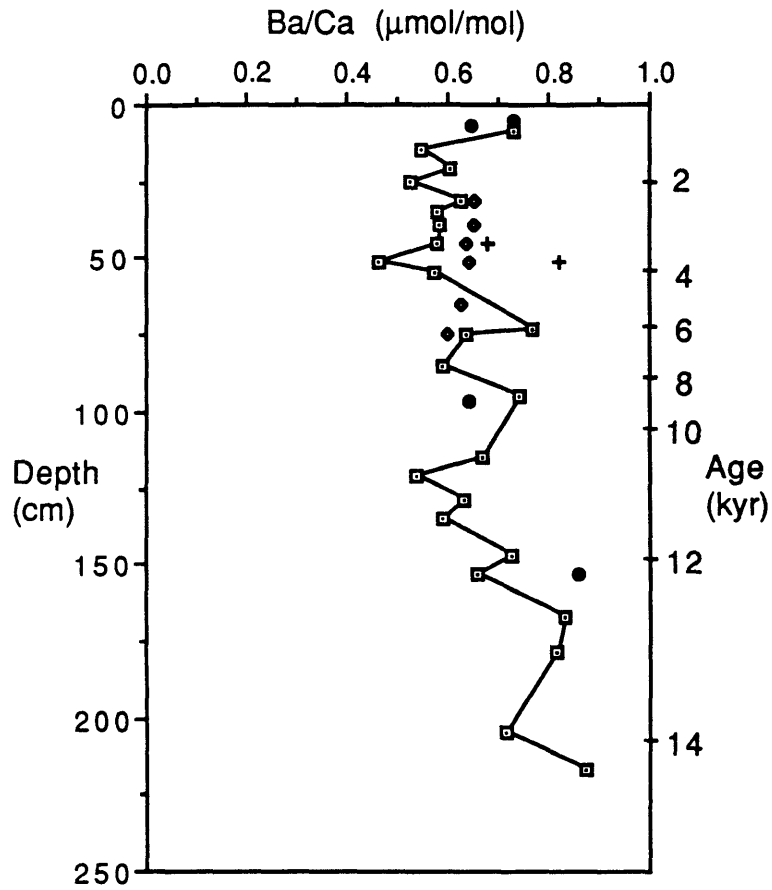


Figure 4.8 Ba/Ca of cleaned *Globigerinoides* species in core EN120-GGC1 from the Bermuda rise (4450 m) plotted as a function of depth. Key to species code: filled circles = *G. conglobatus*; diamonds = *G. sacculifera*; crosses = *G. ruber*; open squares = *Orbulina* spp. Ages from L. Keigwin, pers. comm.

Depth cm	Species	Ba/Ca μmol/mol	SD	n	r
5	conglob	0.73	0.13	4	
5	Orb				2
7	conglob	0.65	0.06	2	
9	Orb	0.73		1	1
15	Orb	0.55	0.14	3	
21	Orb	0.60		1	
25	Orb	0.53		1	
31	Orb	0.62		1	
31	sacc	0.65		1	
35	Orb	0.58		1	
39	Orb	0.58		1	
39	sacc	0.65		1	
45	Orb	0.58	0.19	2	
45	ruber	0.68		1	
45	sacc	0.64	0.01	2	
51	Orb	0.46		1	
51	ruber	0.82		1	
51	sacc	0.64		1	
55	Orb	0.57		1	
65	sacc	0.62		1	
73	Orb	0.77		1	
75	Orb	0.64		1	
75	sacc	0.60		1	
85	Orb	0.59		1	
91	Orb				1
95	Orb	0.74		1	
97	conglob	0.64		1	
97	sacc				1
115	Orb	0.67		1	
121	Orb	0.54		1	
129	Orb	0.63		1	
135	Orb	0.59		1	
147	Orb	0.73		1	
153	conglob	0.86		1	
153	Orb	0.66		1	
167	Orb	0.83		1	
179	Orb	0.82		1	
205	Orb	0.72		1	
217	Orb	0.87		1	

Table 4.5 Planktonic foraminiferal Ba/Ca data from core EN120-GGC1. Codes: conglob = *G. conglobatus*; Orb = *Orbulina spp.*; sacc = *G. sacculifera*; ruber = *G. ruber*.

EN120 -GGC1 foraminifera solutions was reproducible to about 10% over the course of these analyses. The ability to do precise measurements of foraminiferal Ba by inductively coupled plasma mass spectrometry (Chapter 2) suggests that improved planktonic Ba/Ca records can be obtained in the future.

4.8 Conclusions

The Ba content of several species of the planktonic foraminifera *Globigerinoides* and *Globoquadrinia* can be used as a means of reconstructing historical changes in dissolved Ba in surface waters. Ba contents of species of *Globorotalia* examined for this study are enriched over other genera, possibly reflecting food sources high in Ba; therefore these species can not be employed for surface water Ba reconstructions. Recovery of meaningful Ba/Ca values for planktonic foraminifera requires extensive purification of the shells to remove residual sedimentary phases which can contribute Ba to the analysis.

A record of planktonic foraminiferal Ba/Ca record for a North-West Atlantic core covering the last 14 kyr suggests that Ba in surface waters of the Atlantic might have been up to 20% higher during the end of the last glacial period. Higher surface Ba might be an indication of increase in riverine fluxes to the Atlantic.

References--Chapter 4

- Bishop, J. K. B. (1988) The barite-opal-organic carbon association in oceanic particulate matter. *Nature* **332**, 341-343.
- Boyle, E. A. (1981) Cadmium, zinc, copper, and barium in foraminifera tests. *Earth Planet. Sci. Lett.* **53**, 11-35.
- Boyle, E. A., Huested, S. S. and Jones, S. P. (1981) On the distribution of copper, nickel and cadmium in the surface waters of the North Atlantic and North Pacific Ocean. *J. Geophys. Res.* **86**, 8048-8066.
- Boyle, E. A. and Keigwin, L. D. (1987) North Atlantic thermohaline circulation during the past 20,000 years linked to high-latitude surface temperature. *Nature* **330**, 35-40.
- Broecker, W. S. (1982) Ocean chemistry during glacial time. *Geochim. Cosmochim. Acta.* **46**, 1689-1705.
- Broecker, W. S. and Peng, T. -H. (1982) *Tracers in the Sea*. Eldigio Press, 690p.
- Chan, L. H., Drummond, D., Edmond, J. M. and Grant, B. (1977) On the barium data from the Atlantic GEOSECS Expedition. *Deep-Sea Res.* **24**, 613-649.
- Chow, T. J. and Goldberg, E. D. (1960) On the marine geochemistry of barium. *Geochim. Cosmochim. Acta.* **20**, 192-198.
- Church, T. M. (1979) Marine Barite. In *Marine Minerals* (ed. R. G. Burns), pp. 175-209, Mineralogical Society of America, Washington, D.C.
- Collier, R. W. (1981) *The trace element geochemistry of marine biogenic particulate matter*. PH.D. Thesis, MIT/WHOI, WHOI-81-10.
- Dehairs, F., Chesselet, R. and Jedwab, J. (1980) Discrete suspended particles of barite and the barium cycle in the open ocean. *Earth Planet. Sci. Lett.* **49**, 528-550.
- Deuser, W. G., Ross, E. H., Hemleben, C. and Spindler, M. (1981) Seasonal changes in species composition, numbers, mass, size, and isotopic composition of planktonic foraminifera settling into the deep Sargasso Sea. *Paleogeogr., Paleoclimatol., Paleoecol.* **33**, 103-127.
- Fischer, K. and Puchelt, H. (1978) Barium. In *Handbook of Geochemistry* (ed. K. H. Wedepohl), pp. A1-N1, Springer Verlag, Berlin.
- Kitano, Y., Kanamori, N. and Oomori, T. (1971) Measurements of distribution coefficients of strontium and barium between carbonate precipitate and solution-- Abnormally high values of distribution coefficients at early stages of carbonate formation. *Geochem. J.* **4**, 183-206.

Lea, D. and Boyle, E. (1989) Barium content of benthic foraminifera controlled by bottom water composition. *Nature* **338**, 751-753.

Ostlund, H. G., Craig, H., Broecker, W. S. and Spencer, D. W. (1987) *GEOSECS Atlantic, Pacific, and Indian Ocean Expeditions, Vol. 7, Shorebased Data and Graphics*. National Science Foundation, Washington, DC, 200p.

Ringbom, A. (1963) *Complexation in Analytical Chemistry*. Interscience Publishers, 361p.

Sen Gupta, J. G. (1984) Determination of cerium in silicate rocks by electrothermal atomization in a furnace lined with tantalum foil. *Talanta* **31**, 1053-1056.

Shannon, R. D. (1976) Revised effective ionic radii and systematic studies of interatomic distances in halides and chalcogenides. *Acta Crystallogr.* **A32**, 751-767.

Sill, C. W. and Willis, C. P. (1964) Precipitation of submicrogram quantities of thorium by barium sulfate and application to fluorometric determination of thorium in mineralogical and biological samples. *Anal. Chem.* **36**, 622-630.

Spindler, M., Hemleben, C., Salomons, J. B. and Smit, L. P. (1984) Feeding behaviour of some planktonic foraminifers in laboratory cultures. *J. of Foraminiferal Res.* **14**, 237-249.

Von Damm, K. L., Edmond, J. M., Grant, B., Measures, C. I., Walden, B. and Weiss, R. F. (1985) Chemistry of submarine hydrothermal solutions at 21°N, East Pacific Rise. *Geochim. Cosmochim. Acta.* **49**, 2197-2220.

4.9 Appendix to Chapter 4

A simple two box model for the oceans (Broecker, 1982; Broecker and Peng, 1982) demonstrates the relationship between surface Ba concentrations and mean oceanic Ba (Fig. 4.9). Both Ba and P are employed in the model, as surface concentrations of nutrient-like elements (Ba) are tied to a limiting nutrient like P (see below). Eqs.(1) and (2) are for the surface box and (3) and (4) are for the entire ocean:

$$(1) \text{Ba}_s Q = R_{\text{Ba}} + \text{Ba}_d Q - F_{\text{Ba}}$$

$$(2) P_s Q = R_P + P_d Q - F_P = 0 \quad (P_s \ll P_d)$$

$$(3) f_{\text{Ba}} F_{\text{Ba}} = R_{\text{Ba}}$$

$$(4) f_P F_P = R_P$$

where s denotes surface waters and d indicates deep waters, R is the river flux of the subscript element, F is the particulate flux of the subscript element, Q is the oceanic ventilation rate and f is the fraction of the particulate flux of the subscript element lost to the sediments.

The relationship between the particulate fluxes of the two elements is:

$$(5) F_{\text{Ba}} = \alpha \beta F_P \text{Ba}_s / P_s$$

where α is the ratio of the Ba/P ratios in the plankton to that in the water and β is the ratio of the Ba/P ratios in the sinking particulate matter to that in the phytoplankton (Boyle *et al.*, 1981; Collier, 1981). The product $\alpha\beta$ directly expresses the ratio of Ba/P ratios in sinking particulate matter to that in the water.

Combining eqs. (1) through (4) into two equations and then substituting (5) leads to:

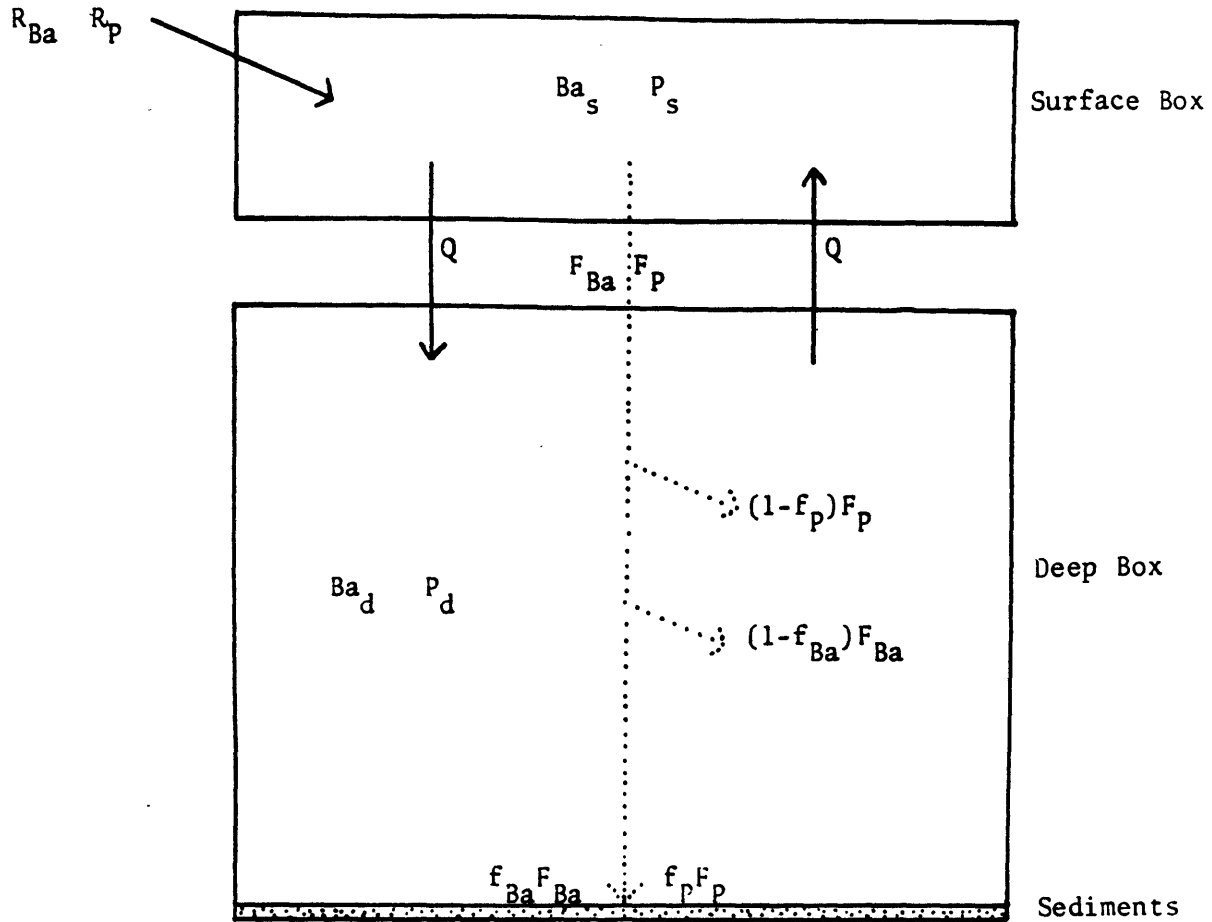


Figure 4.9 Box model described in text. Key to subscripts: s=surface; d=deep; R=river flux; F=particulate flux; Q=mixing flux; f=fraction of the particulate flux that survives destruction and is buried in the sediments.

$$(6) \text{ Ba}_d/\text{Ba}_s = 1 + \{\alpha\beta(1 - f_{\text{Ba}})P_d\}/\{(1 - f_P)P_s\}$$

A test of the validity of Eq. (6) is to substitute values for all variables but α and β for the modern ocean. Using:

$$f_{\text{Ba}} = 0.14$$

$$f_P = 0.01$$

$$P_d / P_s = 2.2 \mu\text{mol/kg} / 0.05 \mu\text{mol/kg} = 44$$

$$\text{Ba}_d / \text{Ba}_s = 110 / 37 = 3$$

eq. (6) yields a value of 0.05 for the product $\alpha\beta$. A range of 0.012 to 0.18 for the product $\alpha\beta$ is calculated for Ba based on measurements of oceanic plankton and particulates (Collier, 1981), so the value calculated from eq. (6) is reasonable.

Eq. (6) shows that the ratio of deep to surface water Ba concentrations is dependent on that same ratio for P. Therefore, surface water Ba values contain information about the oceanic mean values of both Ba and P, since the average Ba and P concentrations in deep waters is approximately the mean oceanic value of those elements. What remains unclear is the paleoceanographic utility of eq. (6), since there is no way as yet to evaluate secular changes in the product $\alpha\beta$, f_{Ba} or f_P . If one assumes *a priori* that these parameters have remained unchanged and surface water P has remained depleted, then solving for Ba_s leads to eq. (7):

$$(7) \text{ Ba}_s = \text{Ba} / (1 + \epsilon P) \text{ where } \text{Ba} = \text{Ba}_d, P = P_d \text{ and } \epsilon = 9 \times 10^5 \text{ (mol P)}^{-1}$$

Fig. 4.10 is a plot of equation (7) with curves drawn for various fixed values of Ba. Note that the curves are fairly steep in the region of modern Ba_s and P values, suggesting that surface Ba concentrations may be quite responsive to changes in mean oceanic P and mean oceanic Ba.

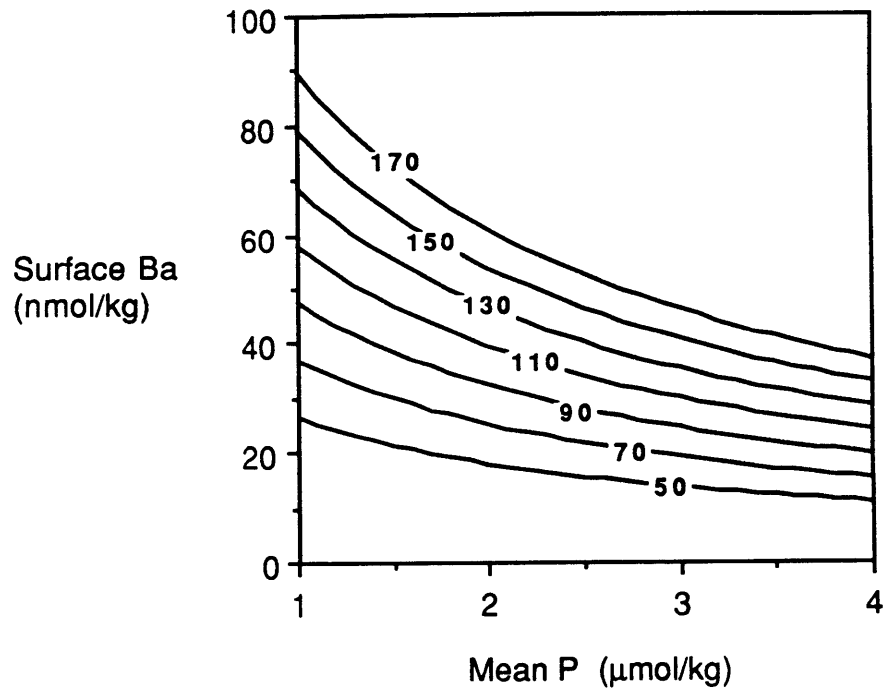


Figure 4.10 Relationship of surface water Ba concentrations to mean ocean P based on model described in text. Separate curves are drawn for various mean ocean Ba contents. Present conditions fall where the number "110" is written.

Core	Latitude	Longitude	Water Depth (m)
All107 65GGC	32° 02' S	36° 11' W	2795
All107 67GGC	31° 55' S	36° 12' W	2587
All107 71GGC	31° 31' S	35° 56' W	1887
CHN82 4PC	41° 43' N	32° 51' W	3427
CHN82 11PC	42° 23' N	31° 48' W	3209
EN66 10GGC	06° 39' N	21° 54' W	3527
EN120 GGC1	33° 40' N	57° 37' W	4450
KNR73 3PC	00° 22' S	106° 11' W	3606
OC173-4 G	31° 54' N	64° 18' W	4469
TR163-27	02° 15' S	86° 35' W	3180
TR163-28	02° 19' S	86° 14' W	3200
TR163-31B	03° 57' S	85° 58' W	3210
TR163-32	02° 29' S	82° 59' W	2890
V22-174	10° 04' S	12° 49' W	2630
WH482-483	5° 22' N	82° 6' W	3885
RC13-228	22° 20' S	11° 12' W	3204

Appendix to Chapter 4: Listing of core locations

Chapter 5: Barium content of benthic foraminifera controlled by bottom-water composition

In recent years the carbon isotope ratio ($\delta^{13}\text{C}$) and cadmium content (Cd/Ca) of benthic foraminifera shells have been employed to reconstruct deep water circulation patterns of the glacial oceans (Boyle and Keigwin, 1982; Boyle and Keigwin, 1985; Boyle and Keigwin, 1987; Curry *et al.*, 1988; Duplessy *et al.*, 1988; Keigwin, 1987; Sarnthein *et al.*, 1988). Both of these tracers co-vary with phosphorus in the modern ocean because they are nearly quantitatively regenerated from sinking biological debris in the upper water column. Hence these tracers can be used to reconstruct the distribution of labile nutrients in glacial water masses. Independent constraints on glacial deep ocean circulation patterns could be provided by a tracer of the distribution of silica and alkalinity, the deeply regenerated constituents of planktonic hard parts. Barium shares key aspects of its behavior with these refractory nutrients since it is removed from solution in surface waters and incorporated into sinking particles which slowly dissolve deep in the water column and in the sediments (Chan *et al.*, 1977). The fractionation of Ba between deep water masses of the major ocean basins is largely controlled by thermohaline circulation patterns, so Ba conforms to different boundary conditions than Cd and $\delta^{13}\text{C}$. Since Ba substitutes into trigonal carbonates (Kitano *et al.*, 1971), it is a potential paleoceanographic tracer *if* the Ba content of foraminifera shells reflects ambient dissolved Ba concentrations. Here data from recent core top benthic foraminifera indicates that the Ba content of some recent calcitic benthic foraminifera does co-vary with bottom water Ba.

The distribution of barium, alkalinity and silica in the world's oceans was extensively mapped during the GEOSECS program (Bainbridge, 1981;

Broecker *et al.*, 1982; Ostlund *et al.*, 1987; Weiss *et al.*, 1983). Figure 5.1 illustrates the similarity between Ba and alkalinity over 9 widely spaced GEOSECS sites. Although the cycling of these two tracers is dominated by different mechanisms (Bishop, 1988; Edmond, 1974), the overprint of thermohaline circulation on two dissolved constituents sharing similar sites of uptake and regeneration results in strong covariance throughout the world's oceans. Thus the distribution of Ba in glacial oceans can provide first order insight into the distribution of refractory nutrients like alkalinity.

To calibrate the response of benthic foraminifera shells to ambient Ba concentrations Ba has been measured in foraminifera recovered from Recent core tops lying below bottom waters whose Ba concentrations can be estimated from nearby GEOSECS stations. Foraminifera were handpicked from disaggregated sediment samples and cleaned with a series of physical and chemical steps designed to remove any extraneous Ba not substituted into the lattice of the foraminiferal CaCO_3 . These cleaning steps begin with the foraminiferal Cd cleaning method (Boyle and Keigwin, 1985) with the addition of a step using alkaline diethylenetriamine-pentaacetic acid (DTPA) (Sill and Willis, 1964) to dissolve associated sedimentary barite (BaSO_4). Typical sample size before cleaning is 0.6 mg (10-30 individuals). Ba concentrations are quantified by isotope dilution flow injection analysis on an inductively coupled plasma--mass spectrometer (ICP-MS). Samples are spiked with ^{135}Ba with subsequent measurement of the 135/138 ratio. Accuracy is based on calibration of isotope dilution determinations to a gravimetric standard. The detection limit of the flow injection method is less than 0.2 nmol/l for a 200 μl injection volume (5 pg Ba). Signal to noise of samples was generally greater than 50:1. Ca is quantified by flame atomic absorption. The inter-run reproducibility for 39 analyses of a consistency standard containing 9.6 nmol/l

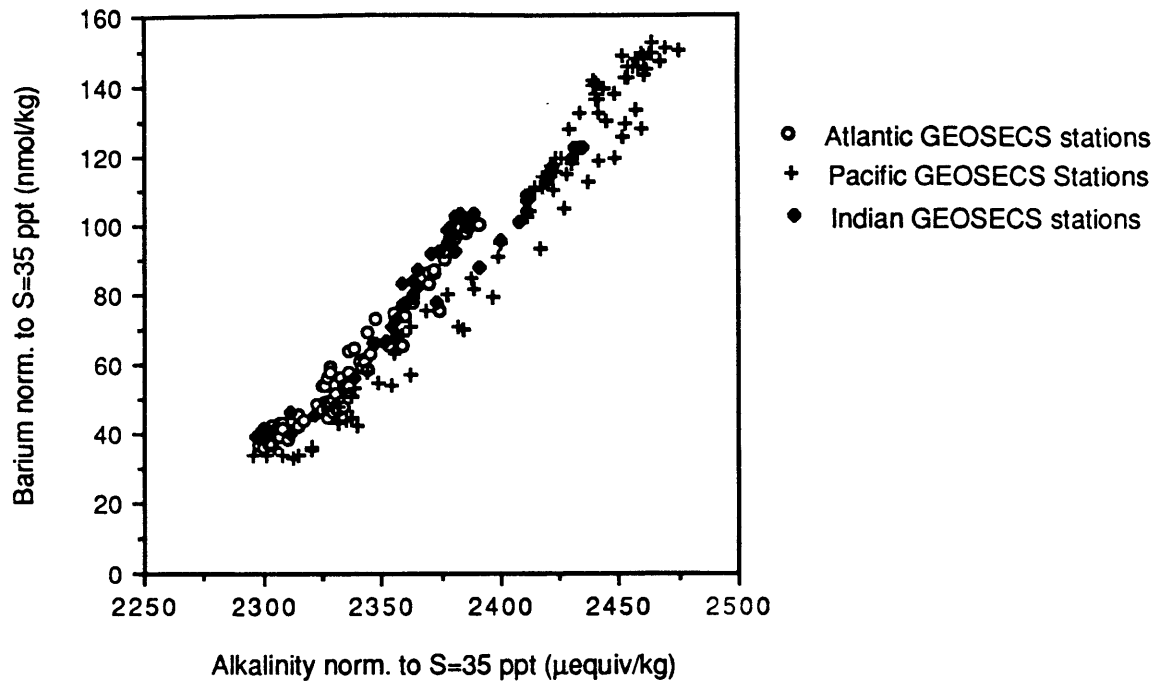


Figure 5.1 Paired Ba and alkalinity data from ocean water samples analyzed for the GEOSECS program (Bainbridge, 1981; Broecker *et al.*, 1982; Ostlund *et al.*, 1987; Weiss *et al.*, 1983). Alkalinity and barium are normalized to a constant salinity of 35 ppt. Included are: Atlantic Ocean stations 29, 82, and 111; Pacific Ocean stations 204, 226, 312, and 322; and, Indian Ocean stations 429 & 452.

Ba and 4.1 mmol/l Ca (Ba/Ca = 2.3 $\mu\text{mol/mol}$) was 2.6% for Ba, 1.5% for Ca and 3.1% for the Ba/Ca ratio. Although contamination during sample preparation and handling is negligible, occasional individual analyses are unreliable due to insufficient cleaning.

The Ba/Ca ratio of the three species studied (Figure 5.2 a,b & c; Table 5.1) increases linearly with increasing concentration in the bottom water. The scatter in the plots exceeds analytical precision and uncertainties in estimating Ba from nearby stations. This scatter may result from either 1) bioturbation, which can mix in older individuals (which may have lived at times when bottom water Ba concentrations were different) into the core top or, 2) a limit on the reliability of certain species of foraminifera as recorders of ambient Ba concentrations. The first factor is probably a primary cause of scatter for *C. wuellerstorfi* (Fig. 5.2a) because the most deviant points (low Ba/Ca ratios for high-Ba Pacific points) are from lower sedimentation rate cores. More limited data for the other two species precludes choice of an obvious cause for the offsets. Of the three species, *C. wuellerstorfi* shows the least scatter. However, one can not conclude that this species is necessarily a more reliable recorder of bottom water Ba because bioturbation combined with temporal abundance variations can bias core tops such that the mean age of each species present might not be the same. Because *Uvigerina spp.* is generally low in abundance during interglacials, *Uvigerina spp.* recovered from core tops are probably less likely to be representative of recent conditions than *C. wuellerstorfi*.

From the data in Fig. 5.2 an effective distribution coefficient $\{(Ba/Ca)_{\text{foraminifera}} = D(Ba/Ca)_{\text{seawater}}\}$ is calculated. $D = 0.36 \pm 0.06$ for the fractionation of Ba in the calcite of the three benthic species. In the present data set there is no evidence for significant differences in individual D for each species, although mean D ranges from 0.33 for *Uvigerina spp.* and 0.36 for

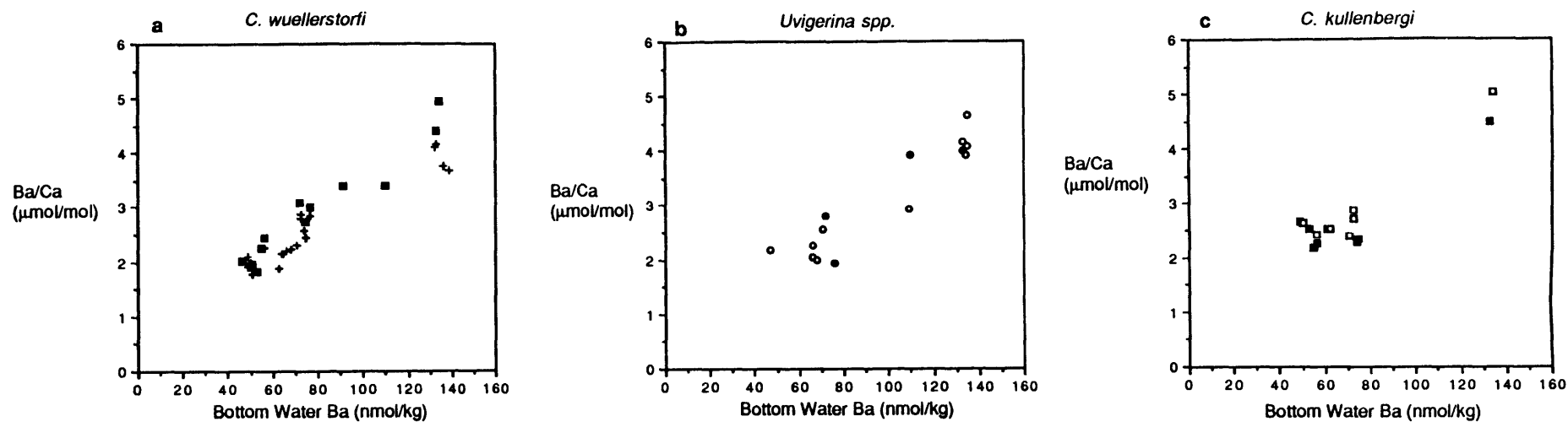


Figure 5.2 Ba/Ca in recent benthic foraminifera plotted against estimated bottom water barium concentrations. Samples from cores with >15 cm of Holocene sediment are indicated by darkened symbols. a, *C. wuellerstorfi* ; b, *Uvigerina spp.*; c, *C. kullenbergi*.

Core	Sample Depth (cm)	Latitude	Longitude	Water Depth (m)	Estimated bottom water Ba (nmol/kg)	Ba/Ca (μmol/mol)			
						<i>C. wuellerstorfi</i>	<i>C. kullenbergi</i>	<i>Uvigerina spp.</i>	
AI154	5PG	2-4	07° 25' S	89° 10' W	4165	133	4.18		4.16
AI1107	65GGC	4-7	32° 02' S	36° 11' W	2795	64	2.15		
AI1107	67GGC	0-2	31° 55' S	36° 12' W	2587	63	1.89 ± 0.06 (n=2)		
AI1107	69GGC	5-7	31° 40' S	36° 01' W	2158	66			2.26
AI1107	70GGC	2-4	31° 36' S	35° 59' W	2079	66	2.20		2.04
AI1107	71GGC	0-2	31° 31' S	35° 56' W	1887	68	2.24		2.00
CHN82	1PC	2-4	36° 06' N	07° 10' W	830	47			2.18
CHN82	3PC	13-16	41° 38' N	27° 20' W	2525	51	1.77		
CHN82	4PC*	0-2	41° 43' N	32° 51' W	3427	56	2.44	2.26 ± 0.01 (n=2)	
CHN82	9PC	7-10	41° 51' N	26° 27' W	2830	52	1.85		
CHN82	11PC*	1-6	42° 23' N	31° 48' W	3209	55	2.25	2.18 ± 0.06 (n=2)	
CHN82	15PC	3-5	43° 14' N	28° 08' W	2155	50	1.98 ± 0.02 (n=3)	2.63 ± 0.16 (n=2)	
CHN82	20PG*	4-7	43° 30' N	29° 52' W	3070	53	1.82	2.52 ± 0.04 (n=2)	
CHN82	21PG	4-8	43° 17' N	29° 50' W	2103	49	1.92	2.67	
EN66	10GGC	1-2	06° 39' N	21° 54' W	3527	74	2.58	2.28	
EN66	16GGC	1-3	05° 28' N	21° 08' W	3152	73	2.79	2.87	
EN66	21GGC*	3-12	04° 14' N	20° 38' W	3995	75	2.75	2.35	
EN66	26GGC	1-3	03° 05' N	20° 01' W	4745	77	2.86		
EN66	32GGC*	0-3	02° 28' N	19° 44' W	5003	77	3.00		
EN66	36GGC	2-3	04° 19' N	20° 13' W	4270	75	2.45		
EN66	38GGC	2-4	04° 55' N	20° 30' W	2931	71	2.31	2.39	2.56
EN66	44GGC	1-2	05° 16' N	21° 43' W	3428	73	2.89	2.72	
IOS82	PCS01	2-4	42° 23' N	23° 31' W	3540	61		2.54	
KNR64	5PG	6-8	16° 32' N	74° 48' W	3047	56	2.26	2.42	
KNR73	3PC*	5-6	00° 22' S	106° 11' W	3608	134	4.95		
OC173	G	4-6	31° 54' N	64° 18' W	4469	65	2.16 ± 0.10 (n=3)		
PS21295-4*		1-2	78° 00' N	02° 25' E	3112	46	2.03		
RC 11-120*		5-7	43° 31' S	79° 52' E	3135	91	3.41		
TR163-14		3-5	05° 41' N	87° 14' W	2365	132	4.12		
TR163-27		2-3	02° 15' S	86° 35' W	3180	135			4.66
TR163-28		1-2	02° 19' S	86° 14' W	3200	135			4.09
TR163-31B*		1-11	03° 57' S	85° 58' W	3210	133	4.41 ± 0.24 (n=3)	4.50	4.02 ± 0.47 (n=3)
TR163-32		2-4	02° 29' S	82° 59' W	2890	134		5.04	3.93 ± 0.15 (n=2)
V18-68*		10-12	54° 33' S	77° 51' W	3972	110	3.43		3.94
V22-174*		9-11	10° 04' S	12° 49' W	2630	76			1.94
V22-197*		14-17	14° 10' N	18° 35' W	3167	72	3.10		2.80
V22-198		4-6	14° 35' N	19° 40' W	1082	62		2.52	
V24-109		5-8	00° 26' N	158° 48' E	2367	136	3.76		
V27-60		5-8	72° 11' N	08° 34' E	2525	49	2.11		
V27-86*		5-8	66° 36' N	01° 07' E	2900	51	1.90		
V28-56*		3-4	68° 02' N	06° 07' W	2941	51	1.97		
V28-304		6-9	28° 32' N	134° 08' E	2942	139	3.69		
V32-159		15-17	48° 40' N	147° 24' E	1235	109			2.94

*indicates cores with >15 cm Holocene sediment

Table 5.1 Ba/Ca ratios in benthic foraminifera from Recent core tops

C. wuellerstorfi to 0.40 for *C. kullenbergi*. The uncertainty of D for each species can be improved by further analyses from high sedimentation rate cores, ultimately allowing us to determine if different benthic species have different effective distribution coefficients.

The estimate of the foraminiferal distribution coefficient applies only to cold deep waters ($\sim 3^{\circ}\text{C}$, $P\sim 300$ bars). Inorganic precipitation experiments performed at 20 to 25°C , 1 bar have generally yielded distribution coefficients of order 0.1, although much higher values are observed during the first stages of precipitation or during rapid precipitation (Kitano *et al.*, 1971). Observed foraminiferal D_{Sr} for chemically similar Sr is about a factor of four times higher than that observed for slow precipitation (Bender *et al.*, 1975; Delaney *et al.*, 1985; Lorens, 1981). Measurements of Ba in planktonic foraminifera indicate an effective distribution coefficient of about 0.2 (Chapter 4), although the restricted range of Ba concentrations in surface waters limits validation of the direct response of planktonic foraminifera to changes in surface water Ba concentrations. That this value is significantly different from the benthic D suggests that variables such as temperature, pressure, and biological factors may play a role in determining D.

In conclusion, the shells of benthic foraminifera preserve a record of ambient bottom water Ba concentrations. Therefore it will be possible to utilize fossil shells from deep-sea cores to reconstruct the distribution of Ba in the bottom waters of past oceans.

References--Chapter 5

- Bainbridge, A. E. (1981) *GEOSECS Atlantic Expedition, Vol.1, Hydrographic Data*. National Science Foundation, Washington, DC, 121p.
- Bender, M. L., Lorens, R. B. and Williams, D. F. (1975) Sodium, magnesium, and strontium in the tests of planktonic foraminifera. *Micropaleontology* **21**, 448-459.
- Bishop, J. K. B. (1988) The barite-opal-organic carbon association in oceanic particulate matter. *Nature* **332**, 341-343.
- Boyle, E. A. and Keigwin, L. D. (1982) Deep circulation of the North Atlantic over the last 200,000 years: Geochemical evidence. *Science* **218**, 784-787.
- Boyle, E. A. and Keigwin, L. D. (1985) Comparison of Atlantic and Pacific paleochemical records for the last 215,000 years: changes in deep ocean circulation and chemical inventories. *Earth planet Sci. Lett.* **76**, 135-150.
- Boyle, E. A. and Keigwin, L. D. (1987) North Atlantic thermohaline circulation during the past 20,000 years linked to high-latitude surface temperature. *Nature* **330**, 35-40.
- Broecker, W. S., Spence, D. W. and Craig, H. (1982) *GEOSECS Pacific Expedition Vol. 3, Hydrographic Data*. NSF, Washington, D.C., 137p.
- Chan, L. H., Drummond, D., Edmond, J. M. and Grant, B. (1977) On the barium data from the Atlantic GEOSECS Expedition. *Deep-Sea Res.* **24**, 613-649.
- Curry, W. B., Duplessy, J. -C., Labeyrie, L. D. and Shackleton, N. J. (1988) Changes in the distribution of $\delta^{13}\text{C}$ of deep water ΣCO_2 between the last glaciation and the Holocene. *Paleoceanography* **3**, 317-342.
- Delaney, M. L., Bé, A. W. H. and Boyle, E. A. (1985) Li, Sr, Mg, and Na in foraminiferal calcite shells from laboratory culture, sediment traps, and sediment cores. *Geochim. cosmochim. Acta.* **49**, 1327-1341.
- Duplessy, J. -C., Shackleton, N. J., Fairbanks, R. G., Labeyrie, L., Oppo, D. and Kallel, N. (1988) Deepwater source variations during the last climatic cycle and their impact on the global deepwater circulation. *Paleoceanography* **3**, 343-360.
- Edmond, J. M. (1974) On the dissolution of carbonate and silicate in the deep ocean. *Deep Sea Res.* **21**, 455-480.
- Keigwin, L. D. (1987) North Pacific deep water formation during the latest glaciation. *Nature* **330**, 362-364.

Kitano, Y., Kanamori, N. and Oomori, T. (1971) Measurements of distribution coefficients of strontium and barium between carbonate precipitate and solution--Abnormally high values of distribution coefficients at early stages of carbonate formation. *Geochem. J.* **4**, 183-206.

Lorens, R. B. (1981) Sr, Cd, Mn and Co distribution coefficients in calcite as a function of calcite precipitation rate. *Geochim. cosmochim. acta.* **45**, 553-561.

Ostlund, H. G., Craig, H., Broecker, W. S. and Spencer, D. W. (1987) *GEOSECS Atlantic, Pacific, and Indian Ocean Expeditions, Vol. 7, Shorebased Data and Graphics*. National Science Foundation, Washington, DC, 200p.

Sarnthein, M., Winn, K., Duplessy, J. C.-. and Fontugne, M. R. (1988) Global variations of surface ocean productivity in low and middle latitudes: influence on the CO₂ reservoirs of the deep ocean and atmosphere during the last 21,000 years. *Paleoceanography* **3**, 361-399.

Sill, C. W. and Willis, C. P. (1964) Precipitation of submicrogram quantities of thorium by barium sulfate and application to fluorometric determination of thorium in mineralogical and biological samples. *Anal. Chem.* **36**, 622-630.

Weiss, R. F., Broecker, W. S., Craig, H. and Spencer, D. W. (1983) *GEOSECS Indian Ocean Expedition Vol. 5, Hydrographic Data*. NSF, Washington, D.C., 48p.

Chapter 6: Ba in the glacial oceans

6.1 Introduction

Since the 1970's a primary goal in the study of Quaternary marine sediments has been elucidation of the deep thermohaline circulation of glacial oceans. Recent studies have generally focused on the use of the distinct chemical properties of individual deep water masses as a means of tracing temporal change in their oceanic distribution. Among the techniques pursued, studies of the $\delta^{13}\text{C}$ and Cd/Ca composition of benthic foraminifera have played a key role in showing that deep circulation of the glacial oceans was very different than today (Boyle and Keigwin, 1982; Boyle and Keigwin, 1985; Boyle and Keigwin, 1987; Curry *et al.*, 1988; Duplessy *et al.*, 1988; Keigwin, 1987). Both of these paleochemical tracers can be used to reconstruct past distributions of labile nutrients like PO_4 and NO_3 , the dissolved constituents of the biogeochemical recycling of organic soft parts of planktonic organisms.

A tracer of the more refractory nutrients Si and alkalinity, which have a different oceanic distribution than the labile nutrients, would provide new constraints on glacial circulation. Si and alkalinity (dominantly the sum of HCO_3^- and $2^*\text{CO}_3^{=}$) are depleted in surface waters because some plankton form hard parts from opal ($\text{SiO}_2 \cdot n\text{H}_2\text{O}$) and calcium carbonate (CaCO_3). These hard parts are recycled less efficiently than labile organic matter, of which the vast majority is oxidized above 1000 meters, and opal and calcium carbonate rich particulates sink into the deep ocean (Edmond, 1974). A large fraction of these particulates winds up in the sediments, where dissolution caused by undersaturated waters results in a flux of the dissolved species out of the sediments and into the bottom waters. The result of this cycle is an enrichment of these reactive species in the deepest waters of the oceans. The overprint of

thermohaline circulation on this cycle of uptake and regeneration results in fractionation of nutrients between ocean basins, with the lowest values in the North Atlantic where deep waters are flushed by nutrient depleted surface waters, to the highest values in the deep Pacific, deep waters farthest from sites of ventilation.

Although no method exists to reconstruct the distribution of this nutrient class directly, Lea and Boyle (1989) (Chapter 5) proposed that similarities between the distribution of Ba and the deeply regenerated nutrients in today's ocean allows paleo-Ba distributions to be used as a proxy for this nutrient class. Ba is removed from surface waters by uptake onto biogenic particulate matter, apparently in the form of the mineral barite (BaSO_4); however, unlike the vast portion of its organic matter host, barite survives destruction in the upper water column and is transported into the deep ocean, ultimately dissolving deep in the water column and/or in the sediments (Bishop, 1988; Chan *et al.*, 1977; Dehairs *et al.*, 1980). Thus oceanic Ba cycle shares some characteristics with Si and alkalinity, although there is no simple direct link between the cycles of the refractory nutrients and Ba. Deep water concentrations of Ba in the North Atlantic are about 55 nmol/kg, while the deep waters of the North Pacific rise to a maximum of about 150 nmol/kg. In today's ocean, foraminifera recovered from recent core tops reflect this basin-to-basin fractionation (Lea and Boyle, 1989)(Chapter 5); therefore one can compare foraminifera from the major ocean basins to see the affects of circulation change on the distribution of Ba.

The principal strategy of the study is to compare Ba/Ca in benthic foraminifera from glacial sections (stage 2 $\delta^{18}\text{O}$ maximum) with core-top values and/or the modern distribution of Ba. Coverage is aimed at elucidating the major features of the distribution of Ba in the glacial oceans, so cores that cover a wide areal extent and depth range are included in the study. However, since

availability of samples is limited, coverage is unequally weighted towards cores from the North Atlantic and Equatorial Pacific in the 2 to 3 km depth range.

6.2 Core Selection

Cores were selected on the basis of availability, the usefulness of coverage, and previously published stratigraphies. Cores are from the WHOI collection (cores beginning with All, CHN, KNR, EN66), URI collection (TR), and LDGO (RC and V). All of the samples from the LDGO collection remained from a companion study of Cd/Ca in glacial benthics; therefore, only certain species and depths for which benthic abundances were large enough were available for the Ba/Ca study.

For most cores Ba/Ca was determined on benthic foraminifera from, at, or near the $\delta^{18}\text{O}$ maximum (Table 6.1, Figure 6.1). However, for several cores complete benthic Ba/Ca records of the last 20 to 30 kyr (i.e. stage 1 and 2) of sedimentation have been recovered. These include three cores from the North Atlantic: CHN82 Sta. 24 Core 4PC (41°43'N, 32°51'W: 3427 m); CHN82 Sta. 31 Core 11PC (42°23'N, 31°48'W: 3209 m); and, CHN82, Sta. 41, core 15PC (43°14'N, 28°08'W: 2155 m); Caribbean core KNR64 Sta. 5 Core 5PG (16°32'N, 74°48'W: 3047 m); and equatorial Pacific core TR163 Core 31B (03°57'S, 85°58'W: 3210 m). Oxygen isotope, carbon isotope, and Cd/Ca records have been recovered for benthic foraminifera from all five cores in previous studies, and accelerator radiocarbon dates on both planktonic and benthic foraminifera are available for equatorial Pacific core TR163-31B (Boyle, 1988; Boyle and Keigwin, 1982; Boyle and Keigwin, 1985; Boyle and Keigwin, 1987; Curry *et al.*, 1988; Shackleton *et al.*, 1988). All five cores contain well-preserved planktonic and benthic foraminifera throughout their length. The sedimentation rate of the Atlantic cores ranges from about 1.5 to 5 cm/kyr over

Core	Map Code (Fig. 6.1)	Latitude	Longitude	Water Depth (m)	Sample Depth (cm)	Uvigerina mean SD ($\mu\text{mol/mol}$)	Ba/Ca n	wuellerstorfi mean SD ($\mu\text{mol/mol}$)	Ba/Ca n	NOTES	Cd/Ca* ($\mu\text{mol/mol}$)		
North Atlantic													
CHN82 Sta24 Core4PC	1	41° 43' N	32° 51' W	3427	54 - 75	3.37	0.21	9	3.50	0.21	2	0.111	
CHN82 Sta31 Core11PC	2	42° 23' N	31° 48' W	3209	73 - 87	3.27	0.27	7	3.54	0.17	4	0.100	
CHN82 Sta41 Core15PC	3	43° 14' N	28° 08' W	2155	26 - 40				2.30	0.17	3	0.040	
CHN82 Sta20 Core20PC	4	43° 30' N	29° 52' W	3070	86 - 106	3.30	0.42	2				0.099	
EN 66-10GGC	5	06° 39' N	21° 54' W	3527	33 - 34				3.17	0.02	2		
EN 66-38GGC	6	04° 55' N	20° 30' W	2931	23 - 27				3.73	0.12	3		
EN 66-44GGC	7	05° 16' N	21° 43' W	3428	28 - 31				3.69	0.03	2		
IOS82-PC SO1/1	8	42° 23' N	23° 31' W	3540	57 - 65.5	3.48	0.26	2				0.137	
KNR64 Sta5 Core5PG	9	16° 32' N	74° 48' W	3047	34 - 41				1.87	0.30	5	inc. kull	0.039
Mediterranean													
RC 9-203	10	36° 13' N	01° 58' W	1287	80 - 100				2.69	0.23	2	Cibs	
South Atlantic													
All107-65GGC	11	32° 02' S	36° 11' W	2795	38 - 44	2.07	0.15	5	3.50	0.38	2		0.120
RC12-294	12	37° 16' S	10° 06' W	3308	40 - 56	3.27	0.08	2	4.60	0.16	2	hi Mn?	0.153
RC13-229	13	25° 30' S	11° 20' E	4191	59 - 85.5	3.51	0.10	3					0.163
Southern Ocean													
RC11-120	14	43° 31' S	79° 52' E	3135	65 - 69	3.86	0.05	2					0.151
Equatorial Pacific													
KNR73 Sta4 Core3PC	15	00° 22' S	106° 11' W	3606	68 - 94	3.96	0.44	2	4.24	0.08	4		0.183
KNR 73 Sta5 Core4PC	16	10° 51' N	110° 16' W	3681	43 - 60	3.22	0.23	5					0.213
TR163-31B	17	03° 57' S	85° 58' W	3210	81 - 103	3.19	0.22	11	3.56	0.28	6		0.200
V19-27	18	00° 28' S	82° 04' W	1373	97 - 134	3.02	0.11	3	3.40	0.35	3		0.125
V19-28	19	02° 22' S	84° 39' W	2720	116 - 143	3.50	0.31	5				all hi Mn	0.190
V19-29	20	03° 35' S	83° 56' W	2673	133 - 155	3.29	0.10	2				all hi Mn	0.177
V21-29	21	00° 57' N	89° 21' W	712	156 - 191	2.10	0.04	4					0.103
V21-30	22	01° 13' S	89° 41' W	617	30 - 44	2.63	0.08	4					0.132
South Pacific													
RC15-61	23	40° 37' S	77° 12' W	3771	58 - 87	3.43	0.36	3				hi Mn	0.162
Western Pacific													
V21-146	24	37° 41' N	163° 02' E	3968	34 - 41				3.93	0.07	2	no DTPA	0.186
V28-235	25	05° 27' S	160° 29' E	1746	35 - 45	4.09	0.54	2	3.60	0.23	3		0.161
Indian Ocean													
RC11-147	26	19° 02' S	112° 27' E	1953	45 - 61	3.15	0.17	3	3.61	0.11	3	inc. kull	0.141

*E. Boyle, pers. comm.

Table 6.1 Ba/Ca measured in benthic foraminifera from glacial (18 kyr) core sections. Core numbering refers to Figure 6.1. Also listed are benthic foraminiferal Cd/Ca averages for glacial sections (E. Boyle, pers. comm.).

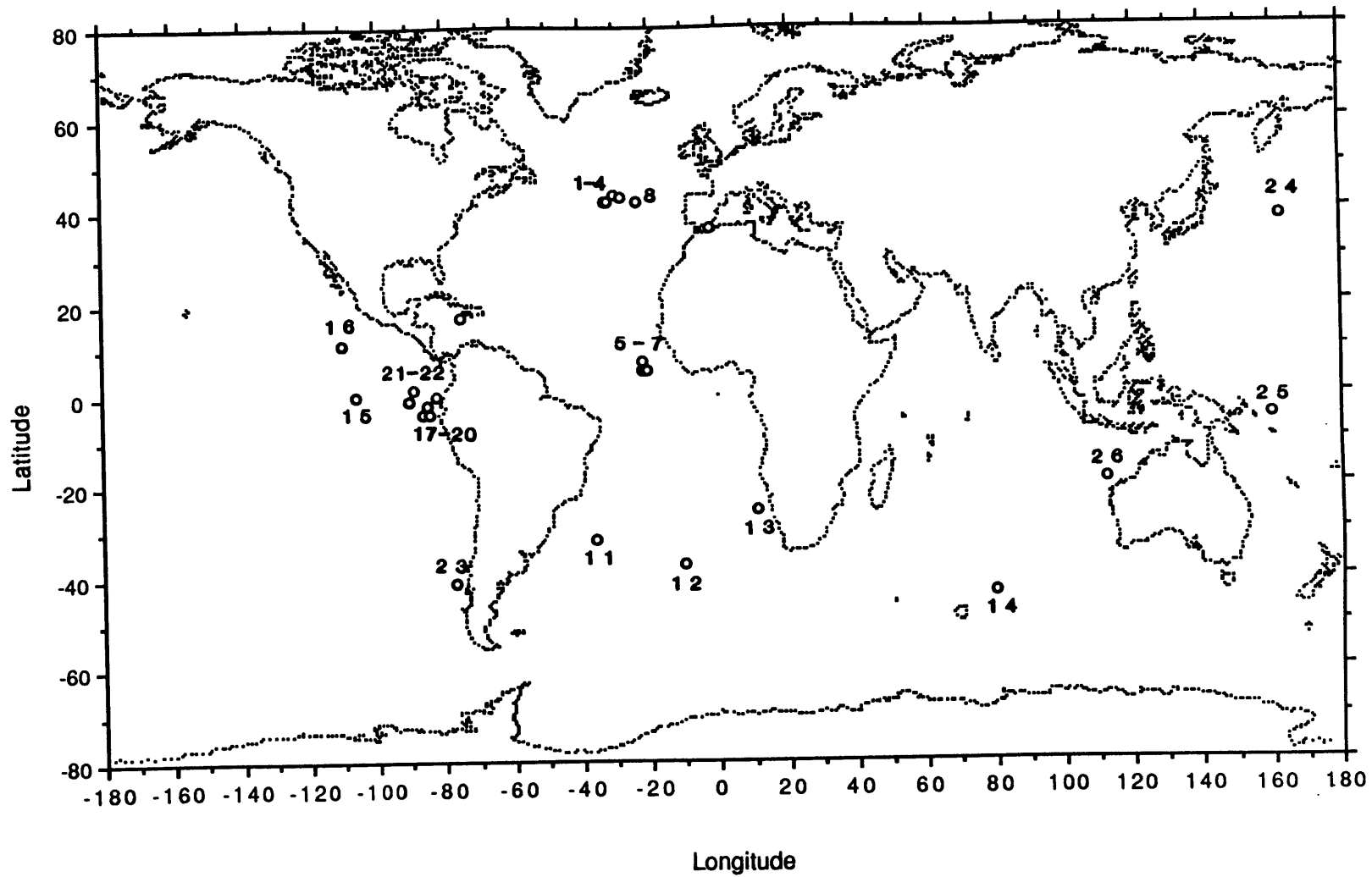


Figure 6.1 Location of cores used in this study. See Table 6.1 for key to core numbering.

the interval studied, while the Pacific core has an average sedimentation rate of about 5.5 cm/kyr.

6.3 Methods

Foraminifera were handpicked from disaggregated sediment samples and cleaned with a series of physical and chemical steps designed to remove any extraneous Ba not substituted into the lattice of the foraminiferal CaCO_3 . These cleaning steps begin with the foraminiferal Cd cleaning method (Boyle, 1981; Boyle and Keigwin, 1985) with the addition of a step using alkaline diethylenetriamine-pentaacetic acid (DTPA) (Chapter 2) to dissolve associated sedimentary barite (BaSO_4). Typical sample size before cleaning is 0.6 mg (10-35 individuals). Generally about 100-200 μg of calcite remains after cleaning; about half of this loss is due to removal of fine CaCO_3 and adhering clays; the other half is due to partial dissolution of the foraminiferal calcite that occurs during the reductive hydrazine-citrate step and the alkaline-DTPA step. The DTPA dissolves calcite quite readily, and therefore cleaning times must be carefully balanced for sample size.

Ba concentrations are quantified by isotope dilution flow injection analysis on a VG plasmaquad inductively coupled plasma--mass spectrometer (ICP-MS). After dissolution in nitric acid samples are spiked with ^{135}Ba and the 135/138 ratios are subsequently measured on the ICP-MS. Accuracy of the Ba determinations is based on calibration of isotope dilution determinations to a gravimetric standard. The detection limit of the flow injection method is less than 0.1 nmol/l for a 200 μl injection volume (5 pg Ba). Signal to noise of samples is generally greater than 50:1. Splits of the samples are quantified for Ca by flame atomic absorption. The inter-run reproducibility for 89 analyses of 300 μl of consistency standard "CN2" containing 9.6 nmol/l Ba and 4.1 mmol/l Ca (Ba/Ca

= 2.4 $\mu\text{mol/mol}$) was 2.6% for Ba, 1.7% for Ca and 3.1% for Ba/Ca (1 standard deviation); 58 analyses of a second consistency standard ("CN3") containing 19.4 nmol/L Ba and 6.2 mmol/L Ca (Ba/Ca = 3.1 $\mu\text{mol/mol}$) were reproducible to 2.2% for Ba, 1.6% for Ca, and 2.6% for Ba/Ca. Laboratory contamination for Ba or Ca is minimal.

Reproducibility of replicate picks of foraminifera from the same samples seldom as good as the analytical reproducibility of consistency standards. In this study the pooled standard deviation for replicates (or difference from the mean when $n=2$) for the 3 cores with the most replicates was ± 0.25 $\mu\text{mol/mol}$ Ba/Ca (7%) for TR163-31B, ± 0.22 $\mu\text{mol/mol}$ (8%) for CHN82-4PC, and ± 0.27 $\mu\text{mol/mol}$ (10%) for CHN82-11PC. The decrease in precision associated with real samples is presumably related to bioturbation which mixes together individuals that lived at different times when Ba contents might have been different (Boyle, 1984; Lea and Boyle, 1989). However, some portion of this variability might be due to imperfect cleaning and/or imperfect nature of the foraminifera as chemical recorders of bottom water Ba. For this reason no single data point on its own should be taken as conclusive.

6.4 Core Data

Down-core Ba/Ca values for foraminifera from North Atlantic cores CHN82 11PC and 15PC have been obtained (Table 6.2 a and b, 7.1; Figure 6.2). Ba/Ca records for these three North Atlantic cores are plotted on a common age scale based on cross correlated oxygen isotope records (Boyle and Keigwin, 1982; Boyle and Keigwin, 1985; Boyle and Keigwin, 1987). Age points are given in the appendix to Chapter 6. Ba/Ca was recovered for *C. wuellerstorfi*, *Uvigerina spp.*, and *C. kullenbergi* where abundances permitted. The records in Fig. 6.2 are based on *C. wuellerstorfi* for cores 11 PC and

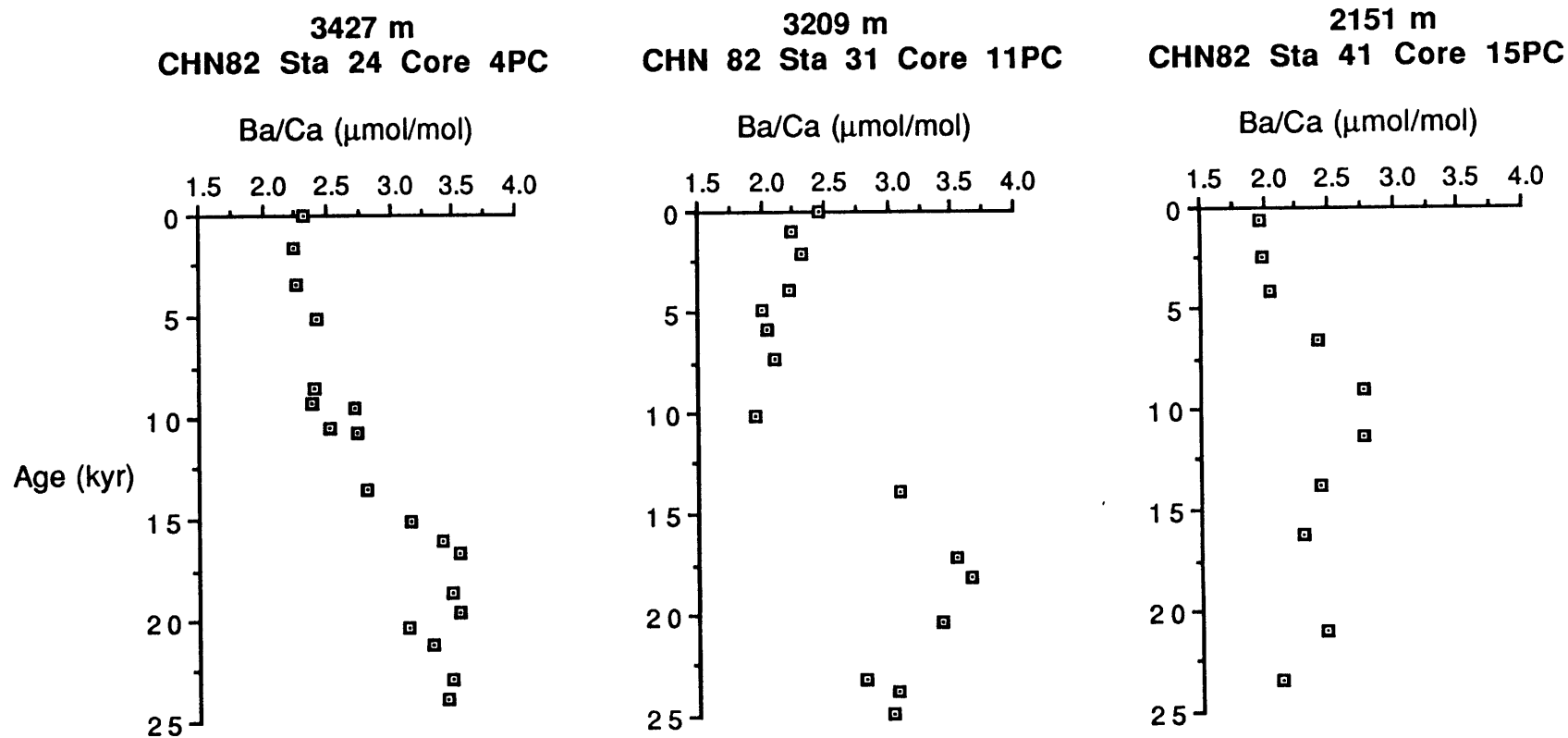


Figure 6.2 Records of benthic foraminiferal Ba/Ca from three CHN82 cores in the North Atlantic. The records are placed on a time scale based on their oxygen isotope records (Boyle and Keigwin, 1982; 1985; 1987). Values for 11PC and 15 PC based on *C. wuellerstorfi*; values for 4PC are based on *C. kullenbergi* and *Uvigerina spp.* (see Chapter 7).

Depth (cm)	Species	Ba/Ca μmol/mol	SD	n	r
0.5 - 2	kull	2.23		1	
0.5 - 2	wuell	2.45		1	
4.5 - 6	kull	2.12		1	
4.5 - 6	wuell	2.25		1	
8.5 - 10.5	kull	2.24		1	
8.5 - 10.5	wuell	2.32		1	
11 - 15	kull	2.16	0.03	2	
16 - 18	kull	2.36		1	
16 - 18	wuell	2.23		1	
20.5 - 22	kull	2.38		1	
20.5 - 22	wuell	2.01		1	
24 - 26	kull	2.57		1	
24 - 26	wuell	2.05		1	
28 - 30	kull	2.48		1	
28 - 34	wuell	2.11		1	
37.5 - 43	kull	2.66		1	
41.5 - 43	wuell	1.96		1	
45 - 47	kull	2.65		1	
49.5-56.5	kull	3.31		1	
54.5 - 61	Uvig	2.45		1	
54.5 - 61	wuell	3.09		1	
69 - 71	wuell	3.54	0.17	2	
73 - 75	Uvig	3.28	0.26	2	
73 - 75	wuell	3.64		1	
76.5-78	Uvig	3.46	0.12	2	
76.5-78	wuell				1
81 - 83	Uvig	2.86		1	
81-86.5	wuell	3.42		1	
84.5-86.5	Uvig	3.16		1	
84.5-86.5	Uvig	3.36		1	
96-97.5	Uvig	2.53		1	
96-97.5	wuell	2.82		1	
99-101	Uvig	2.59	0.51	2	
99-101	wuell	3.06	0.19	2	
104-106	Uvig	3.00	0.30	2	
104-106	wuell	3.03	0.23	2	
108.5-110.5	kull	3.62		1	
108.5-110.5	Uvig	2.83	0.12	2	
108.5-110.5	wuell	2.94		1	
113.5-115.5	Uvig	2.77	0.02	2	
113.5-115.5	wuell	3.03		1	
116-117	Uvig	2.57	0.05	2	
116-117	wuell	2.46		1	
120-122	Uvig	2.68	0.12	2	
120-122	wuell	2.67	0.13	2	
124-126	Uvig	2.53	0.36	4	
124-127	wuell	2.91	0.44	2	
126-127	Uvig	2.68	0.09	2	
129-130	Uvig	2.52	0.26	2	
129-130	wuell	3.38		1	
133.5-135	Uvig	2.98		1	
135-137	Uvig	2.44		1	
137.5-139	Uvig	3.70		1	
140.5-142	Uvig	2.86		1	
140.5-142	wuell	3.79		1	
142-144	Uvig	3.14		1	
142-144	wuell	2.69		1	
144-146	Uvig	2.96	0.31	3	
144-146	wuell	3.03		1	1

Table 6.2 a Ba/Ca in benthic foraminifera from North Atlantic core CHN82 Sta31 Core11PC. Key to species: kull = *C. kullenbergi*; wuell = *C. wuellerstorfi*; Uvig = *Uvigerina spp.* SD = standard deviation; n = number of samples included in mean; r = number of samples rejected from mean.

Interval (cm)	Species	Ba/Ca ($\mu\text{mol/mol}$)	n	r
0 - 2	wuell	1.97	1	
3 - 5	wuell	1.98	1	
6 - 8	wuell	2.05	1	
10 - 12	wuell	2.41	1	
14 - 16	wuell	2.76	1	
18 - 20	wuell	2.77	1	
22 - 24	wuell	2.43	1	
26 - 28	wuell	2.30	1	
24 - 26	wuell	2.47	1	
38 - 40	wuell	2.12	1	

Table 6.2 b Ba/Ca in benthic foraminifera from North Atlantic core CHN82
Sta41 Core15PC.

15 PC; since *C. wuellerstorfi* abundances are low in core 4 PC, this record is based on *C. kullenbergi* in the Holocene and *Uvigerina spp.* in stage 2 (see Chapter 7 for tabulated data for Core 4PC).

In the two deep cores Atlantic cores (Core 4PC: 3427 m; Core 11PC: 3209 m) Late Holocene Ba/Ca averages about 2.3 $\mu\text{mol/mol}$. Ba/Ca at the glacial $\delta^{18}\text{O}$ maximum rises to about 3.5 $\mu\text{mol/mol}$, an enrichment in Ba of approximately 50%. The enrichments in Ba in glacial North Atlantic deep waters coincide with previously observed enrichments for Cd and lower $\delta^{13}\text{C}$ in the last glacial period. Increases in the nutrient contents of the waters that bathed these sediments has been interpreted as an indication of a reduction in the flushing of nutrient-depleted North Atlantic Deep Water (NADW) during glacial periods (Boyle and Keigwin, 1982; Boyle and Keigwin, 1985; Boyle and Keigwin, 1987).

Comparison of the Cd/Ca and Ba/Ca records from core 11PC indicates a strong covariance between these two nutrient indicators; both tracers are at their minimum in the Holocene and reach their maximum values at the glacial $\delta^{18}\text{O}$ maximum (Fig. 6.3) Both tracers increase by about 50% from Holocene to Glacial. Thus all three paleochemical nutrient proxies ($\delta^{13}\text{C}$, Cd/Ca, Ba/Ca) record enrichments in nutrients in the deep waters of the North Atlantic at the last glacial maximum. Such correspondence would be expected if fluctuations in these tracers are caused by changes in the flux of nutrient depleted water to these sites. Changes in the chemistry of the bottom waters due to *in situ* chemical processes would not affect Cd, $\delta^{13}\text{C}$ and Ba similarly because of contrasting chemical controls.

In contrast to the deep water sites, *C. wuellerstorfi* from mid-depth North Atlantic core CHN82-15PC do not show significantly higher Ba/Ca in the glacial section (Fig. 6.2). Values are somewhat higher during deglaciation; Oppo and

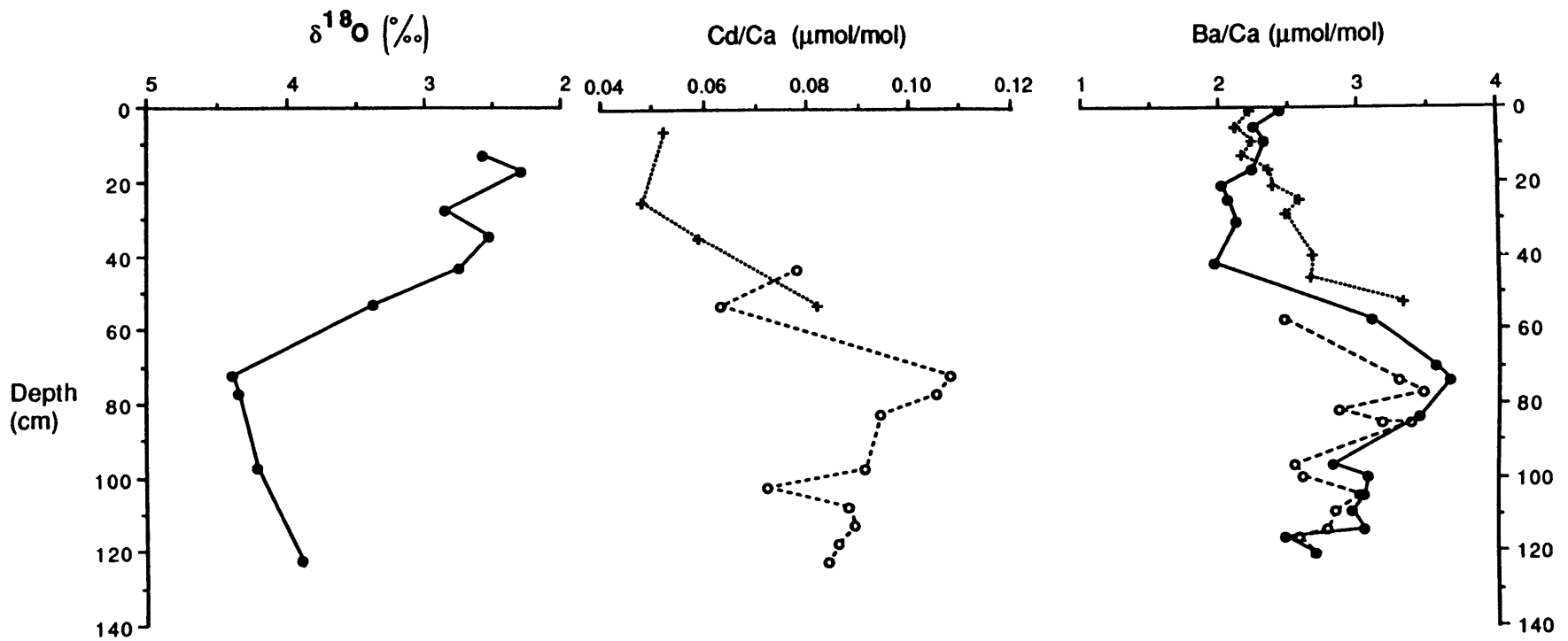


Figure 6.3 Comparison of benthic foraminiferal $\delta^{18}\text{O}$, Cd/Ca and Ba/Ca from CHN82 Sta 31 core 11PC (Boyle and Keigwin, 1982). Crosses indicate *C. kullenbergi*, filled dots indicate *C. wuellerstorfi*, and open dots indicates *Uvigerina* spp. Note coincidence of Cd and Ba maxima with $\delta^{18}\text{O}$ maximum.

Fairbanks (1989) have reported a deglacial benthic $\delta^{13}\text{C}$ minimum (i.e. higher nutrients) in an intermediate depth core. Full glacial Ba/Ca values in 15PC are not significantly higher than late Holocene values. Cd/Ca values are unchanged over the interval studied (Boyle and Keigwin, 1987).

Benthic Ba/Ca from Caribbean core KNR64-5PG substantiates the contrast between intermediate and deep water Ba suggested by the CHN82 records (Fig. 6.4, Table 6.3). Since the Caribbean is filled by North Atlantic waters from 1700~1800 m depth the composition of Caribbean deep waters records changes in the composition of Atlantic intermediate waters (Boyle and Keigwin, 1987). Benthic Ba/Ca of *C. wuellerstorfi* and *C. kullenbergi* recovered from the glacial section of core KNR64-5PG are slightly lower than Holocene values (Fig. 6.4). Although the change is relatively small (about 0.5 $\mu\text{mol/mol}$ or 20%) it is recorded by both benthic species. Ba/Ca of benthic foraminifera recovered from the glacial section of core KNR64-5PG are among the lowest values measured in any sediments studied so far (Lea and Boyle, 1989) (Chapter 5). Boyle and Keigwin (1987) found low Cd/Ca and increased $\delta^{13}\text{C}$ in glacial benthic foraminifera from this core. Thus three proxies for nutrients suggest marked nutrient depletion in the intermediate waters of the glacial North Atlantic.

In order to compare temporal records of bottom water Ba in the Atlantic with the Pacific we have recovered benthic Ba/Ca from core TR163-31B taken at 3210 m on the Carnegie Ridge. This high sedimentation rate core (~5.5 cm/kyr) preserves a foraminiferal record of the last 30 kyrs, although the last 5000 years are not present in the core, possibly due to loss during coring (Shackleton *et al.*, 1988). Fig. 6.5 illustrates down-core records of *C. wuellerstorfi* and *Uvigerina spp.* Ba/Ca for this core (Table 6.4). The major features of both benthic Ba/Ca records are highest values in the Holocene,

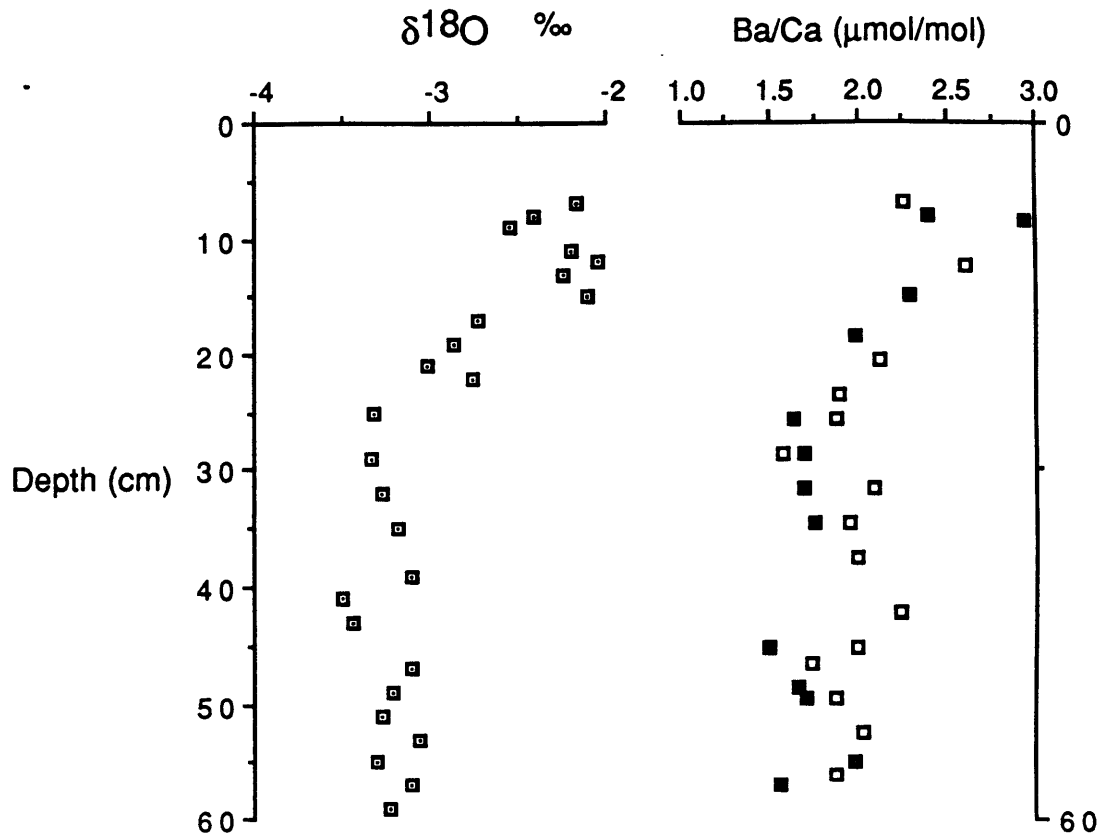


Figure 6.4 Benthic foraminiferal Ba/Ca and $\delta^{18}\text{O}$ (Boyle and Keigwin, 1987) from Caribbean core KNR64 5PG. Open squares are values from *C. wuellerstorfi* and filled squares are from *C. wuellerstorfi*.

Depth (cm)	Species	Ba/Ca ($\mu\text{mol/mol}$)	SD	n	r
6 - 8	wuell	2.28		1	
6 - 10	kull	2.68	0.26	2	
12 - 13	wuell	2.61		1	
13.3-16.7	kull	2.25		1	
16 - 21	kull	1.99		1	
20 - 21	wuell	2.12		1	
23 - 24	wuell	1.90		1	
25 - 26	kull	1.63		1	
25 - 26	wuell	1.88		1	
28 - 29	kull	1.72		1	
28 - 29	wuell	2.24		1	
31 - 32	kull				1
31 - 32	wuell	1.74		1	
34 - 35	kull	1.69		1	
34 - 35	wuell	1.58		1	
37 - 38	wuell	2.09		1	
37 - 41	kull	1.70		1	
40 - 44	wuell	1.88		1	
43.3-46.7	kull	1.47		1	
43.3-46.7	wuell	1.93		1	
46 - 47	wuell	2.03		1	
46.7-50	kull	1.64		1	
49 - 50	kull	1.57		1	
49 - 50	wuell	1.88		1	
50-53.3	kull	1.78		1	
52 - 53	wuell	1.96		1	
53.3-56.7	kull	1.96		1	
55 - 57	wuell	2.00		1	
55 - 59	kull	1.76		1	

Table 6.3 Ba/Ca in benthic foraminifera from Caribbean core KNR64 Sta5 Core5PG. Key to species: kull = *C. kullenbergi*; wuell = *C. wuellerstorfi*.

intermediate values in the glacial to interglacial transition, a clear Ba/Ca minimum associated with the ^{18}O -maximum, and relatively stable values intermediate between the two extremes in the 15 kyrs before the glacial maximum. Ba/Ca in *C. wuellerstorfi* averages about 0.5 $\mu\text{mol/mol}$ higher (10-15%) than Ba/Ca in *Uvigerina spp.*; this offset has previously been observed in Ba distribution coefficients calculated from core top benthic foraminiferal Ba/Ca (Lea and Boyle, 1989) (Chapter 5). Both species show the same major trends, and the agreement between species confirms that the observed Ba/Ca signal does reflect variations in the Ba content of bottom waters.

The Ba/Ca records in core TR163-31B display considerable high frequency variability (events of about 1 to 2 kyr duration). This variability is observed for both species, although peaks do not correspond to better than ± 10 cm in depth. However, this lack of correspondence does not preclude the signals having originated from the same environmental signal since differential changes in species abundance coupled with bioturbation can bias one species versus another over this sediment depth. High frequency variability in this core has previously been observed for both Cd (Boyle, 1988) and $\delta^{13}\text{C}$ (Shackleton, unpublished data). It is likely that this variability, normally smoothed out in cores accumulating at lower sedimentation rates, is seen in TR163-31B because of the high sedimentation rate.

The Pacific record is essentially the mirror image of the deep Atlantic records, although the magnitude of change in Ba/Ca is smaller in the Pacific. Pacific benthic Ba/Ca is about 0.8 $\mu\text{mol/mol}$ lower at the LGM relative to the Holocene, corresponding to a relative change of about 25% as recorded by Ba/Ca records of both species. This change is about one-half to two-thirds of the increase observed in the glacial-interglacial records from the two deep CHN82 cores in the North Atlantic.

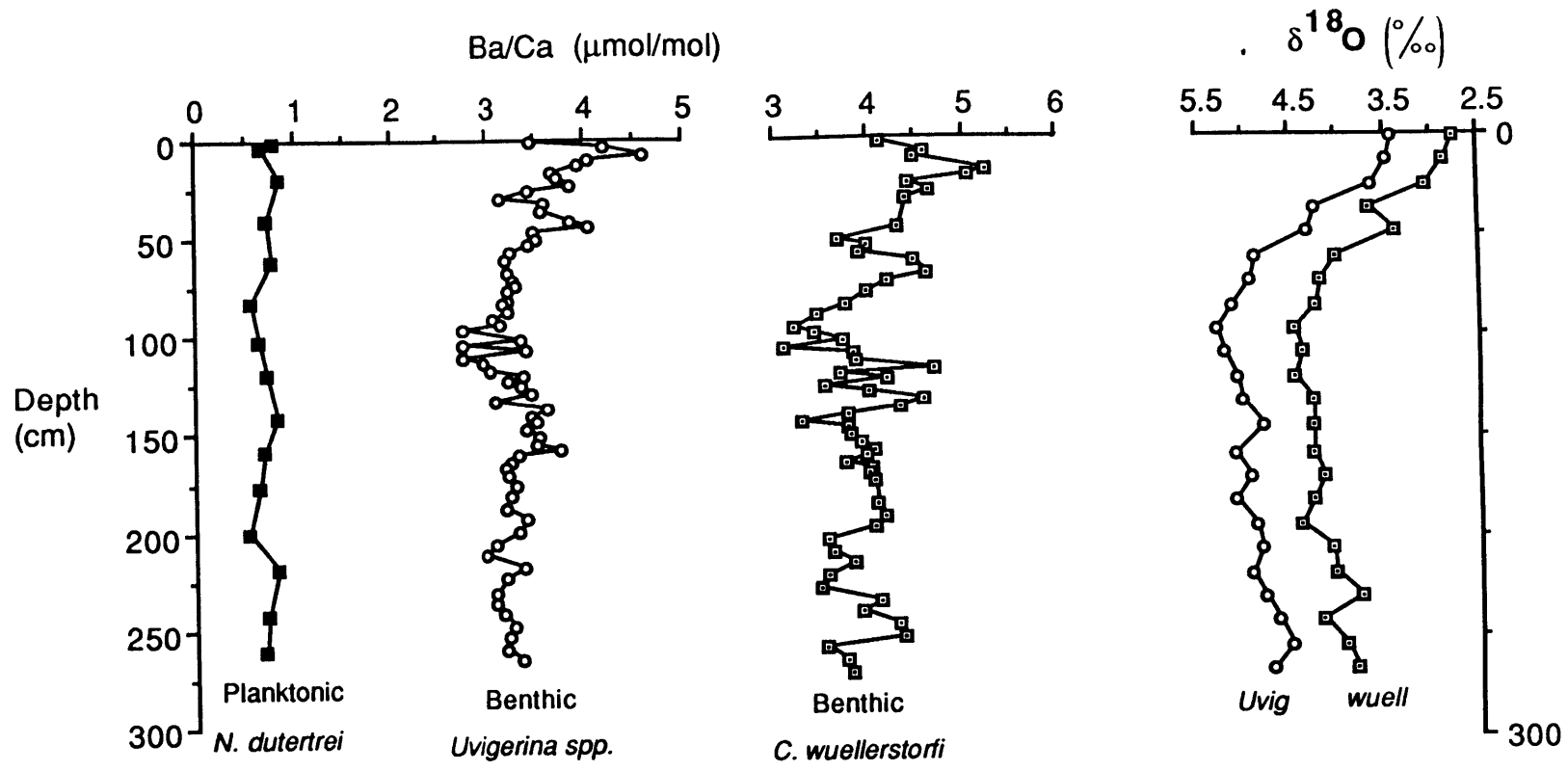


Figure 6.5 Foraminiferal Ba/Ca from Eastern Equatorial Pacific core TR163-31B. Open squares are points from *C. wuellerstorfi*, open circles are points from *Uvigerina* spp., and filled squares are points from the planktonic species *N. dutertrei*. Also shown are *Uvigerina* and *wuellerstorfi* $\delta^{18}\text{O}$ (Shackleton *et al.*, 1988; N. Shackleton, unpublished data).

Depth (cm)	Species	Ba/Ca ($\mu\text{mol/mol}$)	SD	n	r
0 - 2	duter	0.78	0.10	2	
0 - 2	Uvig	3.48	0.24	2	
0 - 5.5	wuell	4.14		1	
3.5 - 5.5	duter	0.67	0.04	2	
3.5 - 5.5	Uvig	4.21		1	
7 - 8.5	Uvig	4.61		1	
7 - 8.5	wuell	4.60		1	
7 - 11.5	kull	4.50		1	
10 - 11.5	Uvig	4.05	0.02	2	
10 - 11.5	wuell	4.50		1	
13 - 14.5	Uvig	3.94	0.10	2	
16 - 17.5	kull	4.80		1	
16 - 17.5	Uvig	3.68	0.16	2	
16 - 17.5	wuell	5.26	0.12	2	
19 - 20	duter	0.85	0.01	2	
19 - 20	Uvig	3.72		1	
19 - 20	wuell	5.07		1	
23 - 24	Uvig	3.85	0.27	2	
23 - 24	wuell	4.42		1	
26 - 27.5	Uvig	3.43		1	
26 - 27.5	wuell	4.64	0.41	2	
29.5 - 30.5	Uvig	3.15		1	
29.5 - 30.5	wuell	4.39		1	
32.5 - 33.5	Uvig	3.60		1	
36.5 - 37.5	Uvig	3.57	0.22	2	
40 - 41	duter	0.72		1	1
40 - 41	Uvig				1
41 - 43	Uvig	3.87		1	
44 - 46	Uvig	4.04	0.42	4	
44 - 46	wuell	4.31		1	
46.5 - 48.5	Uvig	3.50		1	
50 - 51.5	Uvig	3.51		1	
50 - 51.5	wuell	3.68		1	
53 - 55	Uvig	3.44	0.10	2	
53 - 55	wuell	3.99		1	
56.5 - 58.5	wuell	3.92	0.31	2	
56.5 - 58.5	Uvig	3.26	0.14	0	
60.5 - 62	duter	0.76	0.07	2	
60.5 - 62	Uvig	3.21	0.15	3	
60.5 - 62	wuell	4.49		1	
63.5 - 65.5	Uvig				1
63.5 - 65.5	wuell				1
66.5 - 68.5	Uvig	3.24	0.25	3	
66.5 - 68.5	wuell	4.62		1	
71 - 73	Uvig	3.29	0.16	4	
71 - 73	wuell	4.21		1	
74 - 76	Uvig	3.32	0.25	2	

Table 6.4 Ba/Ca in foraminifera from Eastern equatorial Pacific core TR163-31B. Key to species: kull = *C. kullenbergi*; wuell = *C. wuellerstorfi*; Uvig = *Uvigerina* spp.; duter = *N. dutertrei*.

Depth (cm)	Species	Ba/Ca ($\mu\text{mol/mol}$)	SD	n	r
74 - 78.5	wuell	4.00		1	
76.5 - 78.5	Uvig	3.24	0.40	2	
81 - 83	duter	0.55	0.03	2	
81 - 83	Uvig	3.24		1	1
81 - 85.5	wuell	3.78		1	
83.5 - 84.5	Uvig	3.17	0.16	2	
86.5 - 88.5	Uvig	3.22	0.07	2	
86.5 - 88.5	wuell	3.47		1	
90.5 - 92.5	Uvig	3.07		1	
94 - 95.5	Uvig	3.16		1	
94 - 95.5	wuell	3.21		1	
97 - 98	Uvig	2.75		1	
97 - 98	wuell	3.45		1	
97 - 102.5	wuell	3.74	0.28	2	
101.5 - 102.5	duter	0.64	0.05	2	
101.5 - 102.5	Uvig	3.36	0.26	3	
103.5 - 105.5	Uvig	2.74		1	
103.5 - 105.5	wuell	3.11		1	
107 - 108	Uvig	3.41		1	
107 - 108	wuell	3.86		1	
110.5 - 112.5	Uvig	2.75		1	
110.5 - 112.5	wuell	3.87		1	
114 - 115	Uvig	2.95		1	
114 - 115	wuell	4.70		1	
116.5 - 118.5	Uvig	3.05		1	
116.5 - 118.5	wuell	3.71	0.01	0	
119 - 121	duter	0.70	0.13	6	
120 - 121	Uvig	3.38		1	
120 - 121	wuell	4.20		1	
122.5 - 124	Uvig	3.23		1	
122.5 - 124	wuell	3.55		1	
125 - 126.5	Uvig	3.35		1	
125 - 126.5	wuell	4.02		1	
129.5 - 130.5	Uvig	3.47		1	
129.5 - 130.5	wuell	4.59		1	
133.5 - 135	Uvig	3.09	0.08	2	
133.5 - 135	wuell	4.35		1	
136.5 - 138	Uvig	3.62		1	
136.5 - 138	wuell	3.80		1	
140.5 - 142	duter	0.81	0.15	2	
140.5 - 142	Uvig	3.47		1	
140.5 - 142	wuell	3.30	0.43	2	
144 - 145	Uvig	3.53		1	
144 - 145	wuell	3.80	0.15	2	
147 - 148	Uvig	3.41		1	
147 - 148	wuell	3.83		1	
151 - 152	Uvig	3.53		1	
151 - 152	wuell	3.94		1	
154 - 158	Uvig	3.52		1	

Table 6.4 Ba/Ca in foraminifera from core TR163-31B (cont.).

Depth (cm)	Species	Ba/Ca ($\mu\text{mol/mol}$)	SD	n	r
154 - 158	wuell	4.08		1	
158 - 159	duter	0.69	0.13	2	
158 - 159	Uvig	3.77		1	
158 - 159	wuell	4.00		1	
161 - 162	Uvig	3.32		1	
161 - 162	wuell	3.78		1	
164 - 165	Uvig	3.26		1	
164 - 165	wuell	4.05		1	
167 - 168	Uvig	3.21		1	
167 - 168	wuell	4.03		1	
171 - 172	Uvig	3.23	0.20	2	
171 - 172	wuell	4.06		1	
176 - 177	duter	0.63	0.11	2	
176 - 177	Uvig	3.32		1	
176 - 177	wuell				1
182 - 183	Uvig	3.26		1	
182 - 183	wuell	4.09		1	
188 - 189	Uvig	3.21		1	
188 - 189	wuell	4.20		1	
194 - 195	Uvig	3.40		1	
194 - 195	wuell	4.08	0.02	2	
200 - 201	duter	0.52	0.02	2	
200 - 201	Uvig	3.33		1	
200 - 201	wuell	3.58		1	
206 - 207	Uvig	3.10		1	
206 - 207	wuell	3.62		1	
212 - 213	Uvig	2.99		1	
212 - 213	wuell	3.85		1	
218 - 219	duter	0.81	0.16	2	
218 - 219	Uvig	3.39		1	
218 - 219	wuell	3.58		1	
224 - 225	Uvig	3.21		1	
224 - 225	wuell	3.50		1	
230 - 231	wuell	4.12		1	
231 - 232	Uvig	3.08		1	
236 - 237	Uvig	3.09		1	
236 - 237	wuell	3.93		1	
242 - 243	duter	0.71	0.16	2	
242 - 243	Uvig	3.17		1	
242 - 243	wuell	4.32		1	
248 - 249	Uvig	3.28		1	
248 - 249	wuell	4.37		1	
254 - 255	Uvig	3.22	0.33	2	
254 - 255	wuell	3.54		1	
260 - 261	duter	0.68	0.25	2	
260 - 261	Uvig	3.20	0.03	2	
260 - 261	wuell	3.78		1	
266 - 267	Uvig	3.37		1	
266 - 267	wuell	3.81	0.01	2	

Table 6.4 Ba/Ca in foraminifera from core TR163-31B (cont.).

To complement the benthic records from core TR163-31B planktonic Ba/Ca from *N. dutertrei* has been recovered at 20 cm intervals (Fig. 6.5, Table 6.4). Documentation of the response of planktonic foraminifera to surface water Ba is difficult because of the small range of Ba concentrations encountered in surface waters of the temperate and tropical oceans. However, limited study does tend to suggest that certain planktonic foraminifera varieties do record surface water Ba (Chapter 4). Planktonic foraminifera apparently take up Ba with a distribution coefficient of about 0.2, in contrast to calculated distribution coefficients for benthic foraminifera of 0.34-0.41 (Lea and Boyle, 1989) (Chapter 5).

Planktonic foraminifera record small changes in Ba content, but it is difficult to assign with confidence a clear change associated with the single glacial/interglacial cycle represented in this core. Some of the variability in this record might be due to the difficulty of cleaning planktonic foraminifera, since they contain less lattice-bound Ba and have greater surface areas. Average glacial planktonic Ba/Ca is about 0.1 $\mu\text{mol/mol}$ lower than the Holocene; correcting for the difference in distribution coefficients, this planktonic change is equivalent to a benthic change of about 0.2 $\mu\text{mol/mol}$, or about 1/4 the glacial reduction observed for the benthics in TR163-31B. The calculated relative change between Glacial and Holocene conditions in surface water Ba derived from core TR163-31B is an increase of $15\pm 15\%$.

Glacial records of foraminiferal Ba from the cores discussed above suggest significant changes in the distribution of Ba in the deep glacial ocean. To further investigate these distributions Ba has been measured in benthic foraminifera recovered from glacial sections in cores covering most of the important ocean basins (Table 6.1; Figure 6.1). Although these measurements

do not substitute for the detail of a long record, they provide a means of getting a "snapshot" picture of the distribution of Ba/Ca in the glacial oceans.

The majority of the cores studied are from the Atlantic basin; comparison of average Ba/Ca for Holocene and Glacial sections is illustrated in Fig. 6.6. Only those cores for which replicates were measured are included in this compilation. Averages (based on analysis of *Cibicides* and *Uvigerina*) Ba/Ca are used in this plot since the small offset between species is not significant in this context. The picture that emerges is that the Glacial deep Atlantic was filled by a water mass with relatively uniform Ba concentrations averaging about 50% higher than Holocene norms (about 3.5 $\mu\text{mol/mol}$). There is no clear latitudinal variation, but there is a marked depth variation. As noted above, foraminifera from mid-depth cores record Ba depleted water. A few *Uvigerina spp.* points record Holocene-like values in a low sedimentation rate core from 2800 m depth in the South Atlantic; these values will require further investigation before being regarded as significant.

Coverage for the Atlantic is best in the North Atlantic, for which 4 complete 25 kyr records were recovered. The mean and standard deviation of the core-tops and glacial sections of these four cores is plotted in vertical profile in Fig. 6.7.

A vertical profile based on the glacial sections of Eastern Equatorial Pacific cores is plotted in Fig. 6.8. There is a clear indication of a depth gradient, since upper intermediate water Ba (here represented by two cores from about 700 m depth in the Equatorial Pacific) are depleted in Ba at the LGM. The values are somewhat uniform between 1400 and 3600 m, although one of the deepest cores (KNR73-3PC) does record significantly higher Ba than the other deep equatorial Pacific cores. Core top values are not shown for the Pacific because for most cores only glacial samples were available.

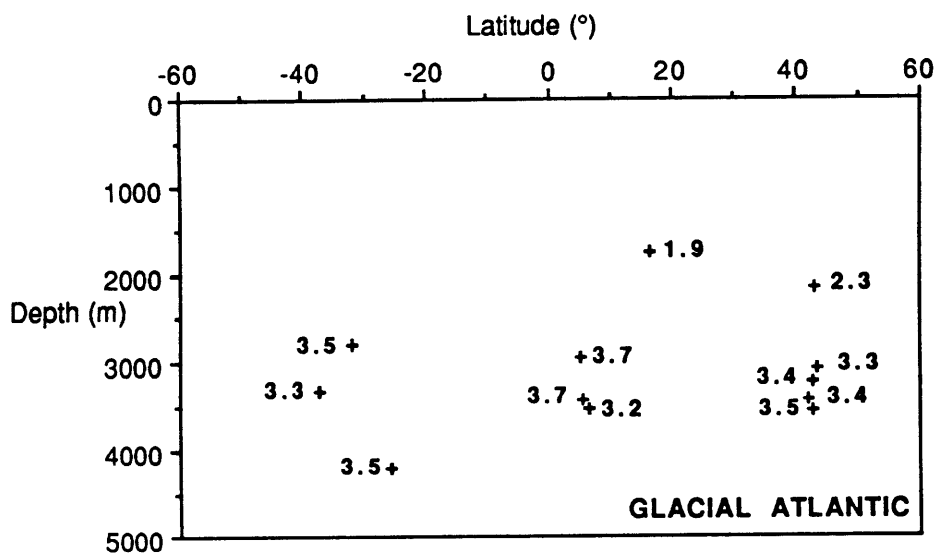
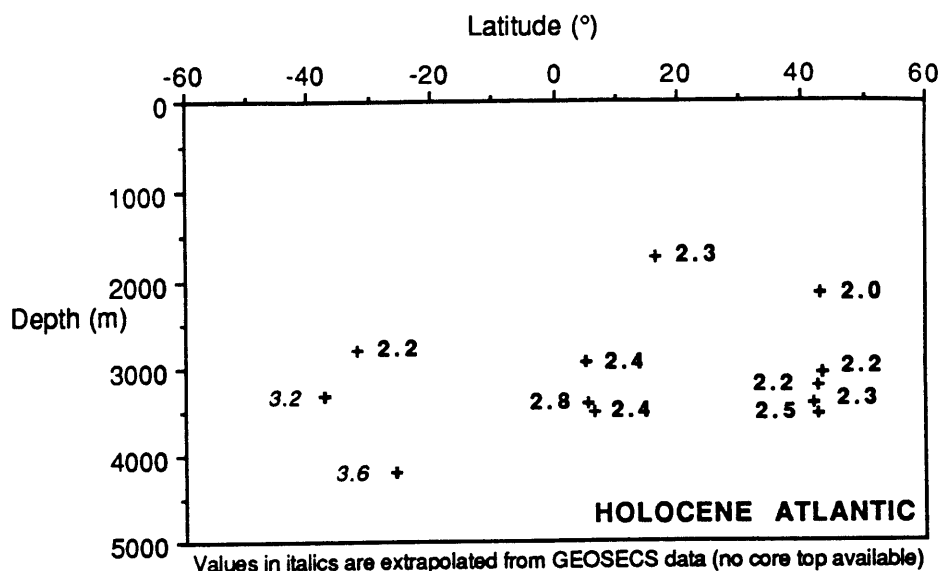


Figure 6.6 Map of Holocene and LGM Ba/Ca ($\mu\text{mol/mol}$) for several cores in the Atlantic ocean. This plot includes data from both the Eastern and Western basins. All values are averages of at least two data points.

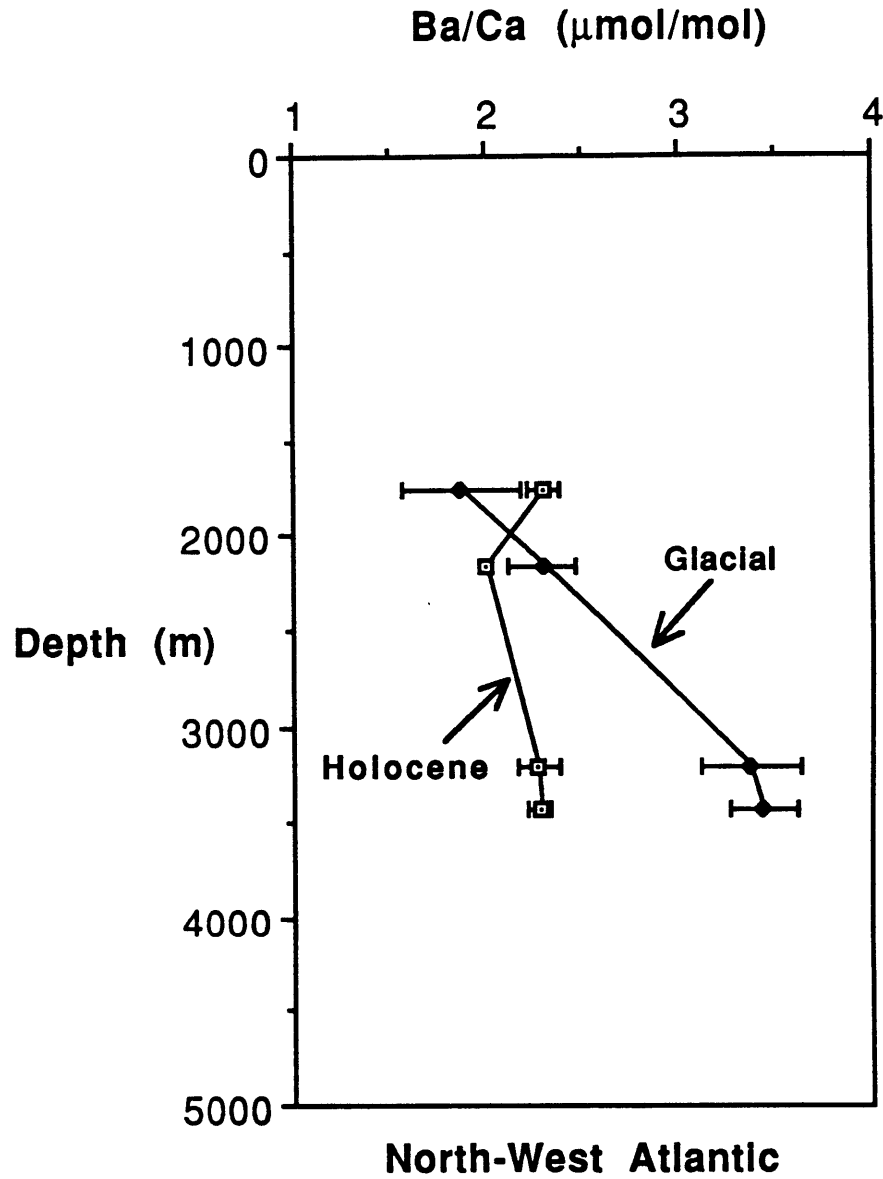


Figure 6.7 Comparison of Ba in the North-West Atlantic in the Holocene and LGM. Means and standard deviations based on the points analyzed in the appropriate sections of four different cores for which complete Ba/Ca records were recovered. See Table 6.1.

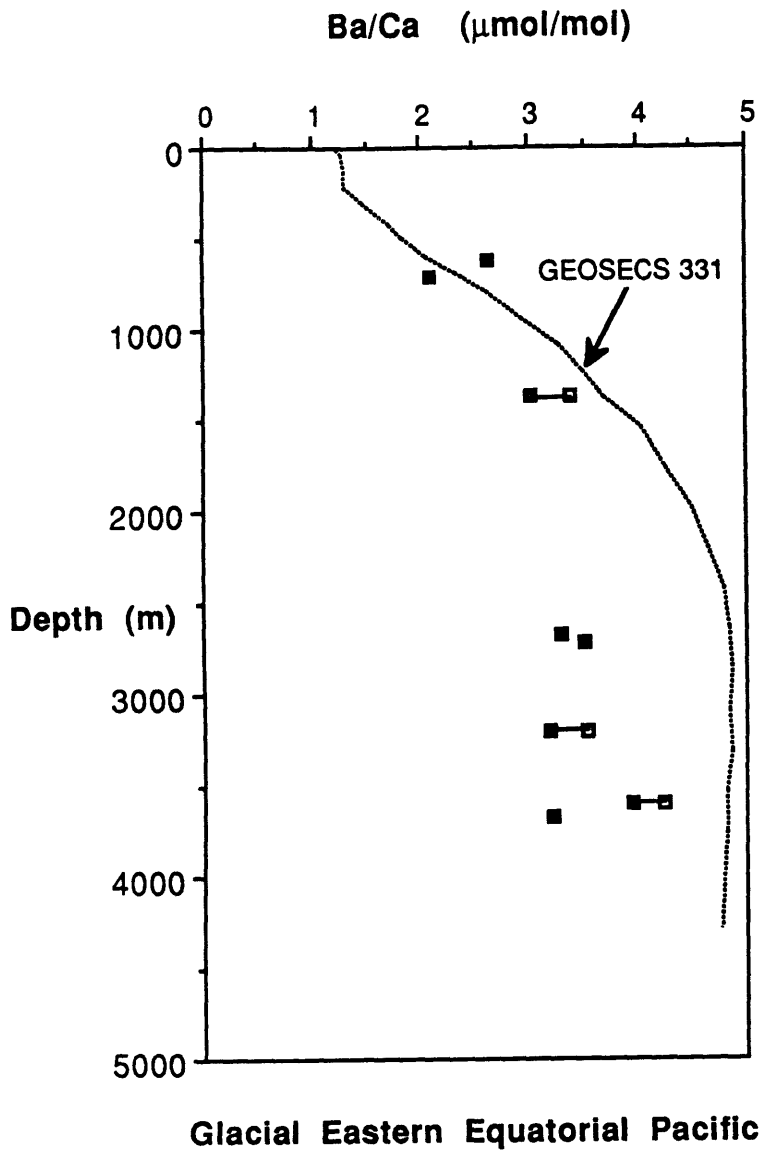


Figure 6.8 Comparison of glacial Ba/Ca with GEOSECS values (Ostlund *et al*, 1987) in the Eastern Equatorial Pacific. St. 331 (4° 36' S; 125° 8'W) Ba concentrations are converted to foram Ba/Ca units using an average benthic foraminiferal distribution coefficient. Filled squares indicate points from *Uvigerina spp.*; open squares indicate points from *C. wuellerstorfi*.

6.5 Changes in the inter-basin distribution of Ba in the glacial oceans

Figure 6.9 compares *C. wuellerstorfi* Ba/Ca records from Atlantic core CHN82-11PC and Pacific core TR163-31B via a time scale based on the radiocarbon measurements made on core TR163-31B. The Atlantic core was placed on this time scale by correlation of oxygen isotope records from the two cores (see Fig. 6.9). Although this age correlation is probably no better than ± 2 kyr, it serves to allow comparison of the records for the changes in Ba distribution associated with glacial-interglacial cycles.

Lea and Boyle (1989) (Chapter 5) found the mean distribution coefficient for Ba in benthic foraminifera to be 0.37 ± 0.06 . Extrapolating from GEOSECS data to these core locations and depths yields dissolved Ba of 56 nmol/kg at the Atlantic site and 133 nmol/kg at the Pacific site (Ostlund *et al.*, 1987). Therefore benthic foraminifera living at these sites today would be expected to record Ba/Ca of about 2 $\mu\text{mol/mol}$ at the North Atlantic site and 4.8 $\mu\text{mol/mol}$ at the Equatorial Pacific site. Measured *C. wuellerstorfi* Ba/Ca for the Holocene sections of the two cores in Fig. 6.9 average about 2.2 $\mu\text{mol/mol}$ in the Atlantic core and 4.6 $\mu\text{mol/mol}$ in the Pacific core; both values are within 10% of the expected values.

Figure 6.9 suggests that the basin-to-basin fractionation for Ba present in the Holocene is absent at the glacial maximum and clearly diminished throughout stage 2. Ba/Ca measured in *Uvigerina spp.* from the $\delta^{18}\text{O}$ maximum in these two cores also do not differ significantly (Tables 6.2, 6.4). It appears that for a few thousand years during the last glacial maximum at sites representative of North Atlantic Deep Water and Pacific Deep water (at 3200 m) there was no difference in the Ba contents of these deep water masses.

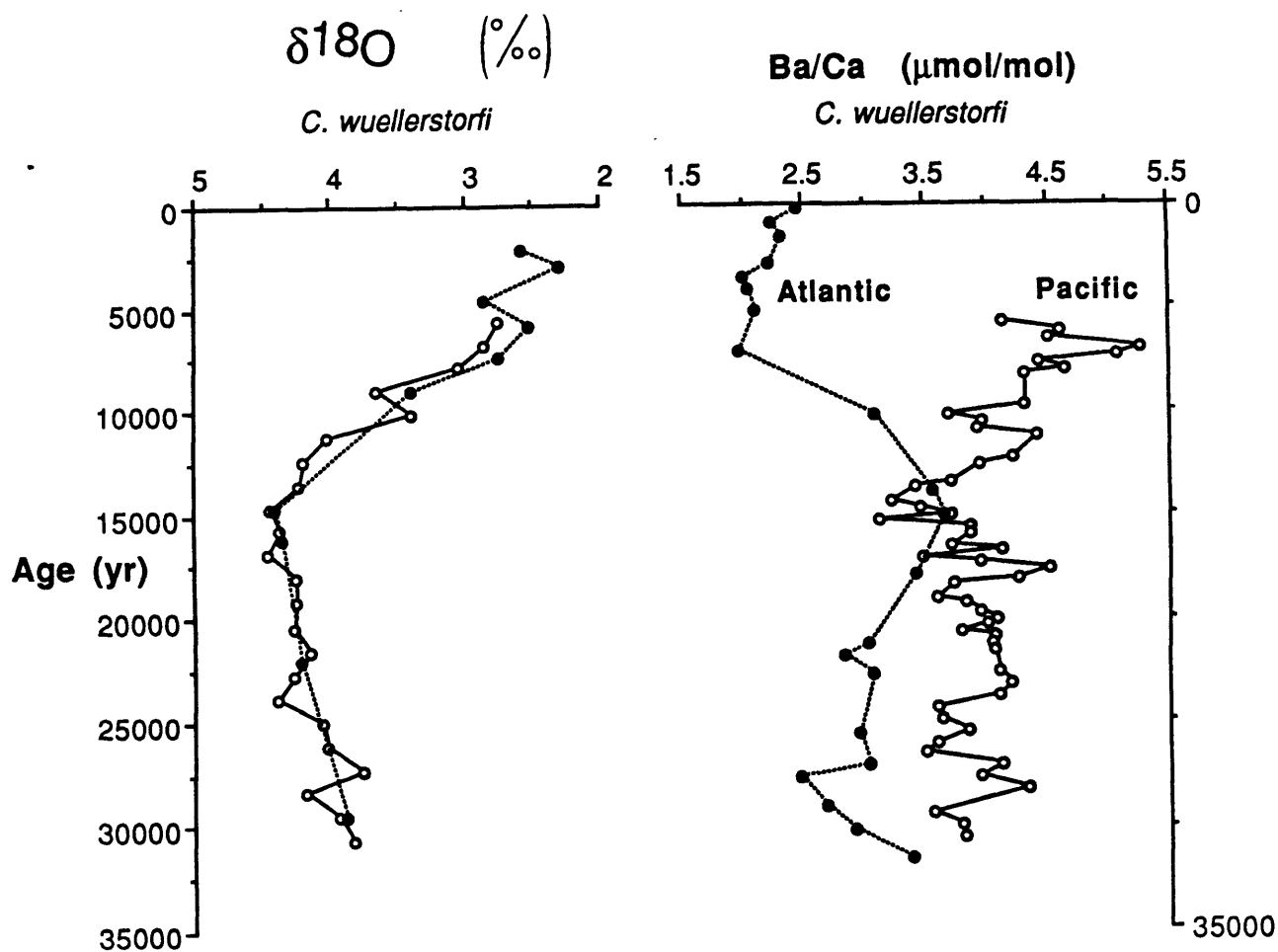


Figure 6.9 Ba/Ca records from *C. wuellerstorfi* for the North Atlantic (CHN82-11PC) and Eastern Equatorial Pacific (TR163-31B) at about 3200 m. The time scale is based on radiocarbon dates for TR163-31B (Shackleton *et al.*, 1988); the values from CHN82-11PC are placed on this time scale by correlation of the oxygen isotope record, as indicated. Oxygen isotopes from Boyle and Keigwin (1982) and Shackleton *et al.*, (1988).

Ba/Ca measured on benthic foraminifera recovered from the glacial sections of other deep ocean cores in the Atlantic and Pacific further confirm this finding (Table 6.1). Ba/Ca of benthic foraminifera from the glacial sections of deep cores (>2800 m) from both the Pacific and Atlantic fall in the range 3.2 to 4.2 $\mu\text{mol/mol}$ Ba/Ca with means close to 3.6 $\mu\text{mol/mol}$. This value is close to the predicted mean Ba content of modern oceanic waters, which in benthic Ba/Ca units is about 3.9 $\mu\text{mol/mol}$ (Ostlund *et al.*, 1987). It should be noted that this mean includes the high Ba waters of the deepest parts of the ocean (4-5 km), while values from this study includes only one core deeper than 3600 m. This factor alone might bring the glacial averages in line with the present day mean.

The glacial sections of 4 North Atlantic cores ranging in depth from 3070 to 3427 m record benthic Ba/Ca of 3.3 to 3.6 $\mu\text{mol/mol}$. This value is not significantly lower than the 3.4 to 3.9 $\mu\text{mol/mol}$ range of Ba/Ca found in Holocene samples from the Southern Ocean (Lea and Boyle, 1989)(Chapter 5). Ba/Ca in glacial benthic samples from the Southern Ocean are in the range 3.3 to 3.9 $\mu\text{mol/mol}$ (Table 6.1 : cores RC13-229, RC12-294 and RC11-120, although RC11-120 is the only core that is truly a Southern Ocean core; see Table 6.1 for depths and locations). Apparently the Ba content of the deep waters of the glacial North Atlantic (NADW) and Southern Ocean (AABW) were not significantly different during glacial times.

6.6 Comparison of glacial distributions of Cd and ^{13}C to Ba

The Cd and carbon isotopic content of benthic foraminifera have been used in many previous studies to reconstruct deep water nutrient chemistry at the LGM. Benthic $\delta^{13}\text{C}$ values for glacial Pacific cores are slightly higher than glacial Southern Ocean benthic $\delta^{13}\text{C}$; they are clearly not lighter (Boyle, 1988; Duplessy *et al.*, 1988). Holocene Cd/Ca is about 0.06 $\mu\text{mol/mol}$ in benthic

foraminifera from cores in the deep North Atlantic, rises to 0.16 $\mu\text{mol/mol}$ in cores from the Southern Ocean, and reaches 0.20 $\mu\text{mol/mol}$ in cores from the deep Pacific. In contrast to Ba, Cd remains depleted in NADW compared to AABW at the LGM; Cd/Ca rises to 0.12 $\mu\text{mol/mol}$ in the glacial sections of deep North Atlantic cores, while benthic foraminifera from the glacial sections of deep cores from the Southern Ocean and Pacific record Cd/Ca of 0.15 to 0.2 $\mu\text{mol/mol}$ (Boyle and Keigwin, 1985; Boyle, pers. comm.)

The ^{13}C content of glacial benthic foraminifera confirm the Atlantic Cd data since benthic foraminifera from deep North Atlantic cores record ^{13}C -enriched (i.e. nutrient-poor) values relative to the deep Antarctic and Pacific at the LGM. However, carbon isotopes apparently record a unique Southern Ocean history since the largest carbon isotope change (0.8 ‰ lower at the LGM) occurs in benthic foraminifera from Southern Ocean cores (Curry *et al.*, 1988). Benthic $\delta^{13}\text{C}$ values for glacial Pacific cores are slightly greater than glacial Southern Ocean benthic $\delta^{13}\text{C}$; they are clearly not lighter (Curry *et al.*, 1988).

6.7 Consideration of factors unique to barium

Differences in the distribution of Ba and Cd (or $^{13}/^{12}\text{C}$) in the glacial ocean suggest that simple lateral variations in the fraction of northern and southern component water will not provide a solution compatible with the glacial distribution of all three tracers. In several respects Cd/Ca and $\delta^{13}\text{C}$ agree more closely than Ba and Cd; however, since both Cd and $\delta^{13}\text{C}$ are tracers of labile nutrients this might be expected.

In consideration of the relative novelty of Ba as a paleo-circulation tracer, problems unique to Ba that might serve as explanation for differences in its glacial distribution are first considered. Temporal change in the oceanic

inventory of any tracer will complicate its utility as a tracer of circulation (Boyle, 1986). The oceanic residence time of Ba is markedly shorter than the estimated 100,000 year residence time of Cd; the best current estimate is on the order of 10,000 years (Chan *et al.*, 1976), although this value is uncertain due to difficulty in estimating the extent of estuarine desorption of Ba and the magnitude of the hydrothermal Ba flux. Since this residence time is on the same time scale as interglacial-glacial change, the possibility of changes in the oceanic inventory of Ba cannot be ruled out.

Change in the Ba inventory of the glacial oceans can be calculated by summing weighted averages for each deep basin. Calculations based on the data summarized in Table 6.1 suggest a decrease in mean ocean Ba of about 15 ± 10 %. This change is barely resolvable within the noise of the data, and is uncertain because very few representative samples are available from the Southern and Indian Oceans and from the deepest parts of all the basins. Two other records can be employed to assess the likelihood of change in mean ocean Ba. Since surface water Ba contents respond directly to changes in Ba inventory (Chapter 3), change in Ba/Ca of planktonic foraminifera can be interpreted as an indication of change in Ba inventory. The record of planktonic Ba recovered from core TR163-31B does not record a clear change in the Ba concentration of surface waters over the last 30 kyr, although there is some indication that glacial values are slightly lower. Finally, study of benthic Ba/Ca over the last 200 kyr in a deep North Atlantic core indicates that the pattern of low Ba in interglacial periods and high Ba in glacial periods is clearly sustained over this time interval. Ba/Ca of benthic foraminifera recovered from the two previous interglacials (stage 5 and 7) have values typical of benthic foraminifera from Atlantic sediments of Holocene age (Chapter 7). Since this record covers a time period much longer than the residence time of Ba in the oceans, the

constancy of interglacial Ba suggest that temporal changes in Ba inventory are probably small relative to changes due to circulation. Ba distributions derived from the model discussed below suggest that a 15% reduction in oceanic Ba gives the best fit to the observed data.

Although changes in the riverine input of Ba might not be large enough to change the oceanic inventory of Ba, such changes could influence surface water distributions. Dissolved Ba is about 20% higher in Atlantic surface waters than Pacific surface waters (Ostlund *et al.*, 1987), presumably in response to the dominance of riverine inputs to the Atlantic basin (J. Edmond, pers. comm.). Such an effect is also seen in the Indian ocean, where the large Ba inputs from the Indus, Ganges and Brahmaputra affect the Ba content of surface waters (Ostlund *et al.*, 1987; K. Falkner, unpublished data).

Change in the patterns of riverine inputs could change the "preformed" Ba content of North Atlantic surface waters that serve as sources for deep water. A 15 kyr record of planktonic Ba/Ca recovered from a core taken on the Bermuda Rise (Chapter 4) indicates that dissolved surface water Ba in the temperate glacial North Atlantic might have been up to 20% higher during glacial periods. However, this change is not clearly resolvable above the noise in the data.

The relationship between pore water fluxes and the concentration of Ba in bottom waters will change as a function of the flushing rate (or residence time) of bottom waters. The bottom waters of rapidly flushed basins such as the western Atlantic accumulate less *in situ* Ba than bottom waters of restricted basins in the Pacific and Indian oceans (Chan *et al.*, 1977). Changes in the Ba content of bottom waters due to this effect can potentially be modeled by considering any changes in the residence times of bottom waters in the glacial ocean (see below).

A final factor that could complicate the interpretation of glacial Ba distributions, as well as any other tracer that derives its characteristics from surface depletion, is temporal change in patterns of productivity and regeneration. In general there is little indication that bottom water Ba is strongly influenced by the productivity of overlying surface waters; however, Bishop (1988) has made the argument that particulate Ba is high in regions of intense organic matter regeneration. If this is the case, dissolution of these Ba-rich particles could cause increases in bottom water Ba. Confirmation for this hypothesis must be sought in studies of the modern ocean.

6.8 Reconciling Ba and Cd distributions in the deep glacial oceans

Although the factors outlined above might account for some of the differences between glacial Ba and Cd (or $\delta^{13}\text{C}$) distributions, there is currently little direct evidence available to assess their relative importance. Therefore the question arises as to whether Ba and Cd distributions can be reconciled without invoking distinct or unique chemical changes.

Figure 6.10 illustrates property-property plots for Ba and Cd in the Holocene and glacial oceans. Each point on the plot represents Holocene or Glacial sections for which analyses of Cd (E. Boyle, pers. comm.) and Ba are available. These cores have been grouped into simplified water masses with boundaries, dependent on availability of cores. The division between intermediate and deep waters is 2500 m.

With the exception of Eastern Tropical Pacific (ETP) intermediate waters, Holocene benthic foraminiferal Ba and Cd display a linear trend consistent with present oceanic distribution. The Ba and Cd content of Holocene foraminifera from North Atlantic deep and intermediate waters is not distinguishable. ETP deep waters are significantly higher than Southern Ocean (SO) waters for both

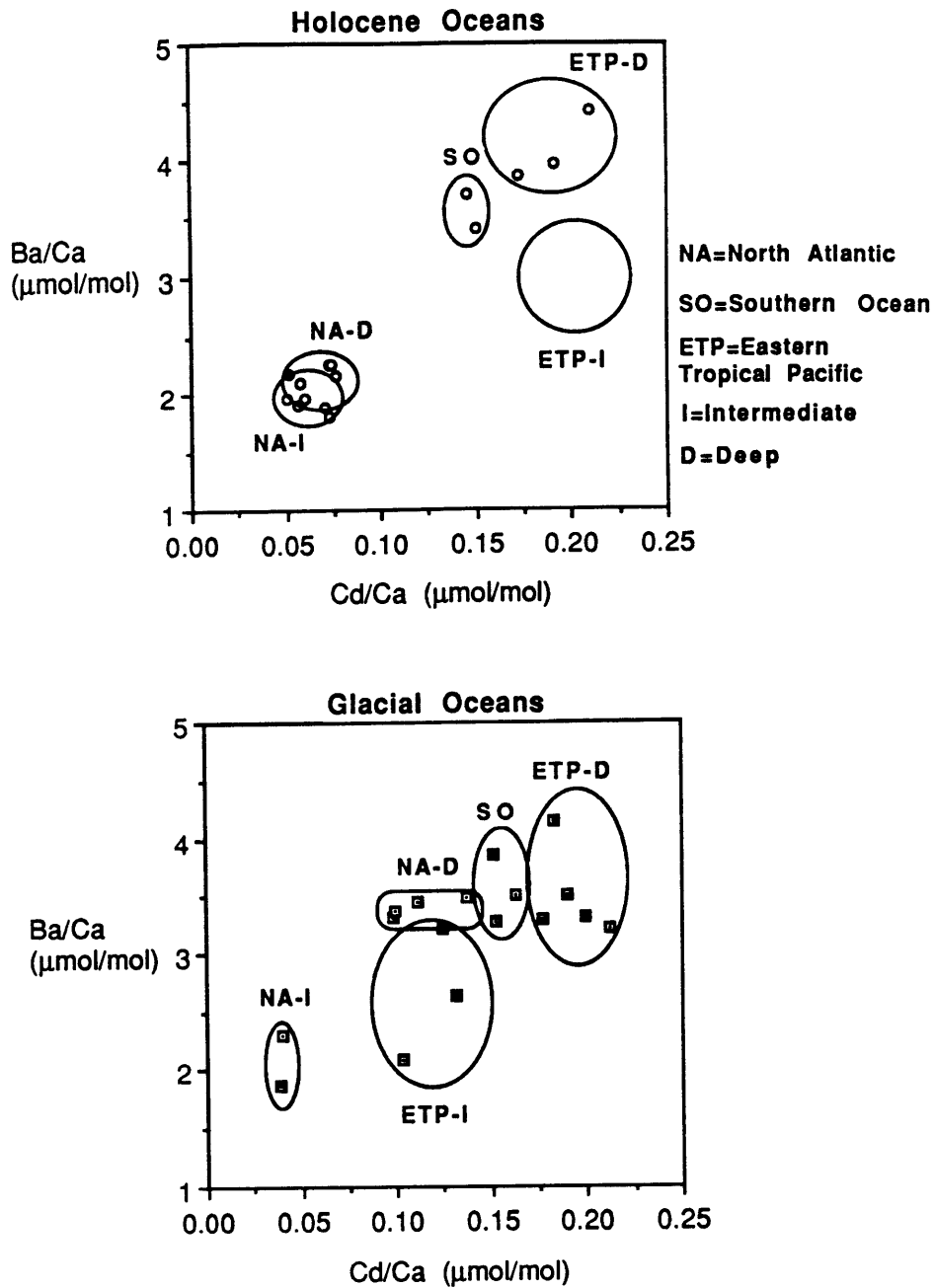


Figure 6.10 Benthic foraminiferal Ba/Ca versus Cd/Ca and the Holocene and Glacial oceans. Points indicate cores for which coincidental analyses exist for both tracers (this work and E. Boyle, pers. comm.). Fields approximately indicate the boundary of definable water masses. The boundary of the field for the intermediate waters of the Eastern Tropical Pacific in the Holocene is placed by conversion of GEOSECS data; no foraminiferal analyses are available.

Ba and Cd. It is only the intermediate waters of the ETP which fall off this linear trend, since these waters are intermediate in Ba content while containing the highest Cd contents (Boyle, 1988; Ostlund *et al.*, 1987). Unfortunately, there are no benthic foraminiferal Ba values for the Holocene sections of cores in this water mass, so the boundary is placed by conversion of GEOSECS Ba and P to foraminiferal units.

The situation for the glacial oceans is markedly different. North Atlantic Intermediate and deep waters are split up into two distinct chemical entities. North Atlantic intermediate waters are lower in Cd with relatively unchanged Ba. North Atlantic deep waters are much higher for both Cd and Ba, but the relative rise in Ba is clearly larger. The slope of the line connecting Holocene NADW and Glacial NADW on this plot is steeper than the Holocene tie line between NADW and Southern Ocean deep waters.

The three Southern ocean points are not very different for Cd and Ba from the Holocene to the Glacial, although it should be emphasized that they are not based on the same cores (see Table 6.1 for glacial cores; see Chapter 5 and Boyle (1988) for Holocene cores). Glacial North Atlantic deep waters are not distinctly different for Ba but remain lower for Cd. Conversely, ETP deep waters are not distinctly different for Ba but remain higher for Cd. ETP intermediate waters appear to be quite lower in Cd in the Glacial oceans; the Ba content of these waters might have been somewhat lower, but it is difficult to judge the magnitude of Ba depletion, if any, without core top Ba/Ca values.

Both Cd and Ba suggest that the nutrient content of Glacial Atlantic deep waters was enriched while that of Atlantic intermediate waters was depleted. The principal difference between Ba and Cd is that Cd remains higher in the deep Pacific relative to the deep Atlantic (implying a significant flux of nutrient depleted water to the deep North Atlantic) while no such difference is apparent

for Ba. This result has been confirmed by results from many cores for both Ba and Cd and therefore is the most important factor that must be reconciled by any model.

A model solution that might reconcile this difference and the other changes described above is sought via a simplified 7-box model along the lines of the PANDORA model (Broecker and Peng, 1986) and the CYCLOPS model (Kier, 1988). This model is not proposed as anything novel but rather is built up along the lines of these previously formulated models, but with omissions of transfers and fluxes unnecessary to considering variations in Ba and Cd. P is used instead of Cd since P is a more familiar property.

The model employs boxes for the following water masses: warm surface, Atlantic intermediate, Atlantic deep, Pacific intermediate, Pacific deep, Circumpolar surface and Circumpolar deep (Fig. 6.11). The volumes are taken such that the Pacific boxes include the Indian ocean volume and the intermediate and deep boxes have equal volumes (see appendix for model details). The concentrations of Ba and P in the two surface boxes are fixed; this results in model computed particulate Ba and P fluxes out of each surface box. These fluxes are then regenerated in the intermediate and deep boxes; although there is only one warm surface box for both the Atlantic and Pacific, the individual particulate fluxes to the Atlantic or Pacific are tied to the upwelling flux from the intermediate waters of the Atlantic and Pacific, respectively. Since the fluxes are completely regenerated, there is no loss to sedimentation in this model.

The two factors that generate differences in the distribution of P and Ba in the model are sites of vertical regeneration and the composition of the fixed surface water concentrations. The model is set-up so that 90% of the particulate flux of Ba removed from surface waters is regenerated in the deep

Warm surface					
Ba=35		P=0.1		20	10
Δ		Q _{pi} > 0		Δ	
Pacific Int	V	CP surface	Atlantic Int	V	V
Ba=95	10	Ba=88	Ba=67	4	16
P=3.0		P=1.5	P=1.7		
	14	20	10		
	Δ	>4	>4	Δ	
Pacific Deep	V	CP deep	Atlantic Deep	V	
Ba=134	10	Ba=105	Ba=69	8	
P=2.5		P=2.0	P=1.0		
	24<		21<		
		>20	>7		
Mean Ba= 100			Mean P= 2.25		
	Atl	Pcf	Circumpolar		
Ba particle flux (mol/s)	322	1198	376	20%	
P particle flux (kmol/s)	16	59	16	17%	
Ba flux (nmol/cm²/yr)	13	16	91		
P flux (μmol/cm²/yr)	0.6	0.8	3.8		
	Atl	Pcf			
Ventilation Ages (years)	293	624			

Figure 6.11 Model run for the Holocene ocean. Model conditions are set up to yield a distribution of P and Ba similar to the GEOSECS distributions. Ba concentrations in nmol/kg; P concentrations in μmol/kg. Water fluxes are in Sverdrups (10⁶ m³/s). Ventilation ages apply to the combined intermediate and deep boxes. CP = circumpolar; Atl = Atlantic; Pcf = Pacific; Q_{pi} = water flux from the Pacific intermediate to the Atlantic intermediate. Percentages to the right of the Circumpolar particle fluxes indicate the % of the total flux accounted for by the flux out of the Circumpolar surface box.

boxes, with 10% regeneration in the intermediate boxes. For P, 90% of the particulate flux is regenerated in the intermediate boxes, with the remaining 10% in the deep boxes. The Ba concentration of the warm surface box is set to the average Ba content of temperate surface waters of 37 nmol/kg (Ostlund *et al.*, 1987); P is set to 0.1 $\mu\text{mol/kg}$. Surface waters of the Circumpolar were initially set to average GEOSECS surface composition for the Southern Oceans (75-90 nmol/kg for Ba, 1.3-1.6 $\mu\text{mol/kg}$ for P); these values were adjusted slightly to generate particulate Ba and P fluxes that matched literature values (Collier, 1981; Dehairs *et al.*, 1980; Kier, 1988; Rhein and Schlitzer, 1988).

Particulate fluxes of P out of the warm surface box account for about 85% of the total P exported out of the two surface boxes; this leads to P fluxes (per unit area) out of the Circumpolar box that are about 5 times higher than fluxes out of the warm surface box, similar to the model generated fluxes in the CYCLOPS model (Kier, 1988). Using the upper limit of GEOSECS Ba concentrations for the Circumpolar surface box (Chan *et al.*, 1977; Ostlund *et al.*, 1987) generates particulate Ba fluxes out of the Circumpolar surface box that account for about 20% of the total Ba export. There is no independent evidence to judge the correctness of this ratio. To minimize artifacts, the fixed concentrations of Ba in the Circumpolar surface box are adjusted in the "glacial" runs described below to yield particulate fluxes out of the Circumpolar surface box that are similar in relative magnitude to the Holocene model.

Eight equations are required to describe the model, with 5 for each of the boxes with variable concentration and 3 for the particulate fluxes. These 8 equations also incorporate mass conservation for Ba or P. The 8 equations are arranged in the form $Ax=b$, and the solution x is found by inverting the 8 x 8 matrix A in a commercial spreadsheet (Excel) program on a Macintosh SE personal computer. Since the calculation is performed rapidly by the

spreadsheet the water fluxes can be adjusted to see quickly what effect changes have on the concentrations of Ba and P in the 5 variable boxes while conserving water volumes.

Figure 6.11 illustrates the model conditions for the Holocene oceans. Ba and P concentrations of each box, water fluxes between the boxes, Ba and P particulate fluxes out of the three surface boxes, and ventilation ages for the Atlantic (I+D) and Pacific (I+D) are indicated. The model does a reasonable job of simulating present day distributions.

Two different model scenarios for the glacial oceans are discussed below. These situations do not by any means represent the only possible ones, but they incorporate two of the more obvious plumbing changes that might have occurred in the glacial conditions. It should be emphasized that these model simulations are not proposed as real "solutions" to the problem of glacial circulation, but rather are used as a means of gaining insight into what is required to move the concentrations in the direction of the changes indicated by paleo Ba and Cd distributions.

Figure 6.12 illustrates Glacial option 3 (G3). This model reduces the flux of nutrient depleted water into the deep Atlantic box from 16 Sv to 8 Sv. The 8 Sv that previously flushed the deep Atlantic is diverted to the intermediate Atlantic box. In addition the water fluxes are tuned to minimize the Ba contrast between the deep Atlantic and Pacific (i.e. fluxes are adjusted in the direction that would lead to a solution most compatible with observed glacial distribution based on benthic Ba and Cd.). Such tuning includes maximizing the exchange between the deep Atlantic and deep Circumpolar boxes and minimizing the exchange between the Ba-depleted intermediate Atlantic and Ba-enriched deep Atlantic. Finally mean Ba ocean contents are adjusted down by about 15% to yield Ba distributions that are more compatible with glacial foraminiferal

Warm surface						
Ba=31			10			
P=0.1	20		Q _{plai} > 0			
	Δ				Δ	
Pacific Int	V	CP surface		Atlantic Int	V	V
Ba=79	10	Ba=70		Ba=46	12	8
P=3.1		P=1.5		P=1.0		
	14	20	8<	2		
	Δ	>4	Δ	>4	Δ	
Pacific Deep	V	CP deep		Atlantic Deep	V	
Ba=113	10	Ba=91	18	Ba=77	0	
P=2.5		P=2.0		P=1.5		
	24<	24<		>18		
		>20				
Mean Ba: 85			Mean P= 2.25			
		Atl	Pcf	Circumpolar		
Ba particle flux (mol/s)		146	958	256	19%	
P particle flux (kmol/s)		9	59	13	16%	
Ba flux (nmol/cm²/yr)		6	13	62		
P flux (μmol/cm²/yr)		0.4	0.8	3.1		
		Atl	Pcf			
Ventilation Ages (years)		216	624			

Figure 6.12 Model run G3. The flux of nutrient depleted surface water to the deep Atlantic is cut by 50%, and the flux of surface water to the intermediate Atlantic is increased by 50%. This run does not yield equivalent deep Atlantic and Pacific Ba under these conditions, even though the fluxes are tuned to minimize the Ba difference. See text for further explanation.

Ba values. Even with tuning, G3 cannot reduce the Pacific-Atlantic Ba contrast to much less than 45%.

Figure 6.13 illustrates glacial option 6 (G6). In this configuration, the flux of surface water to the deep Atlantic is reduced to 0. The net down welling flux to the intermediate Atlantic is increased to 5 Sv, and the net upwelling flux from the intermediate Pacific is decreased to 5 Sv. In addition, upwelling from the intermediate Atlantic is increased by a factor of 2. A few small adjustments to other fluxes are made to minimize the Pacific-Atlantic Ba contrast.

G6 reduces the Pacific-Atlantic Ba contrast to less than 4% while maintaining a sizeable Pacific-Atlantic P contrast (>44%). This differential response is not due to the elimination of the surface water flux to the deep Atlantic, but rather is due to the vigorous exchange between the Atlantic intermediate and surface boxes, which leads to a large particulate flux into the Atlantic. Since that flux is regenerated differentially for Ba and P, with P regeneration predominantly in the intermediate box and Ba regeneration predominantly in the deep box, Ba ends up enriched relative to P in the deep Atlantic. The increase in Atlantic upwelling causes an increase in particulate P fluxes of about 25%.

Figure 6.14 illustrates the relative sensitivity of Ba and P in the deep Atlantic and Pacific to changes in the two key fluxes in G6: Q_{wsad} , which is the flux of water from the warm surface to the Atlantic deep box, and Q_{aiws} , which is the upwelling flux from the intermediate Atlantic to the surface. The evolution of the model proceeds from left to right. With Q_{aiws} kept at the minimum value (lowest possible Atlantic upwelling and particulate flux), Q_{wsad} is reduced incrementally to 0. The Pacific-Atlantic P difference diminishes from 1.5 to 0.85 $\mu\text{mol/kg}$; the Pacific-Atlantic Ba difference diminishes from 54 to 28 nmol/kg . The response to changes in Q_{aiws} is very different. As Q_{aiws} increases, the

Warm surface					
Ba=31		20		20	
P=0.1		Δ		Δ	
Q _{plai} > 0					
Pacific Int	V	CP surface		Atlantic Int	V
Ba=67	15	Ba=75		Ba=54	25
P=2.7		P=1.5		P=1.1	0
	10	20	10<	9	
	Δ	>0	Δ	>3	Δ
Pacific Deep	V	CP deep		Atlantic Deep	V
Ba=110	10	Ba=99	22	Ba=106	7
P=2.6		P=2.2		P=1.8	
	20<		5<		
		>20		>7	
Mean Ba= 85			Mean P= 2.25		

	<u>Atl</u>	<u>Pcf</u>	<u>Circumpolar</u>	
Ba particle flux (mol/s)	461	719	262	18%
P particle flux (kmol/s)	21	53	11	13%
Ba flux (nmol/cm2/yr)	18	10	64	
P flux (μmol/cm2/yr)	0.8	0.7	2.7	

	<u>Atl</u>	<u>Pcf</u>
Ventilation Ages (years)	260	687

Figure 6.13 Model run G6. Fluxes in this model are tuned to give the minimum deep Atlantic-Pacific Ba difference with the maximum deep Atlantic-Pacific P difference. See text.

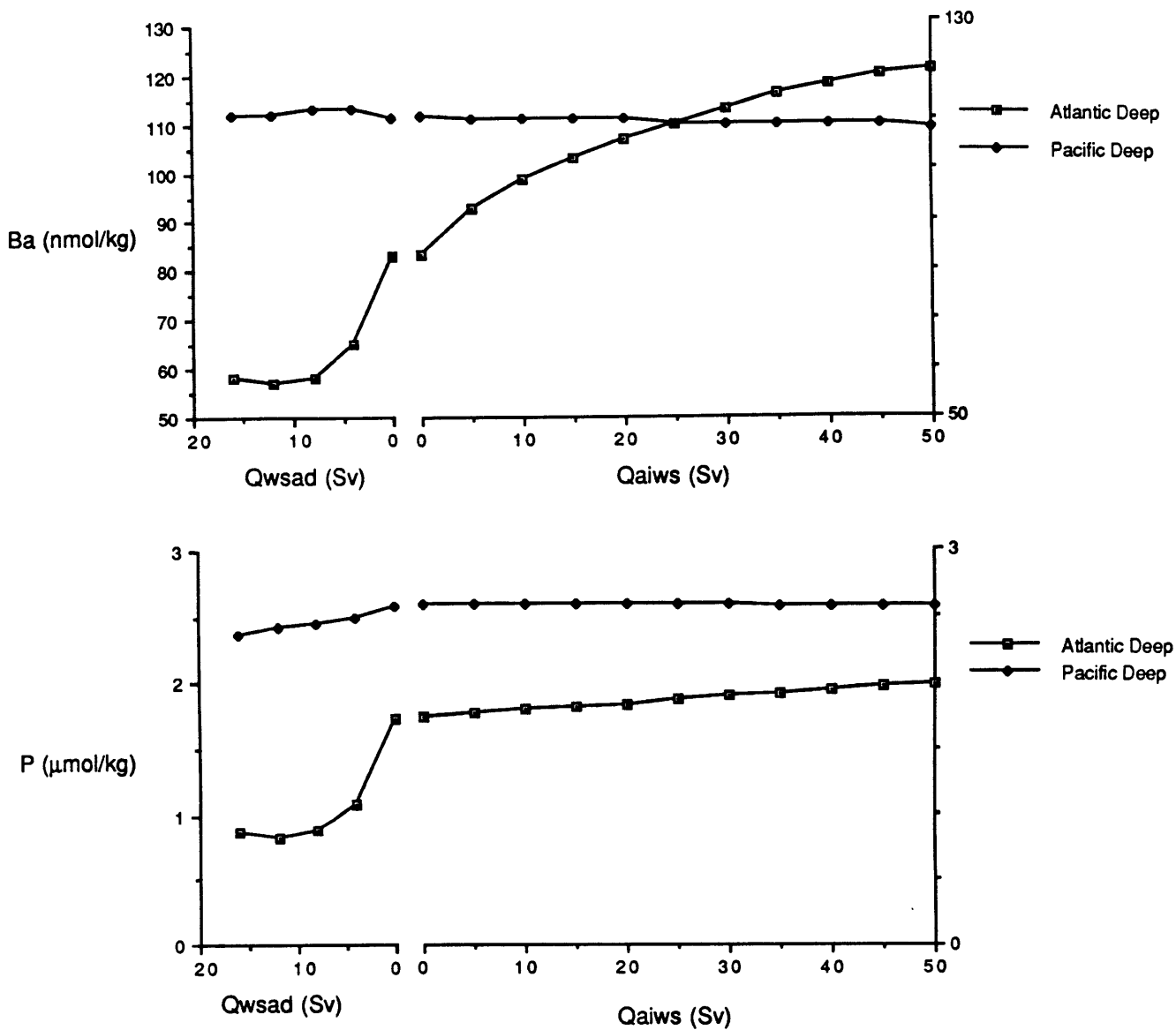


Figure 6.14 Differential response of Ba and P in the deep boxes of G6 to reduction in the flux of surface water to the the deep Atlantic and to increases in the upwelling flux from the Intermediate Atlantic. As Q_{aiws} increases the Atlantic-Pacific Ba fractionation decreases much more rapidly than the Atlantic-Pacific P fractionation. See text for further explanation.

Atlantic particulate Ba flux increases and Ba is fractionated into the deep Atlantic box relative to P. When Q_{aiws} reaches 25 Sv, the Ba content of the deep Atlantic and boxes are equal; as Q_{aiws} increases above 25 Sv deep Atlantic Ba actually rises above deep Pacific Ba. At $Q_{aiws} = 50$ Sv deep Atlantic Ba is 11% **higher** than deep Pacific Ba while P still remains 30% **lower** in the Atlantic.

While there is no evidence that Q_{aiws} reached the high values required by G6, the higher wind strengths suggested for the Glacial oceans from modelling and paleo-climatic evidence might have enhanced exchange between the intermediate and surface Atlantic (Boyle, 1986; COHMAP, 1988; Parkin and Shackleton, 1973). In addition, foraminiferal and chemical evidence suggests that productivity in the Glacial equatorial Atlantic was higher (Lyle, 1988; Mix, 1989); higher productivity would be a direct consequence of increases in Q_{aiws} .

The P and Ba distributions generated by G6 in large part agree with the foraminiferal Ba and Cd evidence. However, since this is a very simple model which includes only a fraction of the real variability in the ocean, the changes that cause the model to yield distributions consistent with what is observed might have little to do with the actual changes that occurred. The important result and the general conclusion that emerges from the modelling experiments is that differences observed in glacial foraminiferal Ba and Cd distributions might arise from contrasting regeneration sites.

6.9 Intermediate waters of the Atlantic; was the Mediterranean a more important source during glacial periods?

Several workers have argued on the basis of glacial carbon isotope distributions that the Mediterranean outflow was a volumetrically more important

source to intermediate depth Atlantic waters during the last glacial period (Oppo and Fairbanks, 1987; Zahn *et al.*, 1987). Since lower sea level in glacial periods would probably result in a reduced Mediterranean outflow (Duplessy *et al.*, 1988), the proposed scenario requires that other sources to the intermediate Atlantic would have to be relatively smaller to yield the proposed increase in Mediterranean influence.

Boyle and Keigwin (1987) presented evidence for nutrient depletion in glacial intermediate water cores and argued that such depletion was a result of the formation of cold intermediate waters in the North Atlantic. They argue that a decrease in salinity in the surface polar North Atlantic during glacial times would have reduced the density of waters formed there such that convection to intermediate depths would have been favored.

Discriminating between these hypotheses requires a tracer that is different in the two source water regions. Cd and carbon isotopes do not meet this criterion since both tracers have similar nutrient-depleted values in both Northern Component Water and the Mediterranean. However, Ba is enriched in the waters of the Mediterranean. The outflow over the sill contains almost a factor of 2 more Ba than the Atlantic surface water that flows in (Fig. 6.15). The reasons for the observed enrichment of Ba in the Mediterranean are not completely understood, but it apparently results from a combination of inflow from high Ba rivers, inflow from the Black Sea (Chan *et al.*, 1976), and possible dissolution of Ba from aeolian dust particles derived from the Sahara (Dehairs *et al.*, 1987).

Because of the enrichment of Ba in waters flowing over the sill, the Mediterranean outflow is a source of Ba to the Atlantic. Therefore an increase in the relative influence of Mediterranean outflow waters to the intermediate depth Atlantic would be recorded by higher Ba values at intermediate depths.

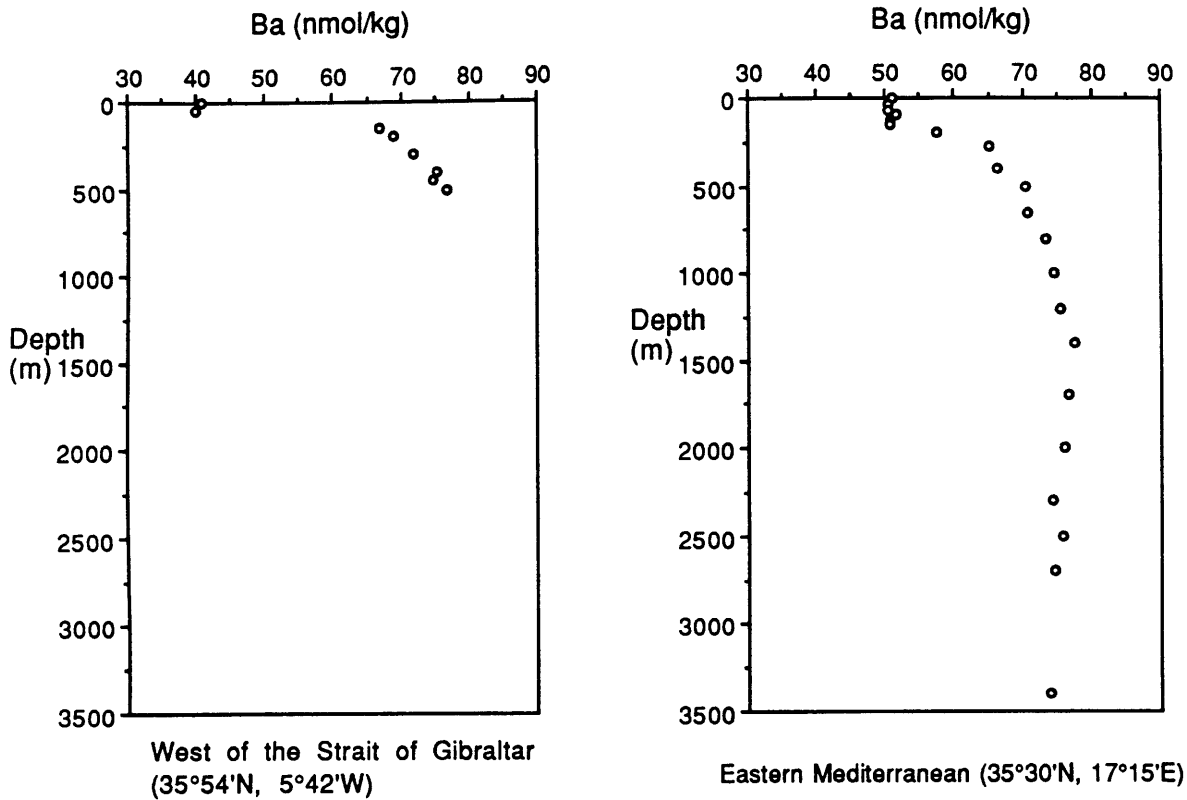


Figure 6.15 Dissolved Ba concentrations at a station just outside of the Straits of Gibraltar, Atlantic Ocean (35.9°N, 5.7°W) and in the Eastern Mediterranean (35° 29.5' N, 17° 14.8' E). The outflowing Mediterranean deep water is enriched in Ba over the in-flowing Atlantic water by about a factor of 2. For the Atlantic station salinity is less than 36.5 ‰ for samples between 0 and 75 m and greater than 38‰ for samples 150 m and deeper. See appendix 1 for tabulated Ba data.

However, as noted above, glacial benthic Ba/Ca at intermediate depths in the North Atlantic was relatively unchanged while a Caribbean core recorded lower glacial Ba values. Clearly this evidence argues against the Mediterranean as an increased source during glacial periods.

One important assumption implicit to this argument is that the Ba content of the Mediterranean remained high during glacial periods. An attempt to confirm this has been made by analyzing benthic foraminifera from the glacial section of a core taken at 1287 m in the Western Mediterranean (Core RC9-203: 36° N, 2°W). A previous study determined an oxygen isotope record for this core indicating glacial values between 85 and 100 cm (Oppo and Fairbanks, 1987). Two samples of *Cibicidoides pachyderma* from 90 and 100 cm yield Ba/Ca = 2.43, 2.89 $\mu\text{mol/mol}$. Expected Ba/Ca for this site based on present Ba/Ca in Mediterranean intermediate waters is about 2.6 $\mu\text{mol/mol}$, so the values determined for the glacial section do not indicate any change in Ba. However, it should be noted that *Cibicidoides pachyderma* has not been previously calibrated for uptake of Ba. Two calibrated species, *Uvigerina spp.* and *C. wuellerstorfi* from 80 cm depth, transitional between glacial and interglacial, had Ba/Ca greater than or equal to the two *C. pachyderma* values.

Glacial RC9-203 benthic Ba strongly suggests that glacial MOW Ba remained higher than glacial Caribbean bottom water Ba, as inferred from the glacial sections of the Caribbean core discussed above. Therefore, a hypothesis that calls on MOW as the source of nutrient depletion in Atlantic Intermediate waters and hence the Caribbean is in direct conflict with the currently available benthic Ba evidence.

6.10 Conclusions

A survey of seawater Ba in the glacial oceans has been made by measuring the Ba content of benthic foraminifera recovered from 15 to 25 kyr sections of a number of deep-sea cores. These Ba determinations indicate changes relative to the Holocene for the dissolved Ba of the following generalized water masses: the deep Atlantic was 30-60% higher, the intermediate Atlantic was slightly lower or unchanged, the deep Southern Ocean was unchanged, and the deep Pacific was 10 to 25% lower. Although these changes are in the same direction as previously observed changes for labile nutrient indicators like Cd and $\delta^{13}\text{C}$, the relative increase of Ba in the Atlantic and the relative decrease of Ba in the Pacific are both greater than the changes observed for the other paleochemical tracers. In accord with the magnitude of these changes and in contrast to Cd and carbon isotopes, there is no significant difference between the Ba content of benthic foraminifera recovered from glacial sections in the deep Atlantic and Pacific.

A 7-box model is used to explore possible causes for unexplained differences in the glacial distribution of Ba and Cd (P). The model suggests that the differences in the primary site of regeneration (intermediate waters for P, deep waters for Ba) can account for the differential effect observed in the glacial data. In particular, the Ba/P ratio of the deep Atlantic is very sensitive to the magnitude of upwelling in the Atlantic and the particulate flux that the upwelling generates. The model suggests that an increase in the Atlantic upwelling by about a factor of 2 can account for the observed glacial Ba distributions while maintaining P distributions that are essentially in agreement with the foraminiferal Cd evidence.

The Ba content of benthic foraminifera recovered from the glacial sections of a Caribbean and Mediterranean core suggest that Mediterranean

Ba was at least 50% higher than Caribbean Ba at the LGM. Therefore the paleo-Ba data are in direct conflict with any scenario that invokes Mediterranean outflow waters as a source of nutrient depletion at intermediate depths in the Glacial Atlantic.

References--Chapter 6

Bishop, J. K. B. (1988a) The barite-opal-organic carbon association in oceanic particulate matter. *Nature* **332**, 341-343.

Bishop, J. K. B. (1988b) Regional extremes in particulate matter composition and flux: effect on the chemistry of the ocean interior. In *Productivity of the oceans present and past* (ed. W. H. Berger, V. S. Smetacek and G. Wefer), pp. n-n, John Wiley and Sons Ltd., Chichester.

Boyle, E. A. (1981) Cadmium, zinc, copper, and barium in foraminifera tests. *Earth Planet. Sci. Lett.* **53**, 11-35.

Boyle, E. A. (1984) Sampling statistic limitations on benthic foraminifera chemical and isotopic data. *Mar. Geol.* **58**, 213-224.

Boyle, E. A. (1986a) Deep ocean circulation, preformed nutrients, and atmospheric carbon dioxide: theories and evidence from oceanic sediments. In *Mesozoic and Cenozoic Oceans* (ed. K. J. Hsü), pp. 153, AGU, Washington, D.C.

Boyle, E. A. (1986b) Paired carbon isotope and cadmium data from benthic foraminifera: implications for changes in deep ocean P and atmospheric carbon dioxide. *Geochim. Cosmochim. Acta.* **50**, 265-276.

Boyle, E. A. (1988) Cadmium: chemical tracer of deepwater paleoceanography. *Paleoceanography* **3**, 471-489.

Boyle, E. A. and Keigwin, L. D. (1982) Deep circulation of the North Atlantic over the last 200,000 years: Geochemical evidence. *Science* **218**, 784-787.

Boyle, E. A. and Keigwin, L. D. (1985) Comparison of Atlantic and Pacific paleochemical records for the last 215,000 years: changes in deep ocean circulation and chemical inventories. *Earth Planet Sci. Lett.* **76**, 135-150.

Boyle, E. A. and Keigwin, L. D. (1987) North Atlantic thermohaline circulation during the past 20,000 years linked to high-latitude surface temperature. *Nature* **330**, 35-40.

Broecker, W. S. and Peng, T. H. (1986) Carbon cycle: 1985 Glacial to interglacial changes in the operation of the global carbon cycle. *Radiocarbon.* **28**, 309-327.

Chan, L. H., Drummond, D., Edmond, J. M. and Grant, B. (1977) On the barium data from the Atlantic GEOSECS Expedition. *Deep-Sea Res.* **24**, 613-649.

Chan, L. H., Edmond, J. M., Stallard, R. F., Broecker, W. S., Chung, Y. C., Weiss, R. F. and Ku, T. L. (1976) Radium and barium at GEOSECS stations in the Atlantic and Pacific. *Earth Planet. Sci. Lett.* **32**, 258-267.

COHMAP. (1988) Climatic changes of the last 18,000 years: Observations and model simulations. *Science* **241**, 1043-1052.

Collier, R. W. (1981) *The trace element geochemistry of marine biogenic particulate matter*. Ph.D. Thesis, MIT/WHOI, 299 pp.

Curry, W. B., Duplessy, J. -C., Labeyrie, L. D. and Shackleton, N. J. (1988) Changes in the distribution of $\delta^{13}\text{C}$ of deep water ΣCO_2 between the last glaciation and the Holocene. *Paleoceanography* **3**, 317-342.

Dehairs, F., Chesselet, R. and Jedwab, J. (1980) Discrete suspended particles of barite and the barium cycle in the open ocean. *Earth Planet. Sci. Lett.* **49**, 528-550.

Dehairs, F., Lambert, C. E., Chesselet, R. and Risler, N. (1987) The biological production of marine suspended barite and the barium cycle in the Western Mediterranean Sea. *Biogeochem.* **4**, 119-139.

Duplessy, J. -C., Shackleton, N. J., Fairbanks, R. G., Labeyrie, L., Oppo, D. and Kallel, N. (1988) Deepwater source variations during the last climatic cycle and their impact on the global deepwater circulation. *Paleoceanography* **3**, 343-360.

Edmond, J. M. (1974) On the dissolution of carbonate and silicate in the deep ocean. *Deep Sea Res.* **21**, 455-480.

Keigwin, L. D. (1987) North Pacific deep water formation during the latest glaciation. *Nature* **330**, 362-364.

Kier, R. (1988) On the late Pleistocene ocean geochemistry and circulation. *Paleoceanography* **3**, 413-445.

Lea, D. and Boyle, E. (1989) Barium content of benthic foraminifera controlled by bottom water composition. *Nature* **338**, 751-753.

Lyle, M. (1988) Climatically forced organic carbon burial in equatorial Atlantic and Pacific oceans. *Nature* **335**, 529-532.

Mix, A. C. (1989) Influence of productivity variations on long-term atmospheric CO_2 . *Nature* **337**, 541-544.

Oppo, D. W. and Fairbanks, R. G. (1987) Variability in the deep and intermediate water circulation of the Atlantic Ocean during the past 25,000 years: northern hemisphere modulation of the Southern Ocean. *Earth Planet. Sci. Lett.* **86**, 1-15.

Ostlund, H. G., Craig, H., Broecker, W. S. and Spencer, D. W. (1987) *GEOSECS Atlantic, Pacific, and Indian Ocean Expeditions, Vol. 7, Shorebased Data and Graphics*. National Science Foundation, Washington, DC, 200p.

Parkin, D. W. and Shackleton, N. J. (1973) Trade wind and temperature correlations down a deep-sea core off the Saharan Coast. *Nature* **245**, 455-457.

Rhein, M. and Schlitzer, R. (1988) Radium-226 and barium sources in the deep East Atlantic. *Deep-Sea Res.* **35**, 1499-1510.

Shackleton, N. J., Duplessy, J. C., Arnold, M., Maurice, P., Hall, M. A. and Cartlidge, J. (1988) Radiocarbon age of last glacial Pacific deep water. *Nature* **335**, 708-711.

Zahn, R., Sarnthein, M. and Erlenkeuser. (1987) Benthic isotope evidence for changes of the Mediterranean outflow during the late Quaternary. *Paleoceanography* **2**, 543-559.

CHN82 Sta24 Core 4PC			CHN82 Sta41 15PC			CHN82 Sta31 11PC		
Depth (cm)	Age (kyr)	Sed. rate (cm/kyr)	Depth (cm)	Age (kyr)	Sed. rate (cm/kyr)	Depth (cm)	Age (kyr)	Sed. rate (cm/kyr)
1	0.0		1	0.0		0	0.0	
40	11.0	3.5	31	18.0	1.7	54	13.0	4.2
64	18.0	3.4				73	18.0	3.8
90	24.0	4.3				110	24.0	6.2

Appendix to Chapter 6: Age models for three North Atlantic cores, based on oxygen isotope records.

Chapter 7: 210 kyr record of Ba in the deep North Atlantic

7.1 Introduction

A long temporal record can be used to evaluate the response of tracer variability over more than one climatic cycle. Since confluence of factors such as orbital forcing varies from one cycle to the next, tracers might respond differently to otherwise similar climate transitions. Long records are important in evaluating the connections between climate variation and deep ocean processes; while a record of a single glacial-interglacial cycle might suggest an association, by itself that record does not confirm a deep ocean-climate link. The importance of this coupling cannot be understated, since deep ocean ventilation affects factors like atmospheric CO₂ that in themselves may drive climate change. Previous studies have shown that deep ocean tracers like Cd and ¹³/₁₂C do respond periodically to climate change over 100 kyr time scales (Boyle and Keigwin, 1982; Boyle and Keigwin, 1985).

Examination of long records by spectral analysis can reveal the presence of orbital frequencies that characterize much of the geochemical and climatological data recovered from marine sediments (Hays *et al.*, 1976). Although the presence of such forcing does not necessarily give mechanistic answers, it provides clues to the source of the observed variations.

A record of benthic Ba/Ca in the deep North-West Atlantic stretching back to Interglacial Stage 7, about 210 kyr before present, has been recovered. This time period encompasses 2 full glacial cycles. The choice of the deep North Atlantic for a first long Ba record was based on the observation that the largest changes observed in Ba in the last 25 kyrs are found in North Atlantic cores, which indicate 40-60% higher Ba in the deep Atlantic during the LGM (Chapter 6). The higher Glacial values are apparently due to a decrease in the flux of Ba-

depleted surface waters to the deep North Atlantic; the Ba enrichments might also be coupled to an increase in the delivery of particulate Ba caused by greater Glacial Atlantic upwelling/productivity (see Chapter 6).

Piston core *CHAIN* 82, station 24, core 4PC was raised from 3427 m on the western flank of the Mid-Atlantic Ridge (41°43'N, 32°51'W). It contains well-preserved planktonic and benthic foraminifera throughout its length. Previous studies have recovered benthic foraminiferal $\delta^{18}\text{O}$, $\delta^{13}\text{C}$, and Cd/Ca (Boyle and Keigwin, 1985). The sedimentation rate averages about 3 cm/kyr, although sedimentation rates are not uniform over the length of the core. This core is located close to the site of core V30-97, for which faunal indices of sea surface temperature through stage 7 are available (Ruddiman and McIntyre, 1981; Ruddiman *et al.*, 1989).

Ba/Ca ratios were determined on samples of *Uvigerina spp.* where available. Certain intervals have low to near zero *Uvigerina spp.* abundances: 0-35 cm (stage 1), 250-300 cm (stage 5a), 450-465 (stage 5e) and 650-670 cm (stage 7a-b) (Boyle and Keigwin, 1985). *C. kullenbergi* Ba/Ca was substituted for *Uvigerina spp.* over 0-30 cm. Calibration of these two species for uptake of Ba indicates no statistically significant difference (Lea and Boyle, 1989) (Chapter 5). *Uvigerina spp.* Ba/Ca were used in the other low abundance intervals; these values should be interpreted with caution since small samples were used for analysis. In addition, bioturbation can bias any foraminiferal parameter measured in zones of low abundance.

In an attempt to fill in some of the low abundance *Uvigerina spp.* intervals, Ba/Ca was determined on samples of both *C. wuellerstorfi* and *C. kullenbergi* from stage 5. However, these values were always significantly higher than coexisting *Uvigerina spp.*, and they displayed poor reproducibility between adjacent depths. These values also bear no clear relation to either the

oxygen isotope record or *Uvigerina spp.* Ba/Ca record. A similar problem has been observed for Cd/Ca determination of these same species in stage 5 of this core as well as others (E. Boyle, pers. comm.). These higher values are probably due to the growth of manganese carbonate overgrowths on the foraminifera shells (Boyle, 1983). These growths presumably "trap" sediment material or coatings onto the shells, the end result being spuriously high metal determinations due to the contribution of these trapped phases. Most of the samples that had high or spurious Ba were checked for Mn content; all samples of *Cibicidoides* from stage 5 for which Mn was determined had Mn/Ca above 290 $\mu\text{mol/mol}$. Values significantly above 100 $\mu\text{mol/mol}$ are taken as evidence for the presence of Mn-carbonate overgrowths (E. Boyle, pers. comm. and Boyle, 1983).

The fact that Mn-carbonate overgrowths are a problem for both Cd and Ba, two tracers with very different chemistries, suggests that Mn must be carefully monitored to have confidence in any foraminiferal metal tracer. It should be noted that these growths affect measured foraminiferal Ba contents even though the Ba content of foraminifera is about a factor of 20 higher than Cd. The "effective" (i.e. including any trapped material) Ba/Mn ratio of these growths must be about 0.002 to account for the observed deviations from expected values. A question that remains unexplained is why these growths are absent on *Uvigerina spp.* shells in this and many other cores (E. Boyle, pers. comm.).

Average Ba/Ca for sampled depths of the core are compiled in Table 7.1 and illustrated in Fig 7.1. The majority of samples were run in duplicate. The pooled average standard deviation (or difference from the mean when $n=2$) for replicates was 0.22 $\mu\text{mol/mol}$ (8%). The reproducibility of samples varied somewhat with depth in the core; for example, samples in intervals where

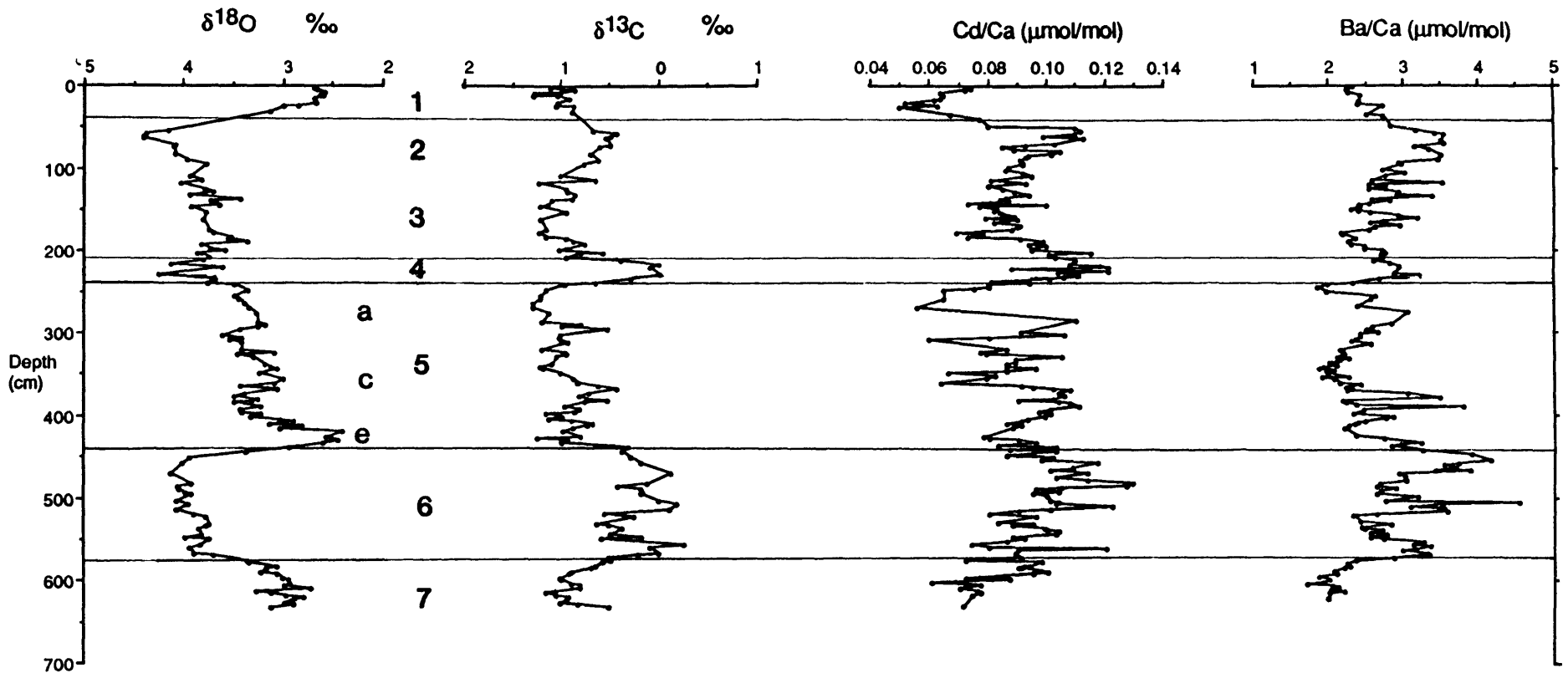


Figure 7.1 Ba/Ca of benthic foraminifera (mostly *Uvigerina spp.*; see Table 7.1) plotted vs. depth in CHN82 Sta24 Core 4PC (42°N, 33°W: 3427 m). Also illustrated are oxygen isotope (*C. wuellerstorfi*), carbon isotope (*C. wuellerstorfi*) and Cd/Ca (mostly *Uvigerina spp.*) data for the same core (Boyle and Keigwin, 1985). Stage boundaries are based on the oxygen isotope record. Note that depths deeper than 348 cm have been corrected by -32 cm because of a core void between 348 and 380 cm.

Interval (cm)	Ba/Ca ($\mu\text{mol/mol}$)	SD	n	r	Species*
0 - 2	2.33	0.06	2		C. kullenbergi
4 - 5	2.24	0.01	2		C. kullenbergi
8 - 9	2.26		1		C. kullenbergi
12 - 13	2.42	0.08	2		C. kullenbergi
19.5-20.5	2.40		1		C. kullenbergi
22 - 24	2.38		1		C. kullenbergi
25 - 26	2.72		1		C. kullenbergi
35 - 36	2.51		1		
37 - 38	2.73		1		
48 - 49	2.81		1		
53.5-54.5	3.16		1		
56 - 59	3.41		1		
59 - 62	3.54	0.02	2	1	
67 - 69	3.49	0.08	3		
70 - 72	3.54		1		
73 - 75	3.14		1		
77 - 79	3.33		1		
84 - 87	3.50		1		
89 - 90	3.46		1		
93 - 95	2.92	0.04	2		
95 - 97	2.97	0.29	2		
100 - 103	2.71		1		
104 - 107	3.00		1		
109 - 111	2.73		1		
114 - 116	2.56	0.22	3	1	
116.5-119	3.52	0.22	2		
119 - 122	2.53		1		
119-126	2.75		1		
123 - 126	2.52		1		
128 - 130	2.92		1		
130 - 133	2.90		1		
133 - 136	3.37		1	1	
136-138.5	2.57		1		
138.5-141	2.80		1	1	
141-143.5	2.53	0.01	2		
143.5-146	2.38	0.09	2		
146-148	2.40		1		
148-150.5	2.28		1		
150.5-153	2.39		1		
153 - 155	2.54	0.06	2		
155-157.5	2.93		1		
157.5-159	2.96	0.20	2		
159.5-162	3.17	0.32	2		
162-164.5	2.72	0.02	2		
164.5-167	2.54	0.12	2	1	
167 - 170	2.95	0.01	2		
170-172.5	2.61		1		
172.5-175	2.53	0.32	2		

Table 7.1 Ba/Ca measured in benthic foraminifera from CHN82 Sta24 Core4PC (42°N, 33°W: 3427 m). All values from *Uvigerina spp.* unless indicated otherwise. Depths listed here are relative to original core liner. Note that there was a core void between 348 and 380 cm. SD = standard deviation; n = number of samples included in mean; r = number of samples rejected from mean. For depths with two replicates standard deviations are differences from the mean.

Interval (cm)	Ba/Ca ($\mu\text{mol/mol}$)	SD	n	r	Species*
177 - 179	2.15	0.03	2		
179.5-181.5	2.16		1		
185 - 187	2.34		1		
187-190	2.25		1		
190 - 193	2.29		1		
193 - 195	2.46		1		
195 - 198	2.47		1		
198 - 201	2.70		1		
201 - 203	2.74	0.04	2		
203 - 205	2.68		1		
207 - 209	2.70	0.16	2		
210 - 214	2.58	0.07	2		
214 - 217	2.80	0.20	2		
217 - 220	2.92	0.06	2		
220 - 222	2.93	0.38	2		
224-226.5	2.88	0.04	2		
226.5-228.5	2.87	0.07	3		
228.5-230	3.19		1	1	
230 - 233	3.00		1		
233 - 236	2.65	0.20	3		
239 - 242	2.30	0.20	3		
241.5-243	1.96		1		
243-246	1.82	0.04	2		
247-252	1.95	0.07	2		
254 - 256	2.61	0.04	1		
255-264	2.55		1		
266-271	2.37		1		
272-279	3.03		1		
286-291	2.82		1		
291-295	2.56		1		
295-298	2.49		1		
298-300	2.64		1		
300 - 303	2.40		1		
303-306	2.40		1		
307 - 309	2.34		1		
310-312	2.29		1		
312-316	2.54		1		
320 - 322	2.12		1		
322-324	2.17		1		
325-328	2.18		1		
328 - 330	2.10		1		
330-332	2.25		1		
333-334	2.13		1		
334-336	2.09		1		
336-338	2.00		1		
339-341	2.09	0.01	2		
341-343	1.92		1		
343-345	1.86		1		
345-347	2.05	0.02	2		
347-348	1.95		1		

Table 7.1 (cont.) Benthic Ba/Ca in CHN82 Sta24 Core4PC.

Interval (cm)	Ba/Ca ($\mu\text{mol/mol}$)	S D	n	r	Species*
381-383	1.98		1		
384.5-7.5	2.25		1		
384.5-387.5	1.89		1		
384.5-387.5	2.05		1		
393-395	2.14		1		
395-397	2.40		1		
398 - 400	2.20		1		
400 - 402	2.29	0.19	2		
402 - 404	2.23	0.05	2	1	
404.5-407	3.04	0.29	4		
410 - 413	3.48		1		
413-415.5	2.17		1		
415.5-418	2.21	0.17	2		
418-420.5	2.35	0.09	2		
421 - 424	3.79	0.25	2		
423 - 426	2.45		1		
426 - 429	2.42	0.27	3	1	
429 - 432	2.31		1		
432 - 435	2.84	0.74	3		
435 - 438	2.75	0.25	2		
438 - 440	2.46	0.29	3		
440 - 442	2.37	0.11	3		
442-444	2.33		1		
444-446	2.24		1		
446-450	2.20		1		
456-458	2.35		1		
458-462	2.72		1		
464-466	3.23		1		
466-468	2.95	0.01	2		
468-470	2.83	0.07	2		
470-471	2.98		1		
472.5-475.5	3.23	0.10	2		
478.5-482	3.91	0.24	2		
485.5-489	4.17		1		
490 - 492	3.74	0.09	2		
492 - 494	3.54		1		
494 - 497	3.70		1		
497 - 500	3.42		1		
499 - 501	3.89	0.28	2		
502 - 504	2.92		1		
504 - 507	3.01		1		
510 - 513	3.02		1		
515 - 517	2.67		1		
517 - 519	2.63		1		
519 - 522	2.89	0.04	2		
523 - 525	2.68		1		
526 - 529	2.62	0.13	2		
529.5-532	3.18	0.08	2		
535 - 537	2.74	0.06	2		
537 - 539	4.53	0.38	2		

Table 7.1 (cont.) Benthic Ba/Ca in CHN82 Sta24 Core4PC.

Interval (cm)	Ba/Ca ($\mu\text{mol/mol}$)	S D	n	r	Species*
539 - 541	3.51	0.47	3		
541 - 544	3.08	0.16	3	2	
544 - 547	3.53	0.06	2		
544 - 547	3.48		1		
547 - 550	3.57	0.31	3	1	
550 - 553	2.62	0.09	2		
553 - 556	2.31	0.16	2		
560 - 563	2.41	0.15	2		
563-565.5	2.82	0.49	4		
566-568.5	2.43	0.24	2		
568 - 571	2.47		1		
571-573.5	2.69	0.07	2		
573.5-575.5	2.55		1		
575.5-578.5	2.75	0.12	3		
578.5-581	2.55	0.11	2		
581 - 584	2.73	0.07	2		
584-587	3.27	0.06	2		
587 - 590	3.12	0.03	2		
590 - 593	3.36		1		
593 - 595	3.16		1		
596 - 598	2.98		1		
598 - 600	3.32	0.03	2		
600 - 603	3.34	0.27	2		
604 - 606	2.87	0.01	2		
607-610	2.35	0.04	2		
610-612.5	2.23	0.00	2		
613 -616.5	2.26		1		
616.5-619.5	2.20		1		
620-623	2.04		1		
623 - 626	2.10	0.02	2		
627-630	1.86		1		
630-633	1.99		1		
633 - 636	1.92	0.18	2		
636-638	1.70		1		
638 - 640	2.04	0.29	2		
640-642	2.11	0.05	2		
642 - 644	2.01		1		
644 - 646	2.20		1		
646 - 648	2.00	0.10	2		
651 - 657	1.96		1		

*Uvigerina spp. unless indicated;

Table 7.1 (cont.) Benthic Ba/Ca in CHN82 Sta24 Core4PC.

Ba/Ca is not changing rapidly (320-350, 550-585, 610-650 cm) showed excellent reproducibility sometimes approaching analytical precision. Conversely, reproducibility during periods of rapid change in Ba/Ca such as the transition from stage 5a to 4 (250-230 cm) was clearly poorer, most probably because of the effect of bioturbation. Ba/Ca determinations between 400 and 440 cm (stage 5d) were less reproducible than in any other interval. Replicate samples from the same depth differed by as much as 50%, while adjacent depths sometimes differed by close to a factor of 2. No explanation is obvious for this phenomenon. High Ba/Ca values are not anticipated for stage 5d (at least based on Cd/Ca and $\delta^{13}\text{C}$), and this section of the core is preceded and followed by some of the most reproducible sections in the core. If these fluctuations are a real indication of variability in bottom water Ba then this interval suggests high frequency variations were present in stage 5d.

7.2 Features of the Ba record

Fig. 7.2 illustrates the Ba record on a time scale based on the accepted timing for the major features of the oxygen isotope record identifiable in this core (Boyle and Keigwin, 1985) (appendix to Chapter 7). The bottom of the core (668 cm) has been assigned to the transition between stage 7a and 7b, or about 220 kyr. This produces a realistic sedimentation rate for stage 7 (~2 cm/kyr) and is justifiable given that the benthic oxygen isotope record never reaches the heavy values (~4‰) characteristic of stage 7b. In addition, the disappearance of *Uvigerina spp.* in the bottom 20 cm of the core is consistent with the same faunal change observed in early stage 7a in neighboring core V30-97.

The major features of the Ba/Ca record show a strong covariance with the classically recognized climate cycles of the last 200,000 years (Emiliani,

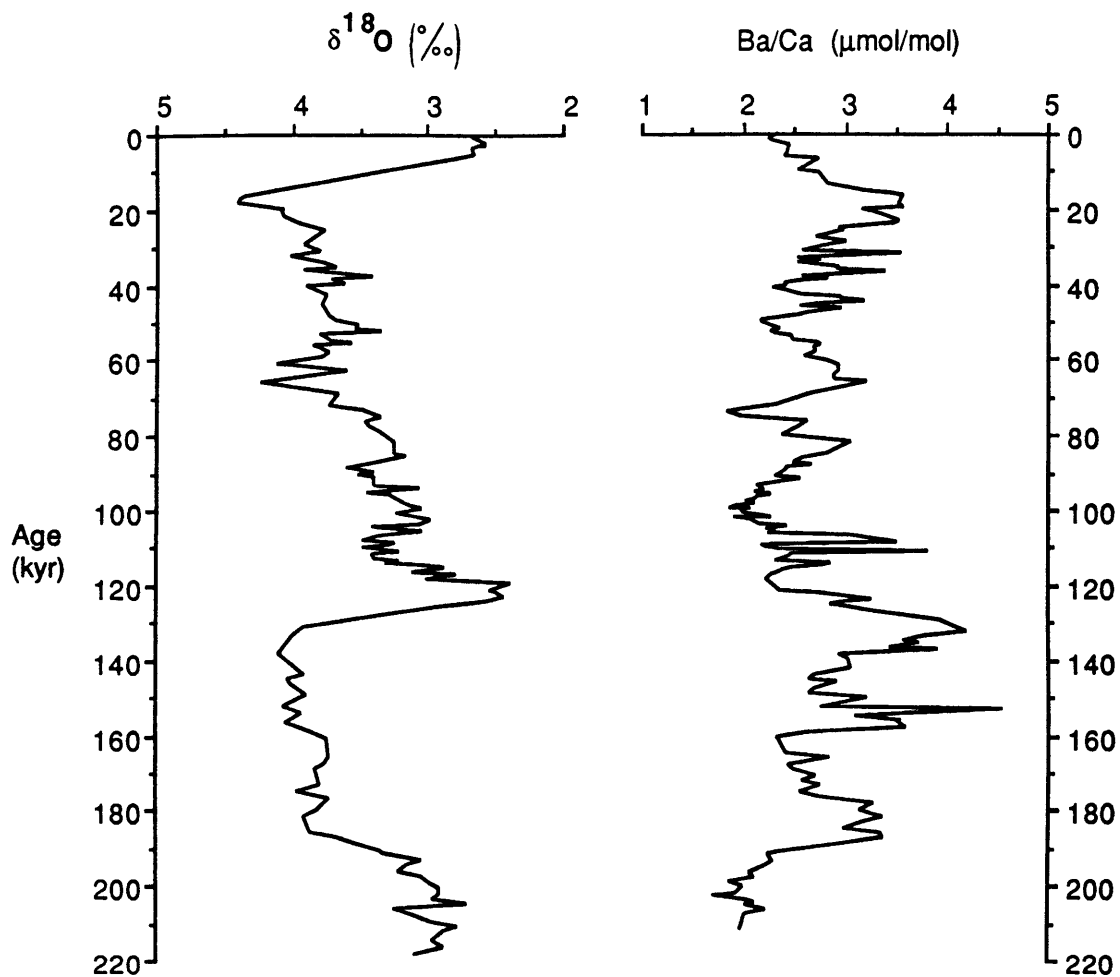


Figure 7.2 Benthic foraminiferal Ba/Ca and $\delta^{18}\text{O}$ (Boyle and Keigwin, 1985) from CHN82 Sta24 Core4PC plotted vs. age. The age model is based on correlation of the oxygen isotope record with a stacked oxygen isotope record (Martinson *et al.*, 1987). See appendix to Chapter 7 for age points.

1966; Shackleton and Opdyke, 1973). Generally, minima in benthic Ba are associated with interglacial stages and maxima are associated with glacial stages. Interglacial stages (1,3,5 and 7) are characterized by Ba/Ca values of about 1.8 to 2.6 $\mu\text{mol/mol}$, and glacial stages (2,4 and 6) are characterized by values of about 2.6 to 4 $\mu\text{mol/mol}$. The most Ba-depleted deep waters at these sites were present in stages 5a, 5c and 7, while the most Ba-enriched deep waters were present during stage 2 and 6.

The most dramatic change in the Ba record is associated with the transition from glacial stage 6 to interglacial stage 5e in which Ba/Ca drops from over 4 $\mu\text{mol/mol}$ to a minimum of 2.2 $\mu\text{mol/mol}$. This change coincides with the ~ 1.6 per mil drop in $\delta^{18}\text{O}$ that defines the transition. This almost two-fold drop in Ba/Ca is clearly larger than the decrease from 3.5 to 2.3 $\mu\text{mol/mol}$ recorded during the transition from stage 2 to stage 1.

The two transitions from interglacial to glacial stages are both characterized by rapid increases in benthic Ba/Ca. In the transition from stage 7 to stage 6, Ba/Ca rises from about 2.1 to 3.6 $\mu\text{mol/mol}$ over only a 10 cm sediment interval (estimated at about 3 kyrs). In the transition from stage 5a to stage 4 Ba/Ca rises from about 1.8 $\mu\text{mol/mol}$ to 3.2 $\mu\text{mol/mol}$ over a 13 cm interval (estimated at about 7 kyrs). These seemingly rapid changes in Ba/Ca at these transitions suggest that Ba in the deep waters of the Northwest Atlantic changes most rapidly during the transitions into glacial periods.

Comparison of the Ba and Cd records for this core reveal that both records are generally similar in confirming high nutrient levels during glacial periods and low nutrient levels during interglacial periods (Fig. 7.1). The two records are most similar in the top 250 cm of the core, both showing minima in the core-top and in stage 3 with maxima during stage 2 and 4. However, there are clear differences over this interval between the two records; in particular, Cd

records an early Holocene minimum not observed in the Ba record and stage 4 is broader and of higher relative magnitude in the Cd record. The records of Ba and Cd are less similar over the rest of the core. The records diverge quite markedly over much of stage 5, actually appearing out of phase over certain intervals. The records do agree in confirming higher nutrient values in glacial stage 6 relative to lower values in interglacial stage 7, but the records show little direct correspondence in the higher frequency variability observed in 6 and 7.

Comparison of the Ba record with the carbon isotope record reveals stronger similarities than those observed between Ba and Cd (Fig. 7.1). Ba/Ca maxima and $\delta^{13}\text{C}$ minima correspond in stage 2, 4, 5d, and 6 (3 different maxima), although the relative magnitude of these peaks varies between the two tracers. In particular, the peaks in stage 6 are more sharply defined for Ba. Another large difference between the two records is that Ba shows more high frequency variability in stage 2 and 3; although this variability is generally supported by the Cd record, it is not clearly apparent in the carbon isotope record.

7.3 Discussion

It is somewhat surprising that there is not more correspondence between Cd and Ba variability, especially given the similarities between the carbon isotope record and Ba. Previous studies have suggested that some of the variability in the carbon isotope record reflects climate mediated transfer of carbon between high latitude forests and the oceans (Shackleton, 1977; Boyle and Keigwin, 1985; Keigwin and Boyle, 1985), so *a priori* one would expect less similarity between the Ba and carbon isotope records. The source of these differences is important in terms of both understanding climate/ocean change as well as evaluating just what physical factor(s) each tracer records.

Ba's short oceanic residence time, estimated at about 10,000 years (Chan *et al.*, 1976), is especially important to any consideration of long term variability. A survey of Ba in the oceans of the LGM suggest that mean ocean Ba might have been ~15% lower (Chapter 6). On the 200,000 time scale of the 4PC record, changes in the Ba content of the oceans are quite possible. However, the variability in Ba recorded by the benthic foraminifera from core 4PC argues against large changes in oceanic Ba content over the last 200 kyr, since the interglacial minima are of similar magnitude between stages 1, 5 and 7. The question of change in oceanic Ba content cannot be answered satisfactorily without a complimentary Pacific record.

Two previous studies of CHN82-4PC suggested that down-core variability in benthic foraminiferal Cd (and some of the down-core variability in $\delta^{13}\text{C}$) can be explained by variations in the flux of nutrient depleted water to this site (Boyle and Keigwin, 1985; Keigwin and Boyle, 1985). Such variations would affect Ba in a similar manner since temperate surface waters from the world's oceans are depleted in Ba. The fact that records of all three tracers indicate higher nutrients in Atlantic deep waters during glacial times (i.e reduced flushing) suggests that at least some of the temporal variability in each tracer is due to variations in surface convection. However, the records are quite different in detail (Fig. 7.1); it is difficult to suggest with any certainty what specific oceanic or climatic factors might be causing these differences. The problem of the relationship between the three paleo-nutrient indicators is dealt with in further detail by spectral analysis.

7.4 Time Series Analysis

Differences between the Ba and the oxygen isotope record indicate that Ba variability at this site is not related in a simple way to change in global ice

volume (Fig. 7.2). During intervals where oxygen isotopes remain heavy (large relative ice volume) there are minima in Ba/Ca comparable to the Holocene (for example stages 3 and 6), and some of the Ba maxima in stage 5 (low relative ice volume) are comparable to glacial values for Ba. In addition, there is a strong indication of a ~20 kyr periodicity in the Ba record. Clearly an objective evaluation of this variability is necessary.

Spectral analysis has been applied to the Ba data from this study and the Cd, carbon and oxygen isotope data from previous studies (Boyle and Keigwin, 1985; Keigwin and Boyle, 1985) to evaluate the frequency response, coherence and phase of these records with respect to the earth's orbital parameters. The technique is based on the Fast Fourier Transform (FFT) method and is described in Keigwin and Boyle (1985).

Fig. 7.3 illustrates periodogram and log power Spectra (2-band averaged) derived by FFT from a 212 kyr detrended and tapered 4PC benthic foraminiferal Ba record. The strongest power is found for frequencies of 0.0094 (106 kyr), 0.0189 (53 kyr), and 0.0425 (23.6 kyr). 100 kyr power is seen in almost all paleo-climatic records and corresponds to the period of eccentricity in the earth's orbit. The 106 kyr power (area under the peak) in the Ba record accounts for about 22% of the total variance. The 23.6 kyr power corresponds to the period of precession in the earth's orbit. The 23.6 kyr peak is the dominant peak for Ba, accounting for about 34% of the total variance in the spectra. The 53 kyr peak does not correspond to previously observed orbital periods in deep sea cores, although Berger (1987) has suggested that several ~50,000 year orbital terms might be expected. The 53 kyr peak accounts for 24% of the total variance present in the periodogram; however, it is not a resolvable peak in the band-averaged log power spectra, in which only the 23.6 peak is present above

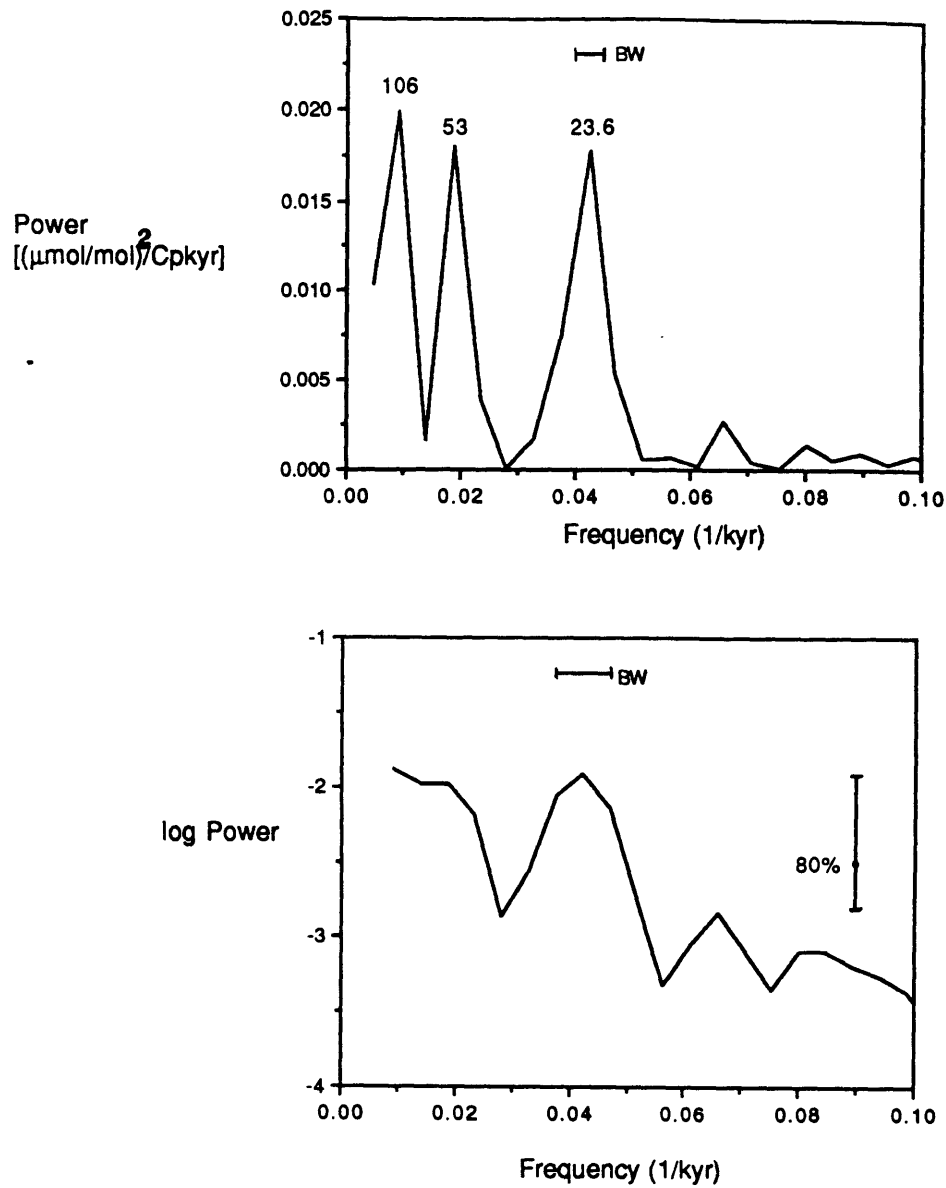


Figure 7.3 Periodogram and log power spectrum for the CHN82-4PC record. Bandwidths (BW) and 80% confidence intervals are indicated. The power spectrum is based on 2-band averaging.

the 80% CI. Power corresponding to the period of changes in the earth's tilt (41 kyr) is conspicuously absent from the Ba spectra.

Figure 7.4 compares log power spectra for Ba, Cd, $\delta^{13}\text{C}$ and $\delta^{18}\text{O}$ derived from CHN82-4PC records with the spectra for combined eccentricity + tilt + precession (ETP) index derived from calculated orbital parameters (Berger, 1977). All the tracers but Ba show at least some increase in power at the 41 kyr tilt frequency (0.024 kyr^{-1}), although they are not close to matching the magnitude of tilt power in the ETP spectra. Ba has very strong power at the 23 kyr precessional frequency (0.043 kyr^{-1}); this power almost matches that present in the orbital ETP spectra. Oxygen isotopes also have strong power at 23 kyr, and both Cd and carbon isotopes display some power at this period. Ruddiman and McIntyre's (1981) spectral analysis of August SST in nearby core V30-97 indicated dominance of precessional power similar to what is observed in the Ba spectra from CHN82-4PC.

Table 7.2 lists the coherence between Ba and the other tracers from CHN82-4PC, ETP and SST from V30-97. Ba is coherent (95% confidence interval) at the precessional frequencies with (from strongest to weakest) oxygen isotopes, carbon isotopes, Cd and ETP. Coherence with the V30-97 SST record at 23 kyr only exceeds the 90% confidence interval, presumably because of deviations that arise in matching time scales from two different cores. Ba coherence also exceeds the 95% CI at the 106 kyr periodicity with ETP, oxygen and carbon isotopes and V30-97 SST.

Phase relationships are summarized in Table 7.2. At the precessional frequencies Ba is in phase with Cd/Ca and $-\delta^{13}\text{C}$ and a half cycle out of phase with $-\delta^{18}\text{O}$ (i.e. in phase with $+\delta^{18}\text{O}$). Ba lags V30-97 SST by 8 ± 2 kyrs (i.e. high Ba is almost in phase with low SST). Summer insolation maxima in precession lead low Ba by 7 ± 2 kyrs. The relation between precession and

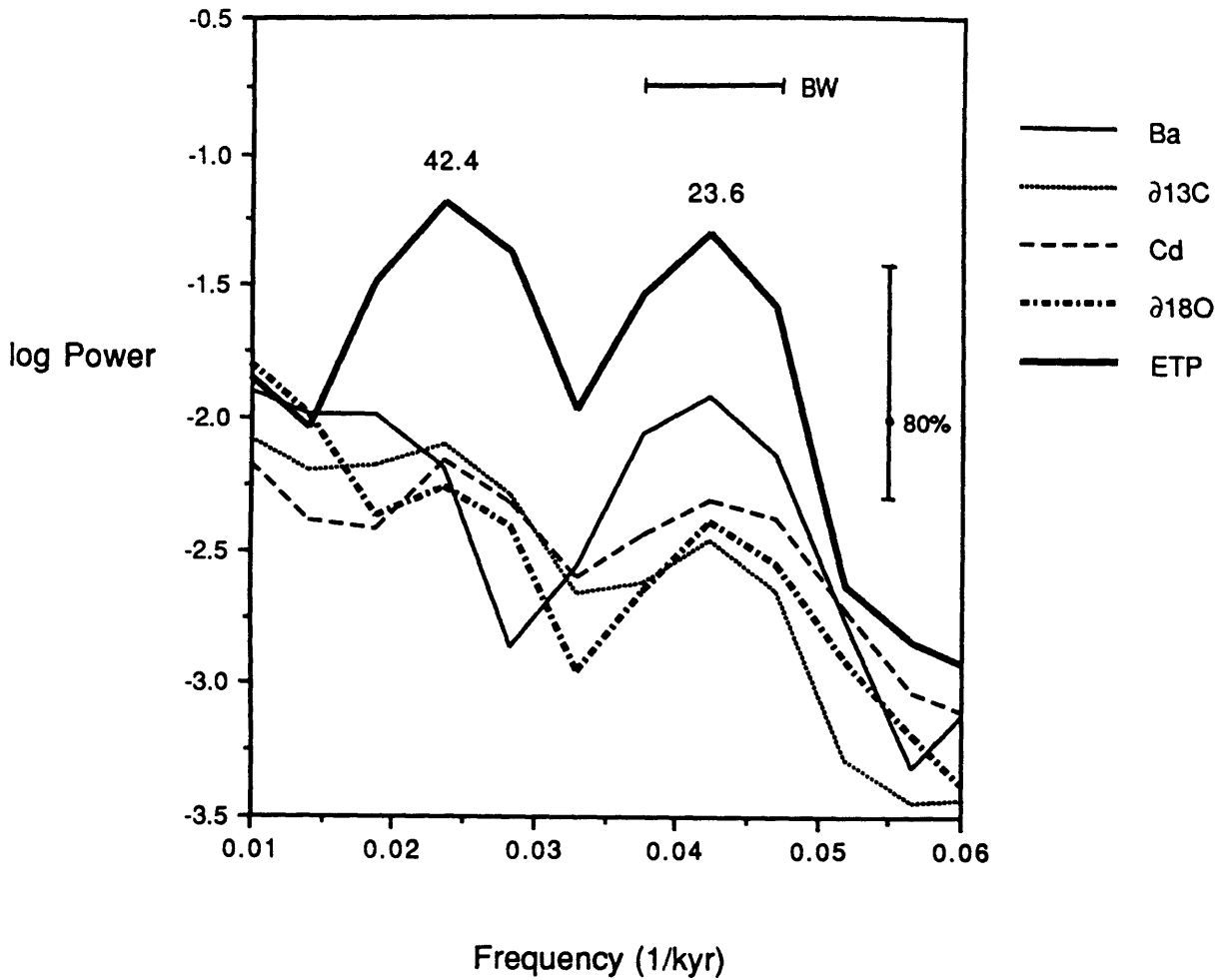


Figure 7.4 Comparison of log power spectra for foraminiferal tracers from CHN82-4PC. Ba from this work, $\delta^{18}\text{O}$, $\delta^{13}\text{C}$ and Cd from Boyle and Keigwin (1985). Also shown is the log power spectra for eccentricity + tilt + precession (ETP) calculated from Berger (1977). Bandwidth (BW) and 80% confidence interval is indicated. Power spectra are based on 2-band averages.

Spectral coherence of climatic parameters with barium

(All coherences on 3-band averages of tapered spectra:

95% confidence interval = 0.881; 90% confidence interval = 0.827.

Phase listed as positive when Ba leads the indicated parameter.)

Period (kyr)	Parameter	Coherence#	Phase (°)*	Phase (kyr)*
106	ETP	0.948	123 ±21	36 ±6
42.4	ETP	0.293		
26.5	ETP	0.857	81 ±40	6 ±3
23.6	ETP	0.878	71 ±36	5 ±2
21.2	ETP	0.887	66 ±34	4 ±2
19.3	ETP	0.502		
106	-δ18O	0.966	128 ±17	38 ±5
42.4	-δ18O	0.624		
26.5	-δ18O	0.863	152 ±39	11 ±3
23.6	-δ18O	0.957	154 ±19	10 ±1
21.2	-δ18O	0.923	155 ±26	9 ±2
19.3	-δ18O	0.732		
106	-δ13C	0.953	-27 ±20	-8 ±6
42.4	-δ13C	0.609		
26.5	-δ13C	0.797		
23.6	-δ13C	0.940	-16 ±23	-1 ±1
21.2	-δ13C	0.941	-10 ±23	-1 ±1
19.3	-δ13C	0.492		
106	Cd	0.852	2 ±41	1 ±12
42.4	Cd	0.308		
26.5	Cd	0.489		
23.6	Cd	0.611		
21.2	Cd	0.920	-7 ±27	0 ±2
19.3	Cd	0.751		
106	SST (V30-97)	0.962	126 ±18	37 ±5
42.4	SST (V30-97)	0.425		
26.5	SST (V30-97)	0.733		
23.6	SST (V30-97)	0.719		
21.2	SST (V30-97)	0.857	-134 ±40	-8 ±2
19.3	SST (V30-97)	0.617		

#Bold indicates coherence exceeding the 90% CI

* Only listed for coherences exceeding the 90% CI

Note: ETP=combined orbital parameters eccentricity, tilt and precession (Berger, 1977).

Table 7.2 Coherence and phase relationships between Ba/Ca and ETP index, negative δ¹⁸O, negative δ¹³C and Cd/Ca in CHN82 Sta24 Core4PC (Boyle and Keigwin, 1985) and summer SST in core V30-97 (Ruddiman and McIntyre, 1981; Ruddiman *et al.*, 1989).

Ba is illustrated in Figure 7.5; shifting the precession index by 7 kyrs aligns insolation minima with Ba maxima.

7.5 Conclusions and speculation

The dominance of the 23 kyr precessional cycle in the Ba spectrum stands out as a key factor that distinguishes the Ba record from that of Cd and carbon isotopes. Since all three tracers potentially record variations in the flux of nutrient depleted waters to the deep Atlantic, this difference hints at either Ba being more sensitive than Cd or $^{13}/^{12}\text{C}$ in picking up precessional forcing of deep water formation; or, variability in these three tracers is forced by more than one mechanism. The latter hypothesis has already been suggested for differences in the deep North Atlantic records of Cd and carbon isotopes. Some of the variability in carbon isotope records has been explained by transfer of carbon from high latitude and tropical forest biomass to the ocean during cold periods (Shackleton, 1977); Boyle and Keigwin (1985) suggest that the relatively strong presence of the 23 kyr precessional cycle in carbon isotope records is due to this transfer.

At present it is difficult to distinguish between these two hypotheses because there are so many unknown factors. It is tempting to speculate that the first hypothesis is less likely, since Cd, which is more depleted in surface waters than Ba (i.e. greater dynamic range), should always be more sensitive to variations in the flux of nutrient depleted surface water.

The second hypothesis is intriguing because it suggest that some of the temporal change in Ba might reflect a process that does not leave a prominent imprint on the temporal records of Cd and carbon isotopes. This hypothesized process or mechanism must be strongly forced at the 23 kyr precessional cycle. A model developed in Chapter 6 suggested that differences in the distribution of

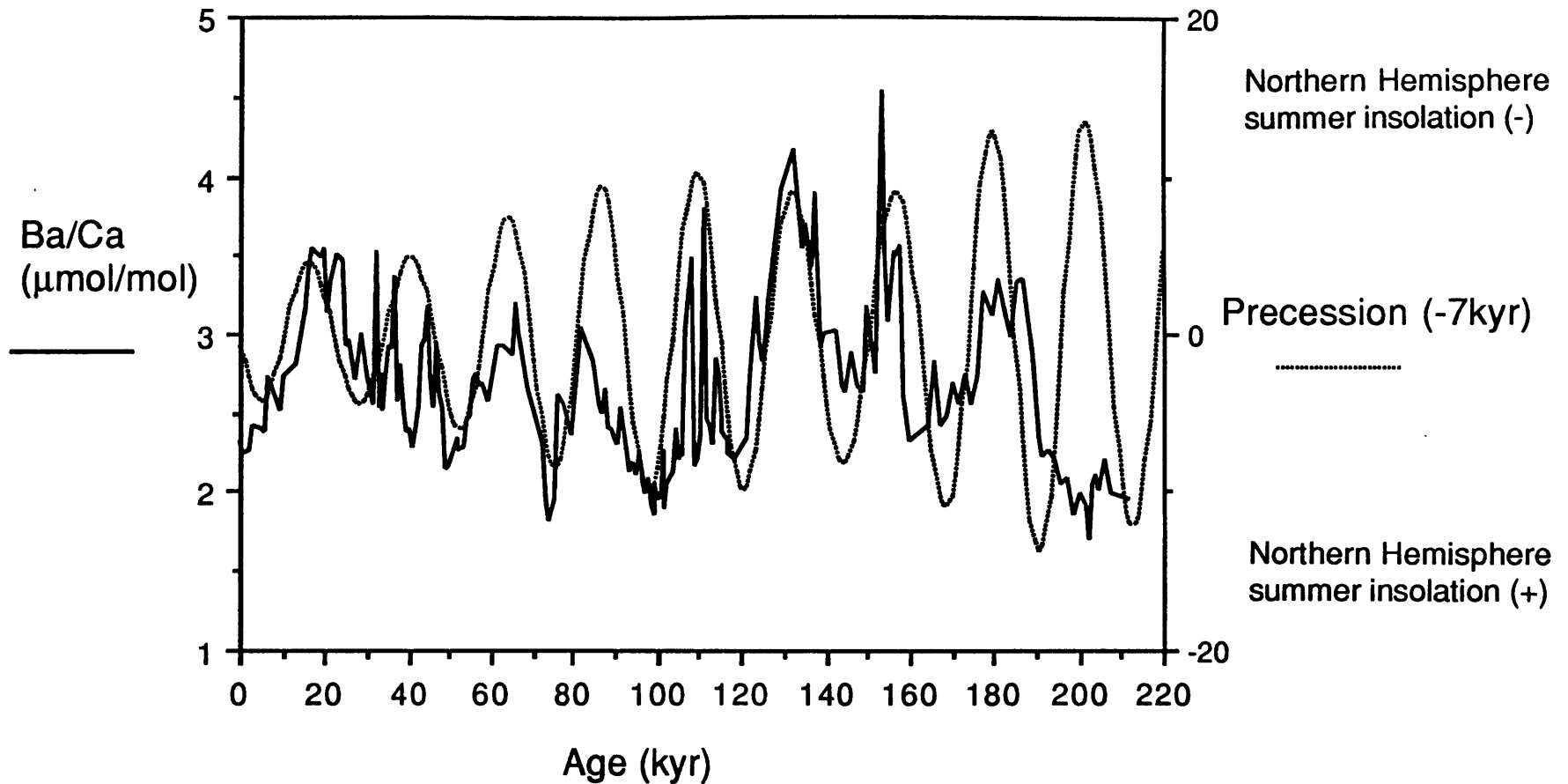


Figure 7.5 Comparison of CHN-4PC Ba/Ca with precession index (Berger, 1977). Precession index is plotted so that Northern Hemisphere summer insolation maxima appear as lows. In addition, the precession index is shifted by -7 kyr to account for the derived phase lag (see Table 7.2 and text).

Ba and Cd (and carbon isotopes) in the oceans of the LGM might be due to the sensitivity of deep Atlantic Ba to enhanced upwelling and the subsequently increased particulate Ba fluxes in the Glacial Atlantic. While there is no obvious reason to tie precessional forcing to enhanced upwelling in the Atlantic, the model does suggest that a second mechanism might be important in explaining Glacial Ba distributions. It is not unlikely that any second mechanism, whether it be greater upwelling in the Atlantic or another factor, might be forced by different orbital parameters than those that drive variations in deep water formation.

Another reason to suspect a second mechanism is that *a priori* one might expect that changes in deep water formation would be forced most strongly by changes in tilt, since deep water formation takes place at polar latitudes. The influence of tilt is large at the poles but small at the equator, in contrast to the effect of precession, which is small at the poles and large at the equator (Imbrie and Imbrie, 1980). Of course, low latitude processes such as upwelling, transport of vapor and origination of surface currents are all critical to deep water formation, and therefore it is not easy to separate out all the relevant factors.

Even if one could be certain that a second factor dominated by precessional forcing and distinct from deep water formation existed, the periodicity that drives this factor does not reveal many clues as to what it might be. However, precession certainly might influence low latitude ocean mixing between the intermediate and surface ocean and hence regulate the transfer of Ba into the deep ocean (Chapter 6); changes in low latitude insolation would affect temperature contrast, wind strength, etc. One cannot answer this question definitively with the present data, but studies might be undertaken to search for

long term periodicities in intermediate depth cores, where benthic Ba might be 180° out of phase with the deep water beat.

References--Chapter 7

- Berger, A. L. (1977) Support for the astronomical theory of climatic change. *Nature* **269**, 44-45.
- Boyle, E. A. (1983) Manganese carbonate overgrowths on foraminifera tests. *Geochim. et cosmochim. acta.* **47**, 1815-1819.
- Boyle, E. A. (1988) Cadmium: chemical tracer of deepwater paleoceanography. *Paleoceanography* **3**, 471-489.
- Boyle, E. A. and Keigwin, L. D. (1982) Deep circulation of the North Atlantic over the last 200,000 years: Geochemical evidence. *Science* **218**, 784-787.
- Boyle, E. A. and Keigwin, L. D. (1985) Comparison of Atlantic and Pacific paleochemical records for the last 215,000 years: changes in deep ocean circulation and chemical inventories. *Earth Planet Sci. Lett.* **76**, 135-150.
- Chan, L. H., Edmond, J. M., Stallard, R. F., Broecker, W. S., Chung, Y. C., Weiss, R. F. and Ku, T. L. (1976) Radium and barium at GEOSECS stations in the Atlantic and Pacific. *Earth Planet. Sci. Lett.* **32**, 258-267.
- Curry, W. B., Duplessy, J. -C., Labeyrie, L. D. and Shackleton, N. J. (1988) Changes in the distribution of $\delta^{13}\text{C}$ of deep water ΣCO_2 between the last glaciation and the Holocene. *Paleoceanography* **3**, 317-342.
- Emiliani, C. (1966) Paleotemperature analysis of Caribbean cores P 6304-8 and P 6304-9 and a generalized temperature curve for the last 425,000 years. *J. Geol.* **74**, 109-126.
- Hays, J. D., Imbrie, J. and Shackleton, N. J. (1976) Variations in the earth's orbit: pacemaker of the ice ages. *Science* **194**, 1121-1132.
- Imbrie, J. and Imbrie, K. P. (1980) *Ice ages--Solving the mystery*. Enslow Publ., New Jersey, 224p.
- Keigwin, L. D. and Boyle, E. A. (1985) Carbon isotopes in deep-sea benthic foraminifera: precession and changes in low-latitude biomass. In *The Carbon Cycle and Atmospheric CO₂: Natural Variations Archean to Present* (ed. E. Sundquist and W. Broecker), pp. 319-328, American Geophysical Union, Washington, D.C.
- Lea, D. and Boyle, E. (1989) Barium content of benthic foraminifera controlled by bottom water composition. *Nature* **338**, 751-753.
- Martinson, D. G., Pisias, N. G., Hays, J. D., Imbrie, J., Moore, T. C. and Shackleton, N. J. (1987) Age dating and the orbital theory of the ice ages: development of high-resolution 0 to 300,000-year chronostratigraphy. *Quat. Res.* **27**, 1-29.

Ruddiman, W. F. and McIntyre, A. (1981) Oceanic mechanisms for amplification of the 23,000-year ice-volume cycle. *Science* **212**, 617-627.

Ruddiman, W. F., Raymo, M. E., Martinson, D. G., Clement, B. M. and Backman, J. (1989) Pleistocene evolution: Northern Hemisphere ice sheets and North Atlantic ocean. *Paleoceanography* **4**, 353-412.

Shackleton, N. J. (1977) ^{13}C in *Uvigerina*: Tropical rainforest history and the equatorial Pacific carbonate dissolution cycles. In *Fate of Fossil Fuel CO₂ in the Oceans* (ed. N. Anderson and A. Malahof), pp. 401-427, Plenum, New York.

Shackleton, N. J. and Opdyke, N. D. (1973) Oxygen isotope and paleomagnetic stratigraphy of equatorial Pacific core V28-238: Oxygen isotope temperatures and ice volumes on a 10^5 and 10^6 year scale. *Quat. Res.* **3**, 39-55.

CHN82	Sta24	Core	4PC
Depth	Age	Sed. rate	
(cm)	(kyr)	(cm/kyr)	
1	0.0		
40	11.0	3.5	
64	18.0	3.4	
90	24.0	4.3	
212	59.0	3.5	
230	66.0	2.6	
242	73.0	1.7	
406	115.0	3.9	
443	127.0	3.1	
520	159.0	2.4	
573	189.0	1.8	
611	205.0	2.4	
636	220.0	1.7	

Appendix to Chapter 7 Age points and derived sedimentation rates for CHN82-4PC. Depths deeper than 348 cm have been corrected by -32 cm because of a core void from 348-380 cm.

Chapter 8: General conclusions

This chapter summarizes and reviews the principal results of this thesis and contains ideas for future work.

High resolution coralline Ba: records of upwelling variability

High resolution measurements of coralline Ba demonstrate that massive corals from the Galapagos Islands contain a detailed Ba stratigraphy that records temporal variability in upwelling of deep waters to the surface ocean. The Ba content of coral time slices record this signal because upwelling in the Equatorial Pacific brings cold (Ba-rich) upper thermocline waters to the ocean surface. Depression of the thermocline during El Niño/Southern Oscillation (ENSO) events results in the coincidence of negative Ba anomalies with the positive temperature anomalies characteristic of these events. As a result, coralline Ba provides a historical record of ENSO events. Similarities between Ba and Sr records in the coral suggest that the Ba/Ca ratio of corals may be partially controlled by a temperature effect.

Ba in planktonic foraminifera: large inter-genera differences

Species of *Globigerinoides* and *Neogloboquadrina* from the Panama Basin, North Atlantic, and Mediterranean have Ba contents consistent with surface Ba in these basins. Records of planktonic-Ba reaching back to the close of last glacial period do not reveal any change in the Ba concentration of temperate Atlantic and Pacific surface waters, although the noise in the data precludes distinguishing small (10-20%) changes. Several species of *Globorotalia* have anomalously higher Ba contents inconsistent with coprecipitation of Ba in the shell. It is hypothesized that high Ba contents of

Globorotalia result from diatom-rich food sources, since precipitation of barite in marine biogenic particulate matter appears to be intimately associated with diatom frustules (Bishop, 1988).

Ba in benthic foraminifera: reconstructing glacial circulation

The Ba content of benthic foraminifera *Cibicidoides* and *Uvigerina* is controlled by bottom water composition. Thus it is possible to reconstruct Ba distributions in the bottom waters of past oceans. Determination of Ba/Ca on benthic foraminifera recovered from glacial sections (15-25 kyr) of cores from the Atlantic indicates that deep waters had ~30-60% higher Ba while intermediate waters had ~0-20% lower Ba. These changes are consistent with previously observed shifts in Glacial Atlantic nutrient distributions. Deep waters of the Glacial Pacific were about 25% lower in Ba (~3000 m); there is no significant difference in the Ba content of deep waters of the two basins at the LGM.

A simple seven-box ocean model is used to explore several scenarios for reconciling Glacial Ba distributions with inferred P distributions based on foraminiferal Cd determinations (Boyle, 1988; Boyle and Keigwin, 1985; Boyle and Keigwin, 1987). While the changed distribution of both tracers suggests diminishment in the flux of nutrient depleted waters to the deep Atlantic during the LGM, model Ba distributions can be matched to the foraminiferal Ba data by increasing Atlantic upwelling rates (and particle fluxes due to that upwelling) in the model.

212 Kyr record of deep North Atlantic Ba

A long record of benthic foraminiferal Ba in the deep North Atlantic indicates that although a general pattern of high Ba during glacial periods and

low Ba during interglacials has persisted for 200 kyrs, variability in benthic Ba is not strictly linked to glacial-interglacial ice-volume. Spectral analysis of the Ba time series indicates dominance of the 23 kyr precessional period of change in the earth's orbit. Since the power at the precessional frequencies is greater in the Ba time series than in the time series of Cd and carbon isotopes from the same core, Ba variations may also be recording a second process distinct from variations in the flux of nutrient depleted water to the core site. It is tempting to speculate that this second mechanism might be an increase in Atlantic upwelling/enhanced particulate fluxes, as suggested to explain differences in Ba and Cd at the LGM.

Future work

The results of this thesis demonstrate that Ba is a powerful paleoceanographic tracer in a number of different settings. Some promising areas for future work are:

- 1) Long coral Ba records could be used to reconstruct changes in upwelling of cold source waters to prehistoric oceans. The resolution of these records could be improved over the current work by closer-spaced sampling; since Ba is relatively free from artifacts due to contamination, closely-spaced samples could potentially be drilled out, with subsequent analysis of the drilling "dust". Confirmation of the temperature effect on the incorporation of Ba into corals might be sought in studies of Ba variability in corals from waters with limited source water variation but large temperature variation, such as the corals of Bermuda.

- 2) Sources of inter-genera variability in the Ba content of planktonic foraminifera might be investigated via live culturing of planktonic species.

Varying food sources might be used to investigate the origin of the enriched Ba content of *Globorotalia* shells.

3) Further study of the the distribution of Ba in the glacial oceans will enhance the effectiveness of Ba as a paleo-circulation tracer. There are particularly important gaps in the current data set for the Southern, Indian and Western Pacific Oceans. A long Pacific record to complement the Atlantic record is a high priority for the future. The source and persistence of precessional forcing in Ba-time series requires further evaluation; in particular, a record of benthic Ba in the intermediate waters and the Southern hemisphere might show a contrasting (inverse?) relationship between Ba and precession.

References--Chapter 8

Bishop, J. K. B. (1988) The barite-opal-organic carbon association in oceanic particulate matter. *Nature* **332**, 341-343.

Boyle, E. A. (1988) Cadmium: chemical tracer of deepwater paleoceanography. *Paleoceanography* **3**, 471-489.

Boyle, E. A. and Keigwin, L. D. (1985) Comparison of Atlantic and Pacific paleochemical records for the last 215,000 years: changes in deep ocean circulation and chemical inventories. *Earth planet Sci. Lett.* **76**, 135-150.

Boyle, E. A. and Keigwin, L. D. (1987) North Atlantic thermohaline circulation during the past 20,000 years linked to high-latitude surface temperature. *Nature* **330**, 35-40.

Appendix 1: Ba in Mediterranean seawater

Ba was measured in a number of samples of Mediterranean seawater by the isotope dilution method on the ICP-MS. 250 μL of acidified seawater was spiked with the appropriate volume of ^{135}Ba -enriched spike (Chapter 2) and diluted to about 10 mL with 0.1N HCl. $^{135}/^{138}\text{Ba}$ ratios were then determined on the ICP-MS with typical counting times of about 6 minutes. Standardization was accomplished by normalizing to solutions of known spike/standard ratio (SGS), as described in Chapter 2. The precision of the determinations is estimated at 2 %.

Cruise, station, description	Lat, Long	Depth	Ba nM
OC176 St. 15, Niskin cast	35°54'N, 5°42'W	0	41.6
OC176 St. 15, Niskin cast	35°54'N, 5°42'W	50	40.9
OC176 St. 15, Niskin cast	35°54'N, 5°42'W	150	68.8
OC176 St. 15, Niskin cast	35°54'N, 5°42'W	200	70.9
OC176 St. 15, Niskin cast	35°54'N, 5°42'W	300	74.0
OC176 St. 15, Niskin cast	35°54'N, 5°42'W	400	77.7
OC176 St. 15, Niskin cast	35°54'N, 5°42'W	450	77.0
OC176 St. 15, Niskin cast	35°54'N, 5°42'W	500	78.9
OC176 St. 15, Niskin cast	35°54'N, 5°42'W	50	40.0
OC176 St. 15, Niskin cast	35°54'N, 5°42'W	300	75.6
KNR134-7 St. 3, Niskin cast	35°28.1'N, 17°13.8'E	0	53.1
KNR134-7 St. 3, Niskin cast	35°28.1'N, 17°13.8'E	30	52.3
KNR134-7 St. 3, Niskin cast	35°28.1'N, 17°13.8'E	70	52.5
KNR134-7 St. 3, Niskin cast	35°28.1'N, 17°13.8'E	90	53.6
KNR134-7 St. 3, Niskin cast	35°28.1'N, 17°13.8'E	130	52.7
KNR134-7 St. 3, Niskin cast	35°28.1'N, 17°13.8'E	150	52.8
KNR134-7 St. 3, Niskin cast	35°28.1'N, 17°13.8'E	200	59.9
KNR134-7 St. 3, Niskin cast	35°28.1'N, 17°13.8'E	275	67.7
KNR134-7 St. 3, Niskin cast	35°28.1'N, 17°13.8'E	400	69.0
KNR134-7 St. 3, Niskin cast	35°28.1'N, 17°13.8'E	500	73.1
KNR134-7 St. 3, Niskin cast	35°28.1'N, 17°13.8'E	650	73.6
KNR134-7 St. 3, Niskin cast	35°28.1'N, 17°13.8'E	800	76.3
KNR134-7 St. 3, Niskin cast	35°28.1'N, 17°13.8'E	1000	77.5
KNR134-7 St. 3, Niskin cast	35°28.1'N, 17°13.8'E	1200	78.3
KNR134-7 St. 3, Niskin cast	35°28.1'N, 17°13.8'E	1400	80.5
KNR134-7 St. 3, Niskin cast	35°28.1'N, 17°13.8'E	1700	79.4
KNR134-7 St. 3, Niskin cast	35°28.1'N, 17°13.8'E	2000	79.0
KNR134-7 St. 3, Niskin cast	35°28.1'N, 17°13.8'E	2300	77.1
KNR134-7 St. 3, Niskin cast	35°28.1'N, 17°13.8'E	2500	78.7
KNR134-7 St. 3, Niskin cast	35°28.1'N, 17°13.8'E	2700	77.3
KNR134-7 St. 3, Niskin cast	35°28.1'N, 17°13.8'E	3400	76.8
Franchti SS2 filtered	Franchti, Greece	0	61.3
Franchti SS1 filtered	Franchti, Greece	0	81.8
Uzes 9/16/87 decanted only	Uzes, Sicily	0	51.2
ME5/6 St. 722 SS2	35°28.9'N, 25°51.7'E	0	52.9
ME5/6 St. 724 SS3	34°00.1'N, 28°00.1'E	0	57.3
ME5/6 St. 727 SS2	35°29.9'N, 28°29.9'E	0	57.7
ME5/6 St. 729 SS2	35°30.9'N, 29°30.0'E	0	59.2
ME5/6 St. 733 SS1	34°30.0'N, 30°30.4'E	0	56.8
ME5/6 St. 735 SS2	35°29.9'N, 30°29.9'E	0	60.2
ME5/6 St. 737 SS2	35°30.0'N, 31°29.7'E	0	59.1
ME5/6 St. 739 SS2	34°30.5'N, 31°29.7'E	0	57.6
ME5/6 St. 741 SS2	34°00.0'N, 33°00.1'E	0	58.8

Cruise, station, description	Lat, Long	Depth	Ba nM
ME5/6 St. 743 SS2	33°15.6'N, 33°44.5'E	0	56.7
ME5/6 St. 742 SS2	34°00.2'N, 33°59.9'E	0	59.7
ME5/6 St. 744 SS2	32°30.0'N, 33°29.6'E	0	57.5
ME5/6 St. 745 SS2	33°08.6'N, 32°15.1'E	0	56.3
ME5/6 St. 747 SS2	33°48.4'N, 29°05.0'E	0	56.5
ME5/6 St. 748 SS2	33°30.1'N, 26°29.4'E	0	52.5
ME5/6 St. 750 SS2	32°45.4'N, 24°32.2'E	0	50.2
ME5/6 St. 751 SS1	34°33.1'N, 26°15.0'E	0	55.5
ME5/6 St. 753 SS2	35°48.0'N, 25°18.1'E	0	53.5
ME5/6 St. 754 SS2	35°35.3'N, 26°45.5'E	0	54.3
ME5/6 St. 756 SS2	34°11.8'N, 24°42.3'E	0	58.7
ME5/6 St. 758 SS2	35°41.0'N, 23°00.0'E	0	54.2
ME5/6 St. 760 SS2	35°30.2'N, 21°30.0'E	0	47.4
ME5/6 St. 762 SS2	36°38.1'N, 20°05.0'E	0	44.9
ME5/6 St. 764 SS2	38°30.0'N, 19°59.9'E	0	51.0
ME5/6 St. 765 SS2	39°44.9'N, 19°19.8'E	0	50.7
ME5/6 St. 725 SS2	34°29.7'N, 28°29.6'E	0	58.6
ME5/6 St. 767 SS2	39°41.9'N, 18°52.9'E	0	50.6
ME5/6 St. 768 SS2	38°49.6'N, 17°06.2'E	0	48.9
ME5/6 St. 770 SS2	38°30.1'N, 17°59.5'E	0	50.0
ME5/6 St. 772 SS2	36°30.0'N, 18°30.1'E	0	46.1
ME5/6 St. 774 SS2	34°31.0'N, 19°00.9'E	0	50.6
ME5/6 St. 775 SS2	33°30.1'N, 18°59.6'E	0	50.8
ME5/6 St. 777 SS2	35°30.2'N, 17°30.0'E	0	47.7
ME5/6 St. 779 SS2	35°35.6'N, 16°00.2'E	0	50.7
ME5/6 St. 780 SS2	35°11.9'N, 14°26.9'E	0	52.2
ME5/6 St. 782 SS2	37°11.0'N, 11°35.8'E	0	48.0
ME5/6 St. 786 (784?) SS2	37°33.1'N, 11°34.2'E	0	50.1
ME5/6 St. 786 SS2	39°15.1'N, 13°14.7'E	0	52.1
ME5/6 St. 766 SS3 filtered	41°14.7'N, 18°15.4'E	0	51.2
KNR134-7 St. 2 SS2	38°03.3'N, 06°00.8'E	0	52.1
KNR134-7 St. 1 SS1	37°28.4'N, 02°30.4'E	0	51.4
KNR134-7 St. 3 SS1	35°28.1'N, 17°13.8'E	0	53.3
KNR134-7 Pole samp lvng. St. 4	33°12.4'N, 25°21.0'E	0	53.8

Appendix 2: Description of Model VIV* (Chapter 6)

The following pages illustrate all equations in Model VIV*. The model includes 7 boxes. Concentrations are fixed in the two surface boxes. There are eight equations for the model: 1 each for the 5 boxes with variable concentrations, 1 each for 3 model generated particulate fluxes (Atlantic, Pacific and Circumpolar surface). Solutions are calculated by inverting the matrix A for each tracer and then multiplying $A^{-1}b$ to find the solution x.

Key to abbreviations used:

fPi	Fraction of the P particle flux regenerated in intermediate boxes.
fPd	Fraction of the P particle flux regenerated in deep boxes.
fBai	Fraction of the Ba particle flux regenerated in intermediate boxes.
fBad	Fraction of the Ba particle flux regenerated in deep boxes.
Q(box1)(box2)	Water flux from box 1 to box 2 (Sv). Box abbreviations: ws=warm surface; pi=Pacific intermediate; pd=Pacific deep; cs=Circumpolar surface; cd=Circumpolar deep; ai=Atlantic intermediate; ad=Atlantic deep.
V(box)	Fractional volume of box. Box abbreviations as above.
P(box)	P content of box ($\mu\text{mol/kg}$). Box abbreviation as above.
Ba(box)	Ba content of box (nmol/kg). Box abbreviations as above.
meanP	Mean oceanic P ($\mu\text{mol/kg}$)
meanBa	Mean oceanic Ba (nmol/kg)
ABaf	Atlantic particulate Ba flux (mol/s)
APf	Atlantic particulate P flux (10^3 mol/s)

PBaf	Pacific particulate Ba flux (mol/s)
PPf	Pacific particulate P flux (10^3 mol/s)
CBaf	Circumpolar particulate Ba flux (mol/s)
CPf	Circumpolar particulate P flux (10^3 mol/s)
Avent	Atlantic (intermediate + deep) ventilation age (years)
Pvent	Pacific (intermediate + deep) ventilation age (years)
Mmult	Excel matrix multiplication function
Minverse	Excel matrix inverse function
Pmatrix	8x8 matrix A for P
Bamatrix	8x8 matrix A for Ba
bP	1x8 matrix b for P
bBa	1x8 matrix b for Ba

P matrix A:

										x
-1	0	0	0	0	0	0	=Qaiws	0		APf
0	-1	=Qpiws	0	0	0	0	0	0		PPf
0	=fPi	=(Qpiws+Qpipd+Qpics+Qpia)	=Qpdpi	0	0	0	0	0		PI
0	=fPd	=Qpipd	=(Qpdpi+Qpdcd)	0	=Qcdpd	0	0	0		PD
0	0	=Qpics	0	=-1	=Qcdcs	=Qaics	0	0		CPf
0	0	0	=Qpdcd	1	=(Qcdcs+Qcdad+Qcdpd)	0	=Qadcd			CD
=fPi	0	=Qpia	0	0	0	=(Qaiad+Qaiws+Qaics)	=Qadai			AI
=fPd	0	=Vpi	=Vpd	0	=Qcdad+Vcd	=Qaiad+Vai	=(Qadcd+Qadai)+Vad			AD

Ba matrix A:

										x
-1	0	0	0	0	0	0	=Qaiws	0		ABaf
0	-1	=Qpiws	0	0	0	0	0	0		PBaf
0	=fBai	=(Qpiws+Qpipd+Qpics+Qpia)	=Qpdpi	0	0	0	0	0		PI
0	=fBad	=Qpipd	=(Qpdpi+Qpdcd)	0	=Qcdpd	0	0	0		PD
0	0	=Qpics	0	=-1	=Qcdcs	=Qaics	0	0		CBaf
0	0	0	=Qpdcd	1	=(Qcdcs+Qcdad+Qcdpd)	0	=Qadcd			CD
=fBai	0	=Qpia	0	0	0	=(Qaiad+Qaiws+Qaics)	=Qadai			AI
=fBad	0	=Vpi	=Vpd	0	=Qcdad+Vcd	=Qaiad+Vai	=(Qadcd+Qadai)+Vad			AD

Warm surface										
35										
0.1	20							10		
	Δ			$Q_{pia} >$	0			Δ		
Pacific Int	V			Circumpolar surface				Atlantic Int	V	V
-B _{pi}	10			88				-B _{ai}	4	16
-P _{pi}				1.4				-P _{ai}		
		14	10		20	0			10	
		Δ			Δ				Δ	
Pacific Deep	V			Circumpolar deep	V			Atlantic Deep	V	
-B _{pd}	10			-B _{cd}	10			-B _{ad}	8	
-P _{pd}				-P _{cd}		21		-P _{ad}		
			24							
				20				7		
Mean B_a=			100			Mean P_a=		2.25		

B_a particle flux (mol/s)
P particle flux (kmol/s)
B_a flux (nmol/cm²/yr)
P flux (μmol/cm²/yr)

A_{tl}
 -A_{Baf}
 -A_{Pf}
 -A_{Baf}/(0.257*3.08)*0.0315
 -A_{Pf}/(0.257*3.08)*0.0315

P_{cf}
 -P_{Baf}
 -P_{Pf}
 -P_{Baf}/(0.743*3.08)*0.0315
 -P_{Pf}/(0.743*3.08)*0.0315

Circumpolar
 -C_{Baf}
 -C_{Pf}
 -C_{Baf}/0.13*0.0315
 -C_{Pf}/0.13*0.0315
 -C_{Baf}/(C_{Baf}+P_{Baf}+A_{Baf})
 -C_{Pf}/(C_{Pf}+P_{Pf}+A_{Pf})

Warm surface										
35		20		Q _{pi} >		0		10		
0.1		Δ						Δ		
Pacific Int			Circumpolar surface			Atlantic Int			V	V
-B _{pi}		V		88		-B _{ai}		4		16
-P _{pi}		10		1.4		-P _{ai}		10		
		14		20		4		Δ		
		Δ		4		0				
Pacific Deep			Circumpolar deep			Atlantic Deep			V	V
-B _{pd}		V		-B _{cd}		-B _{ad}		8		
-P _{pd}		10		=P _{cd}		-P _{ad}		7		
		24		20		21				
Mean B _∞		100		Mean P _∞		2.25				

B_a particle flux (mol/s)
 P particle flux (kmol/s)
 B_a flux (nmol/cm²/yr)
 P flux (μmol/cm²/yr)

Ventilation Ages (years)

<u>Ati</u>	<u>Pcf</u>	<u>Circumpolar</u>
-AB _a f	-PB _a f	=CB _a f / (CB _a f + PB _a f + AB _a f)
-AP _i f	-PP _i f	=CP _i f / (CP _i f + PP _i f + AP _i f)
=AB _a f / (0.257 * 3.08) * 0.0315	=PB _a f / (0.743 * 3.08) * 0.0315	=CB _a f / 0.13 * 0.0315
=AP _i f / (0.257 * 3.08) * 0.0315	=PP _i f / (0.743 * 3.08) * 0.0315	=CP _i f / 0.13 * 0.0315
<u>Ati</u>	<u>Pcf</u>	
-A _{vent}	-P _{vent}	

Biographical Note

The author was born on March 30, 1961 in Philadelphia, PA and grew up in Philadelphia and Berlin, West Germany. He graduated from Cheltenham High School in 1979 and entered Haverford College the same year. After a year of musical studies on the oboe in Detmold, West Germany (1981-82), the author chose to pursue geology studies at Haverford's sister school, Bryn Mawr College. An interest in geochemistry was stimulated by a summer (1983) working in Hugh Taylor's oxygen isotope lab at Caltech. The author entered the MIT/WHOI Joint Program in fall 1984 in Marine Geology and in 1985 switched to Chemical Oceanography and joined Ed Boyle's group at MIT. He received a Joint Oceanographic Institutions/Ocean Drilling Program Fellowship for 1987-88.

Publications

Shen, G.T., Boyle, E.A. and Lea, D.W. (1987) Cadmium in corals as a tracer of historical upwelling and industrial fallout. *Nature* **328**, 794-796.

Lea, D.W., Larson, P.B., Taylor, H.P.Jr., and Crawford, M.L. (1989) Oxygen isotope and fluid inclusion study of rocks from the Mineral Point Area, Eureka graben, Colorado. In press, *Economic Geology*.

Lea, D.W. and Boyle, E.A. (1989) Barium content of benthic foraminifera controlled by bottom water composition. *Nature* **338**, 751-753.

Lea, D.W., Shen, G.T. and Boyle, E.A. (1989) Coralline barium records temporal variability in Equatorial Pacific upwelling. *Nature* **340**, 373-376.